



**Large-scale production of high-value bioactive
substances from microalgae**

by

Song Wang

a Thesis submitted in partial fulfillment
of the requirements for the degree of

**Doctor of Philosophy
in Geoscience with specialization in Oceanography**

Approved Dissertation Committee

Prof. Dr. Laurenz Thomsen
Jacobs University Bremen

Prof. Dr. Matthias Ullrich
Jacobs University Bremen

Prof. Dr. Guanpin Yang
Ocean University of China

Date of Defense: 21st September 2018

Department of Physics and Earth Sciences

Acknowledgment

First and foremost, I would like to give my deepest gratitude to my first academic supervisor Prof. Dr. Laurenz Thomsen for his constant support, and patient guidance through my whole Ph.D. study. He has taught me how to be an independent scientific researcher and encouraged me to overcome obstacles and impediments I have encountered. His suggestions could always inspire me and help me improve my work. I appreciate the freedom he gave to me in experimental design. His dedication to work has provided a perfect example for me as a qualified scientist.

My sincere thanks to my second academic supervisor Prof. Dr. Matthias Ullrich for his supervision and guidance. He paid attention to every step of my experiment and detail in each of manuscript. He always spent time answering all kinds of questions I had and helped me find solutions. His advice is invaluable to me in my career. His enthusiasm for research always motivates me to move forward.

I am also thankful to Prof. Dr. Guanpin Yang and Prof. Dr. Kehou Pan. They supervised me for three years in my master study at Ocean University of China. They helped me start my career in algal research and supported me to pursue my Ph.D. study in Germany. They always give me insightful suggestions in my career.

I am also grateful to Prof. Dr. Nikolai Kuhnert for the valuable scientific suggestions which help improve my work a lot.

I am extremely thankful to Dr. Claudia Thomsen who was always supportive and encouraging. I learned a lot from her experience in large-scale algae production. I really appreciate the funding support from Phytolutions.

A special thanks to all the co-authors of the manuscripts in this thesis: Dr. Inamullah Hakeem Said, Dr. Sujit K. Verma, Candice Thorstenson, Dr. Diana Sirbu, and Dr. Jichang Han. Without your input and assistance, I will not be able to finish my Ph.D. in such a way. I would also like to thank

the colleagues from OceanLab: Damianos Chatzievangelou, Benjamin Gillard, Dr. Charlotte Kleint, Luise Britta Heinrich, David Ernst, Ann Noowong, Sophie Paul, Dr. Erika Kurahashi and Nadine Weimar, and colleagues from Microbiology Lab: Dr. Neha Kumari, Veronika Will, and Warren John for creating such a lovely atmosphere and the fantastic group activities. My particular thanks to the responsible and dedicated technicians: Annika Moje, Maike Last and Nina Louise Böttcher for your excellent assistance.

I wish to express my gratitude to my family members. My parents raised me up with all their love, shaped my characters and always encouraged me to pursue my dream. It's your support that helps me face every challenge in my life. My cousins always keep me accompanied and cheer me up.

I also want to say thank you to the bachelor students who worked with me. They are Jiemin Du, Enis Bardhi, Ruchen Tian, Yann Guezenec and Lisa Schallwig. It's a pleasant experience to work with all of you.

Thanks for the Ph.D. scholarship from China Scholarship Council (CSC) that funded my study in Germany.

The days in Bremen would surely be the most memorable moment in my life that I will permanently cherish.

Song Wang
Bremen
August 2018

Table of Contents

Acknowledgment.....	i
Abbreviation.....	vii
Abstract.....	viii
1. Introduction.....	1
1.1 Microalgae	1
1.2 Microalgae for human food and animal feed	2
1.3 High-value bioactive compounds from microalgae	3
1.3.1 Carotenoids	3
1.3.2 Polyunsaturated fatty acids	5
1.3.3 Other bioactive compounds	6
1.4 Microalgae as feedstock for biofuel production.....	6
1.5 Photobioreactor (PBR).....	8
1.6 Reference	11
2. Aims of the Ph.D. study	17
2.1 Reference	19
3 Pilot-scale production of antibacterial substances by the marine diatom <i>Phaeodactylum</i> <i>tricornutum</i> Bohlin	20
3.1 Abstract.....	21
3.2 Introduction.....	21
3.3 Materials and Methods.....	23
3.3.1 Microalgal species and cultivation conditions.....	23
3.3.2 Photo-bioreactor (PBR)	23
3.3.3 Growth kinetics and biomass productivity	24
3.3.4 Preparation of crude extract of <i>P. tricornutum</i>	24
3.3.5 Flash column and thin-layer chromatography	25
3.3.6 Disc diffusive assay and minimal inhibitory concentration (MIC)	25

3.3.7 Electro spray Ionization-Tandem Mass Spectrometry (ESI-MSn) and micro Time of Flight Mass Spectrometry (ESI-microTOF).....	26
3.3.8 Quantification of EPA productivity of <i>P. triornutum</i> biomass by fatty acid methyl esterification (FAME).....	26
3.3.9 Preparation of phytohormones and synthesis of coronatine to potentially induce the production of antimicrobial compounds.	27
3.3.10 Induction of synthesis of antibacterial substance(s) in <i>P. triornutum</i> and antibacterial effects analysis	28
3.4 Results and Discussion.....	28
3.4.1 Algal growth kinetics and productivity.....	28
3.4.2 Activity guided fractionation	29
3.4.3 Antibacterial activity against potentially human pathogenic <i>Vibrio vulnificus</i> , <i>Vibrio cholerae</i> , and <i>Vibrio parahaemolyticus</i>	33
3.4.4 Comparison of minimum inhibitory concentration of fraction B and J (eicosapentaenoic acid) with eicosapentaenoic acid standard, a commercial antimicrobial product	34
3.4.5 Inducibility of the defense system of <i>P. triornutum</i>	36
3.5 Conclusions	37
3.6 Reference	39
3.7 Supplementary material.....	44
4 Changes in the fucoxanthin production and protein profiles in <i>Cylindrotheca closterium</i> in response to blue light-emitting diode light	47
4.1 Abstract.....	48
4.2 Introduction.....	49
4.3 Materials and Methods.....	51
4.3.1 Microalgae species and culture conditions	51
4.3.2 Equipment	51
4.3.3 Experimental design.....	52
4.3.4 Measurement of growth kinetics, biomass productivity, and specific growth rate	53
4.3.5 Fucoxanthin extraction, identification, and quantification	54
4.3.6 Protein extraction using SDS-DTT buffer	55

4.3.7 Determination of protein concentration	55
4.3.8 Sodium dodecyl sulfate-polyacrylamide gel electrophoresis (SDS-PAGE).....	55
4.3.9 Two-dimensional protein gel electrophoresis	56
4.3.10 In-gel protein digestion	56
4.3.11 MALDI-TOF-MS analyses of proteins.....	57
4.3.12 Data analysis	57
4.4 Results	57
4.4.1 Screening for species with highest fucoxanthin production	57
4.4.2 Predictions by “Design of Experiment” software	60
4.4.3 Test for large-scale production in bag PBRs	63
4.4.4 Protein content and sodium dodecyl sulfate-polyacrylamide gel electrophoresis analyses using sodium dodecyl sulphate–dithiothreitol buffer	65
4.4.5 Protein annotation via MALDI-TOF-MS analyses.....	67
4.5 Discussion	68
4.5.1 Screening for species with the highest fucoxanthin production	68
4.5.2 Predictions by “Design of Experiment” software	69
4.5.3 Test for large-scale production in bag PBRs	69
4.5.4 Protein annotation via MALDI-TOF-MS analyses.....	70
4.6 Conclusions.....	72
4.7 Reference	74
4.8 Supplementary material.....	80
5. Comparative lipidomic studies of <i>Scenedesmus</i> sp. (Chlorophyceae) and <i>Cylindrotheca closterium</i> (Bacillariophyceae) reveal their differences in lipid production under nitrogen starvation	85
5.1 Abstract.....	86
5.2 Introduction.....	86
5.3 Materials and Methods.....	89
5.3.1 Algae and culture condition	89
5.3.2 Chemicals and agents.....	89
5.3.3 Total lipids extraction	90

5.3.4 Fatty acids methyl esterification preparation and measurement by gas chromatography	90
5.3.5 High-performance liquid chromatography	91
5.3.6 High-resolution mass spectrometry	91
5.3.7 Tandem mass spectrometry.....	92
5.3.8 Statistical analysis	92
5.4 Results	92
5.4.1 Total lipid content and growth kinetics under nitrogen starvation	92
5.4.2 Fatty acids profile under nitrogen starvation	94
5.4.3 Relatively quantitative analysis of glycerolipids and pigments.....	95
5.4.4 Lipid and pigment molecules alteration.....	98
5.5 Discussion	103
5.5.1 Total lipid content and growth kinetics under nitrogen starvation	103
5.5.2 Fatty acids profile under nitrogen starvation	103
5.5.3 Relative quantitative analysis of glycerolipids and pigments.....	104
5.5.4 Lipid and pigment molecules alteration.....	105
5.6 Conclusions	108
5.7 Reference	110
5.8 Supplementary material.....	115
6. Conclusions and Prospective Researches.....	125
6.1 Reference	127

Abbreviation

ACN	Acetonitrile
BBM	Basal Bold Medium
BCA	BicinChoninic Acid
COR	Coronatine
DDA	Disc Diffusive Assay
DGDG	Digalactosyldiacylglycerol
DGTS	Diacylglycerolstrimethylhomoserine
DMSO	Dimethylsulfoxide
DOE	Design of Experiment
EPA	Eicosapentaenoic Acid
ESI-microTOF	Electro Spray Ionization micro Time of Flight Mass Spectrometry
ESI-MSn	Electro Spray Ionization-Tandem Mass Spectrometry
FAME	Fatty Acid Methyl Esterification
FCP	Fucoxanthin-Chl a/c protein Complex
FID	Flame Ionization Detector
GC	Gas Chromatography
HPLC	High-Performance Liquid Chromatography
H ₂ SO ₄	Sulfuric Acid
KCl	Potassium Chloride
KOH	Potassium Hydroxide
LED	Light-Emitting Diode
MALDI-TOF-MS	Matrix-Assisted Laser Desorption/Ionization-Time of Flight-Mass Spectrometry
MeJA	Methyl Jasmonate
MGDG	Monogalactosyldiacylglycerol
MIC	Minimal Inhibitory Concentration
PAR	Photosynthetic Active Radiation
PBR	Photobioreactor
PE	Polyethylene
PE	Phosphatidylethanolamines
PG	Phosphatidylglycerol
PUFA	Polyunsaturated Fatty Acid
rt	Retention time
RuBisCO	Ribulose-1,5-Biphosphate Carboxylase/Oxygenase
SA	Salicylic Acid
SDS-PAGE	Sodium Dodecyl Sulfate Polyacrylamide Gel Electrophoresis
SDS-DTT	Sodium Dodecyl Sulphate – Dithiothreitol
SQDG	Sulfoquinovosyl Diacylglycerol
TAG	Triacylglycerol
TLC	Thin-Layer Chromatography
UV	Ultra-Violet

Abstract

Aside from serving as feedstock for animal feeds, human food, and bio-diesel production, microalgae hold the promise as the reservoir of bioactive compounds for pharmaceutical and nutraceutical purposes. A variety of bioactive substances have been extracted and identified from microalgae such as fatty acids (especially long-chain polyunsaturated fatty acids), polysaccharides, polypeptides, pigments as well as polyphenols. They are found out to be active against oxidants, microbe, cancer, inflammation, and obesity. Although this topic is gaining increasing attention, mass production of microalgae-derived bioactive compounds is still restricted by several factors such as the low yield of algal biomass, the poor productivity of target compounds, immature extraction techniques, high capital and running costs, and insufficient knowledge in biosynthesis pathways.

In this thesis, several critical obstacles in the large-scale production of high-value bioactive compounds were addressed including the selection of appropriate algal species, the establishment of identification and purification methods, optimization of environmental conditions, and modification of photobioreactors. In **Chapter 3**, by using a photobioreactor greenhouse installation, continuous biomass production of the marine pennate diatom *Phaeodactylum tricornutum* Bohlin was achieved on pilot scale (3,000 L). By a recently established high-resolution chromatography method, two fractions that showed antibacterial effects against *Bacillus subtilis* were eluted, from which one was identified as pure polyunsaturated fatty acid – eicosapentaenoic acid (EPA), and the other designated as potential novel anti-bacterial compound(s). The EPA displayed more potent antibacterial effect against *B. subtilis* than a commercialized antibacterial substance. Furthermore, the obtained EPA, as well as the other antibacterial fraction, exhibited an inhibitory effect against three human pathogens: *Vibrio vulnificus*, *V. parahaemolyticus*, and *V. cholerae*. Consequently, we proposed that EPA and the raw algal biomass containing both active fractions could be used as food supplements and animal feed as an alternative to antibiotics.

Fucoxanthin is a major carotenoid in nature, known for multiple bioactive properties, particularly the anti-obesity effect. In **Chapter 4**, one benthic diatom, *Cylindrotheca closterium*, was selected from four tested species yielding the highest content of fucoxanthin and productivity. A “design of experiment” approach was employed to comprehensively determine the optimal light conditions (light source, intensity, and regime) for fucoxanthin production. Light emitting diode (LED) technology was assessed as the replacement to fluorescent light. The optimal light condition, producing maximum fucoxanthin productivity and minimizing energy consumption, was predicted to be Blue LED light, under a light regime of 18h light/6 h darkness, and light intensity of 100 $\mu\text{mol}/\text{m}^2/\text{s}$. The predicted light conditions were tested in bottle photobioreactors to prove the validity and in bag photobioreactors to estimate the viability of the mass production. The modified bag photobioreactors illuminated by LEDs produced the fucoxanthin at concentration as high as 25.5 mg/ (g in dry biomass). The light regime was observed as the most influential factor for fucoxanthin synthesis. The proteome of biomass grown under 18 h light /6 h darkness light regime was compared to that under 24 h constant light. The proteins were extracted by an optimized buffer and separated by two-dimensional gel electrophoresis based on pH and isoelectric point. Of particular note is that the differentially synthesized proteins were all annotated to be essential proteins involved in photosynthesis with the Matrix-Assisted Laser Desorption/Ionization-Time of Flight-Mass Spectrometric method.

Algal biomass is perceived as an excellent feedstock for biofuels production. The lipid, especially triacylglycerol, in algal biomass could be used to produce biodiesel. To better understand the metabolism of lipid accumulation in response to nitrogen starvation in diatoms and green algae, the lipidomes of the benthic marine diatom – *Cylindrotheca closterium* and the freshwater green alga – *Scenedesmus* sp. – were compared by an HPLC – coupled Micro-TOF mass spectrometric method in **Chapter 5**. By combining total lipids content, growth kinetics, fatty acids profiles, glycerolipids and pigment contents, and the most abundant triacylglycerols under nitrogen starvation, further light was shed onto the triacylglycerol synthesis pathways among different microalgal taxa. Nitrogen starvation for 96 h resulted in an elevated triacylglycerol content in both species.

In conclusions, the techniques developed in this project aimed to reveal the commercial feasibility of large-scale production of high-value bioactive substances and lipids. In the next step, the production performance of high-value bioactive substances will be evaluated in a scaled-up photobioreactor. Complete utilization of biomass with an underlying bio-refinery concept is imperative to eventually achieve commercialization in the future.

1. Introduction

1.1 Microalgae

Microalgae are unicellular photosynthetic microorganisms, which encompass eukaryotes and prokaryotes (Duong et al., 2012). By using light and absorbing CO₂, microalgae accumulate biomass and convert energy by photosynthesis. Mixotrophic and heterotrophic cultivation of algae were successfully carried out in several species by supplementing organic carbon sources (Perez-Garcia et al., 2011; Zhan et al., 2017). Microalgae are widely distributed in a variety of aquatic ecosystems, such as freshwater, seawater, brackish and even wastewater (Duong et al., 2012). Based on the number of species catalog in AlgaeBase (<http://www.algaebase.org>), an estimation of 72,500 species has been made, and the names for 44,000 of them have been published (Guiry, 2012). Microalgae from different taxa are incredibly diverse in morphology. Typical micrographs of microalgae from the culture collection of the OceanLab at Jacobs University Bremen are shown in **Fig. 1**. Microalgae mainly include organisms from Bacillariophyta (diatoms), Chlorophyta (green algae), Chrysophyta (golden algae) and Cyanophyta (Cyanobacteria) (Bleakley and Hayes, 2017).

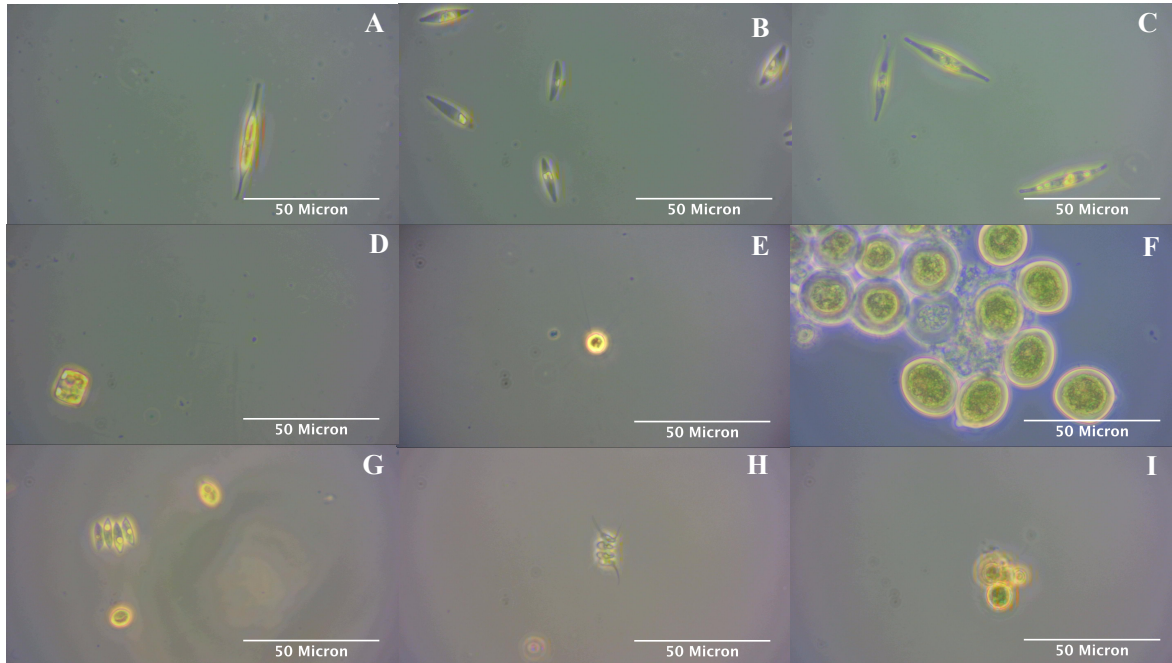


Figure 1. Micrographs of microalgae from different taxa in the culture collection of the OceanLab at Jacobs University Bremen. A: *Cylindrotheca closterium*; B: *Pheodactylum tricornerutum*; C: *Nitzschia* sp.; D: *Thalassiosira weissflogii*; E: *Micractinium* sp.; F: *Exuviaella pusilla*; G: *Scenedesmus* sp. (Israel); H: *Scenedesmus* sp. (Rotenburg); I: *Chromochloris zofingiensis*. All images were taken under a microscope at 400 x magnification.

1.2 Microalgae for human food and animal feed

It was predicted that there would be an increase of at least 50 % in global food demand by the middle of this century due to the growing global population (Royal Society of London, 2009). The rise of food production needs to be achieved in an environmentally sustainable way (Godfray et al., 2010). Microalgae could serve as the potential protein sources for human beings to face the challenge (Becker, 2007). Due to their high protein content and beneficial health effects Cyanobacteria, like *Spirulina*, are considered as foods sources (Lupatini et al., 2017). Some food products supplemented with *Spirulina* biomass, such as beverages, biscuits, puddings, etc., were recently developed in the Federal University of Rio Grande (Vaz et al., 2016). Characterized by high protein content (>50% of dry biomass) as well as excellent amino acids composition, the green algae *Chlorella* sp. is of great interest as food supplements (Becker, 2007; Bleakley and

Hayes, 2017). The exploitation of algal biomass in terms of animal feeds has also gained more popularity. The feed for chicken supplemented with *Porphyridium* sp. dry biomass resulted in a reduced level of cholesterol in serum and less food consumption, compared to the control group without supplementation (Ginzberg et al., 2000). The addition of *Laminaria digitata* into the diet of pigs could lead to an increased iodine content in meat products as well as an increase in meat production (He et al., 2002). Diatoms, like *Chaetoceros gracilis*, were considered as an essential feed for the larvae of shrimp (Chu, 1989). The possibility of the *Coccomyxa onubensis* biomass as a functional food for animals was proven by Navarro et al. (Navarro et al., 2016).

1.3 High-value bioactive compounds from microalgae

1.3.1 Carotenoids

In algae, a variety of carotenoids are synthesized either as essential components in photosynthetic apparatus or as protective tools shielding microalgae from reactive oxygen species (Grossman et al., 2004). Carotenoids with the distinct structure of 40-carbon chain as a backbone are classified into two groups: primary and secondary carotenoids (Guedes et al., 2011). As demonstrated in **Fig. 2**, pigments from *P. tricornutum* biomass were separated by a flashing column chromatography established in our lab. Currently, only several carotenoids are commercially produced in particular astaxanthin and β -carotene (Spolaore et al., 2006). Astaxanthin and β -carotene are antioxidants and their health benefits have received extensive studies summarized in previous reviews (Guerin et al., 2003; Sathasivam and Ki, 2018). Fucoxanthin, rich in diatoms and brown algae, is gaining increasing interests due to its anti-obesity (Gammone and D'Orazio, 2015), anti-oxidant (Xia et al., 2013) and anti-inflammatory properties (Heo et al., 2010). The structures of the carotenoids of commercial interests are listed in **Fig. 3**. In **Chapter 4** of this thesis, special attention was paid to prove the feasibility of commercial production of fucoxanthin.

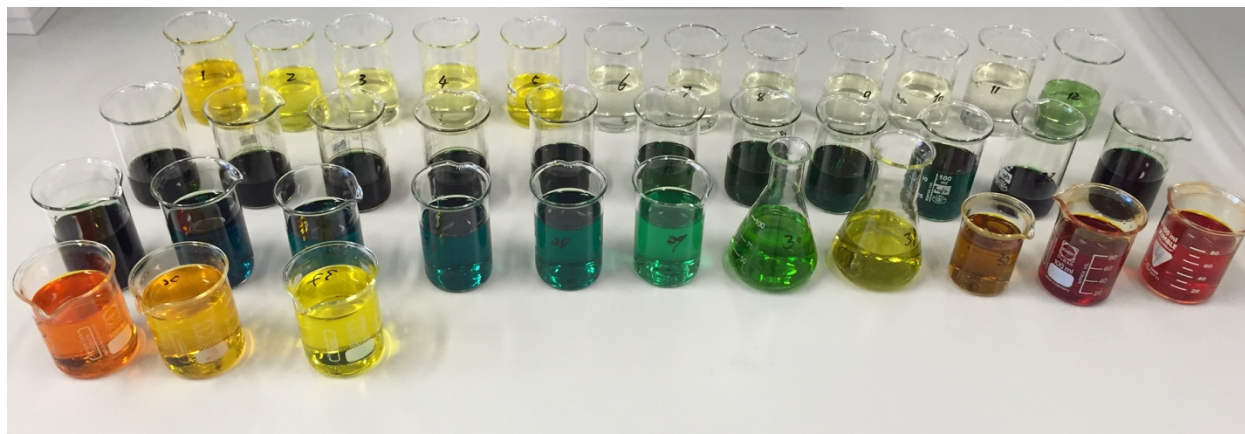


Figure 2. Pigments separated with a flash column chromatography approach from *P. tricornutum* biomass.

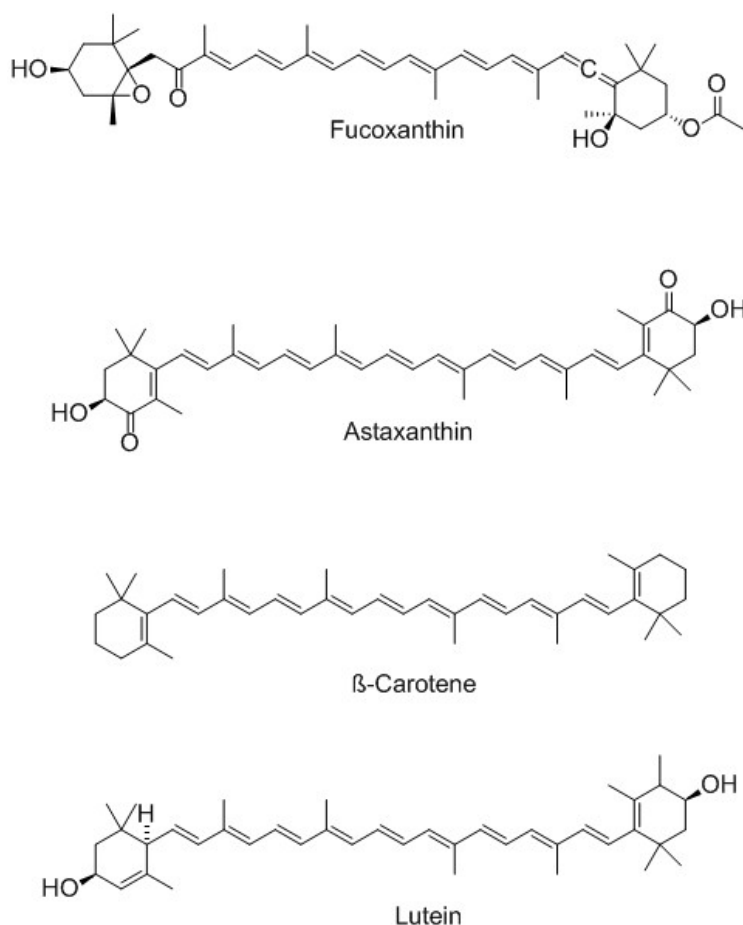


Figure 3. Structures of carotenoids of commercial interests from microalgae. The production of fucoxanthin by marine diatom was discussed in **Chapter 4**.

1.3.2 Polyunsaturated fatty acids

Polyunsaturated fatty acids (PUFAs) are essential compounds for human health. The intakes of PUFAs primarily depend on the diet (Murff and Edwards, 2014). Both EPA and docosahexaenoic acid (DHA) possess multiple health benefits. EPA is beneficial to reducing the risk of cardiovascular diseases (Ohnishi and Saito, 2013) and displays an antibacterial effect against human and animal pathogens (Desbois et al., 2008; Wang et al., 2018). DHA is an important component in the grey matter of the brain, the retina of eyes, and heart tissue (Spolaore et al., 2006). The recommended intake of EPA+DHA by the health authorities in different countries

ranges from 200 to 680 mg/d for adults (Ian Givens and Gibbs, 2008). EPA and DHA are synthesized in a high percentage from total fatty acids of marine microalgae. *P. tricornutum* could accumulate EPA up to 4.4 % of the dry biomass cultivated in an outdoor photobioreactor system (Steinrucken et al., 2018). *Nannochloropsis* has been considered as another excellent producer of EPA in many studies, where different experimental conditions were applied to induce its maximum productivity (Chen et al., 2015; Shene et al., 2016). A previous study selected one strain of *Isochrysis galbana* from 19 candidates as a potential producer of DHA, with the productivity of DHA reaching 13.6 mg/L/d in an outdoor bioreactor (Liu et al., 2013).

1.3.3 Other bioactive compounds

Various phytosterols have been identified in microalgae, which could be potentially used as equivalents of plant-derived phytosterols for healthcare and pharmaceutical use (Luo et al., 2015). Sterol extract of *Schizochytrium* sp. displayed cholesterol level-lowering activity in hamsters (Chen et al., 2014). Anti-inflammatory and anti-cancer effects were observed in the sterol-containing fraction from the marine microalgae *Nannochloropsis oculata* (Sanjeeva et al., 2016). Marine algae are an attractive source for bioactive peptides, which show multiple health benefits after hydrolysis (Fan et al., 2014). A polypeptide isolated after extraction and hydrolysis in a green alga, *C. pyrenoidosa*, displayed inhibitory effect on cancer cells (Wang and Zhang, 2013). Peptides showing antioxidant activity were purified in the marine green algae *C. vulgaris* in previous studies (Sheih et al., 2009). Apart from lipids and proteins, marine microalgae are producers of extracellular polysaccharides (EPS), which exhibited several bioactive benefits including antiviral effect. EPS showing an antiviral effect were mainly found in cyanobacteria, rhodophytes, dinoflagellates (de Jesus Raposo et al., 2013; Rwehumbiza et al., 2014). A sulfated polysaccharide found by ultrafiltration in the medium of *Arthrospira platensis* displayed an anticoagulant effect (Majdoub et al., 2009).

1.4 Microalgae as feedstock for biofuel production

It was proposed that the continually growing human population results in a 50 % increase in energy consumption by 2030 (Maness et al., 2009). Harmful effects of the overuse of fossil fuels and their

limited availability emphasize the need for renewable energy sources. Biofuels are recognized as a replacement for fossil fuels (Milano et al., 2016). Biofuels, such as bio-diesel and bio-ethanol, are sustainable energy carriers, which can be used in the current engines of vehicles with minor modification as substitutions of diesel and gasoline (Mata et al., 2010). However, the first and second generations of biofuels with crops and non-edible plants as feedstocks were constrained by the limited amount of arable land (Mubarak et al., 2015). Microalgae as the feedstock for biofuel production outcompete first and second generations of fuels due to multiple advantages such as higher photosynthetic efficiency, higher biomass productivity, lipid content and simple requirements for nutrients (Li et al., 2008; Mata et al., 2010). Nevertheless, so far the commercialization of microalgal biofuels has been hindered by the high costs and environmental impacts (Singh et al., 2017). Meanwhile, various of techniques and approaches have been put forward to cut down the cost of the mass production of biofuels from microalgae biomass (Barry et al., 2015). Furthermore, the energy and carbon equilibrium, along with the impact upon environment also determines the fate of microalgal biofuels, as reviewed by Slade and Bauen (Slade and Bauen, 2013).

Among the steps in microalgae-based bio-diesel production, lipid extraction was proposed to contribute a lot to the overall costs (Iqbal and Theegala, 2013; Mubarak et al., 2015). The most commonly used techniques are organic solvents and supercritical fluid extraction (Lee et al., 2010; Santana et al., 2012). Although extraction methods based on chloroform are effective, the toxicity of chloroform hampers its application (Halim et al., 2011). Mixtures of dichloromethane/methanol and n-hexane/isopropanol were tried as substitutions for chloroform and methanol (Cequier-Sánchez et al., 2008; Halim et al., 2011). The lipid extraction with supercritical CO₂ has been tested in several species, thereby avoiding the use of the toxic organic solvents (Santana et al., 2012). The performance of lipid extraction could be improved with a cell disruption process, which usually involves ultra-sonication, microwave, and bead mill (Halim et al., 2012).

1.5 Photobioreactor (PBR)

A variety of closed PBRs were designed to provide an accurately controlled environment and effectively prevent the occurrence of contamination with additional benefits such as low water evaporation rate and high photosynthetic efficiency as reviewed by Huang et al. (Huang et al., 2017). The currently available photobioreactors can be categorized into four types, namely: adapted column PBR (**Fig. 4**, designed in OceanLab, Jacobs University Bremen), tubular PBR (Torzillo and Chini Zittelli, 2015), flat PBR (Huang et al., 2014) and bag PBR (**Fig. 5**, patented by Phytolutions, Bremen, Germany). Although higher biomass productivities compared to open pond system were obtained in closed PBRs, their exploitation is still restricted by high operation cost as well as investment (Posten, 2009). Column PBRs are usually equipped with air spargers to generate air bubbles for mixing. The radius and the height of a column PBR are limited up to 0.2 m and to 4 m respectively to achieve a high surface/volume ratio and gas transfer efficiency (Wang et al., 2012). One promising solution to increase the light distribution is to use an internal LED light system as shown in **Fig. 4**. However, this modification inevitably increased both running and operational cost. Therefore, despite a high gas exchange rate in the column PBRs, their applications are limited by the high investment and large efforts for maintenance. Tubular PBRs are characterized by large surface area for light penetration, but the drawbacks are also evident, for instance, high initial investment and subsequently high running costs, O₂ accumulation, and laborious cleaning procedure, as are reviewed by Huang et al. (Huang et al., 2017). Flat-plate PBRs feature for high photosynthetic efficiency owing to high surface-volume-ratio and short light penetration path but the high capital costs (Huang et al., 2017). The performance of the bag PBR patented by Phytolutions was tested in a 500 m² pilot plant with controlled temperature and pH, with the goal to reduce costs to 25 €/m² (Thomsen et al., 2012). Therefore, we perceive vertical bag PBRs as a promising way for mass production with regards to the robustness, low cost, long lifespan, and expandability.

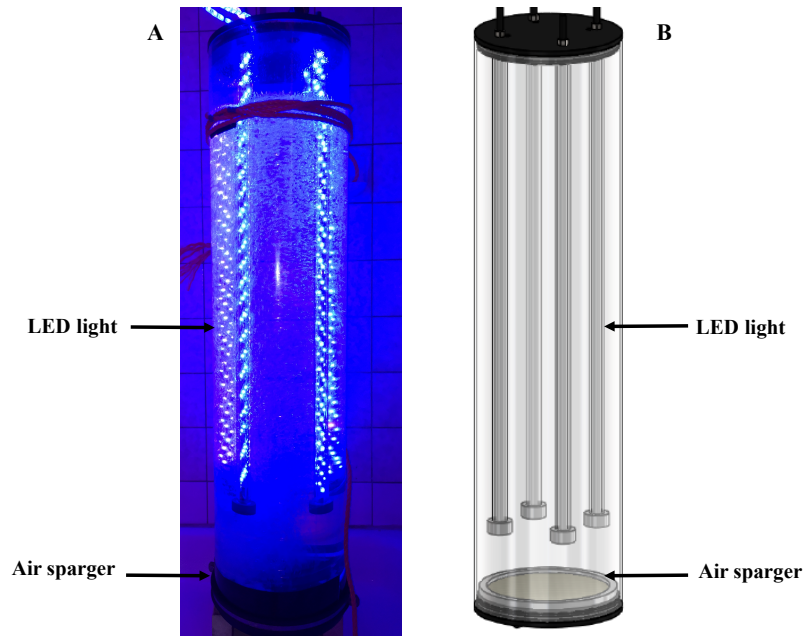


Figure 4. Column PBR designed in OceanLab with LEDs providing illumination. A: the picture of the real PBR; B: the schematic picture of the PBR.



Figure 5. Project Aufwind/Jülich: Phytoplant (500m²) installation with the objective bio-kerosene and byproducts

1.6 Reference

- Barry, A.N., Starkenburg, S.R. and Sayre, R.T. (2015) Strategies for optimizing algal biology for enhanced biomass production. *Frontiers in Energy Research* **3**.
- Becker, E.W. (2007) Micro-algae as a source of protein. *Biotechnology Advances* **25**, 207-210.
- Bleakley, S. and Hayes, M. (2017) Algal proteins: Extraction, application, and challenges concerning production. *Foods (Basel, Switzerland)* **6**.
- Cequier-Sánchez, E., Rodríguez, C., Ravelo, Á.G. and Zárata, R. (2008) Dichloromethane as a solvent for lipid extraction and assessment of lipid classes and fatty acids from samples of different natures. *Journal of Agricultural and Food Chemistry* **56**, 4297-4303.
- Chen, C.Y., Chen, Y.C., Huang, H.C., Ho, S.H. and Chang, J.S. (2015) Enhancing the production of eicosapentaenoic acid (EPA) from *Nannochloropsis oceanica* CY2 using innovative photobioreactors with optimal light source arrangements. *Bioresource Technology* **191**, 407-413.
- Chen, J., Jiao, R., Jiang, Y., Bi, Y. and Chen, Z.Y. (2014) Algal sterols are as effective as beta-sitosterol in reducing plasma cholesterol concentration. *Journal of Agricultural and Food Chemistry* **62**, 675-681.
- Chu, K.H. (1989) *Chaetoceros gracilis* as the exclusive feed for the larvae and postlarvae of the shrimp *Metapenaeus ensis*. *Aquaculture* **83**, 281-287.
- de Jesus Raposo, M.F., de Morais, R.M.S.C. and Bernardo de Morais, A.M.M. (2013) Bioactivity and applications of sulphated polysaccharides from marine microalgae. *Marine Drugs* **11**, 233-252.
- Desbois, A.P., Lebl, T., Yan, L. and Smith, V.J. (2008) Isolation and structural characterisation of two antibacterial free fatty acids from the marine diatom, *Phaeodactylum tricornutum*. *Applied Microbiology and Biotechnology* **81**, 755-764.
- Duong, V.T., Li, Y., Nowak, E. and Schenk, P.M. (2012) Microalgae isolation and selection for prospective biodiesel production. *Energies* **5**, 1835-1849.
- Fan, X., Bai, L., Zhu, L., Yang, L. and Zhang, X. (2014) Marine algae-derived bioactive peptides for human nutrition and health. *Journal of Agricultural and Food Chemistry* **62**, 9211-9222.
- Gammone, M.A. and D'Orazio, N. (2015) Anti-obesity activity of the marine carotenoid fucoxanthin. *Marine Drugs* **13**, 2196-2214.

- Ginzberg, A., Cohen, M., Sod-Moriah, U.A., Shany, S., Rosenshtrauch, A. and Arad, S. (2000) Chickens fed with biomass of the red microalga *Porphyridium* sp. have reduced blood cholesterol level and modified fatty acid composition in egg yolk. *Journal of Applied Phycology* **12**, 325-330.
- Godfray, H.C.J., Beddington, J.R., Crute, I.R., Haddad, L., Lawrence, D., Muir, J.F., Pretty, J., Robinson, S., Thomas, S.M. and Toulmin, C. (2010) Food security: The challenge of feeding 9 billion people. *Science* **327**, 812-818.
- Grossman, A.R., Lohr, M. and Im, C.S. (2004) *Chlamydomonas reinhardtii* in the landscape of pigments. *Annual review of genetics* **38**, 119-173.
- Guedes, A.C., Amaro, H.M. and Malcata, F.X. (2011) Microalgae as sources of carotenoids. *Marine Drugs* **9**, 625-644.
- Guerin, M., Huntley, M.E. and Olaizola, M. (2003) Haematococcus astaxanthin: applications for human health and nutrition. *Trends in Biotechnology* **21**, 210-216.
- Guiry, M. (2012) How many species of algae are there? *Journal of Phycology* **48**, 1057-1063.
- Halim, R., Danquah, M.K. and Webley, P.A. (2012) Extraction of oil from microalgae for biodiesel production: A review. *Biotechnology Advances* **30**, 709-732.
- Halim, R., Gladman, B., Danquah, M.K. and Webley, P.A. (2011) Oil extraction from microalgae for biodiesel production. *Bioresource Technology* **102**, 178-185.
- He, M.L., Hollwich, W. and Rambeck, W.A. (2002) Supplementation of algae to the diet of pigs: a new possibility to improve the iodine content in the meat. *Journal of Animal Physiology and Animal Nutrition* **86**, 97-104.
- Heo, S.J., Yoon, W.J., Kim, K.N., Ahn, G.N., Kang, S.M., Kang, D.H., Affan, A., Oh, C., Jung, W.K. and Jeon, Y.J. (2010) Evaluation of anti-inflammatory effect of fucoxanthin isolated from brown algae in lipopolysaccharide-stimulated RAW 264.7 macrophages. *Food and Chemical Toxicology* **48**, 2045-2051.
- Huang, J., Li, Y., Wan, M., Yan, Y., Feng, F., Qu, X., Wang, J., Shen, G., Li, W., Fan, J. and Wang, W. (2014) Novel flat-plate photobioreactors for microalgae cultivation with special mixers to promote mixing along the light gradient. *Bioresource Technology* **159**, 8-16.
- Huang, Q., Jiang, F., Wang, L. and Yang, C. (2017) Design of photobioreactors for mass cultivation of photosynthetic organisms. *Engineering* **3**, 318-329.

- Ian Givens, D. and Gibbs, R.A. (2008) Current intakes of EPA and DHA in European populations and the potential of animal-derived foods to increase them. *Proceedings of the Nutrition Society* **67**, 273-280.
- Iqbal, J. and Theegala, C. (2013) Microwave assisted lipid extraction from microalgae using biodiesel as co-solvent. *Algal Research* **2**, 34-42.
- Lee, J.Y., Yoo, C., Jun, S.Y., Ahn, C.Y. and Oh, H.M. (2010) Comparison of several methods for effective lipid extraction from microalgae. *Bioresource Technology* **101**, S75-S77.
- Li, Y., Horsman, M., Wu, N., Lan, C.Q. and Dubois-Calero, N. (2008) Biofuels from microalgae. *Biotechnology Progress* **24**, 815-820.
- Liu, J., Sommerfeld, M. and Hu, Q. (2013) Screening and characterization of *Isochrysis* strains and optimization of culture conditions for docosahexaenoic acid production. *Applied Microbiology and Biotechnology* **97**, 4785-4798.
- Luo, X., Su, P. and Zhang, W. (2015) Advances in microalgae-derived phytosterols for functional food and pharmaceutical applications. *Marine Drugs* **13**, 4231-4254.
- Lupatini, A.L., Colla, L.M., Canan, C. and Colla, E. (2017) Potential application of microalga *Spirulina platensis* as a protein source. *Journal of the Science of Food and Agriculture* **97**, 724-732.
- Majdoub, H., Ben Mansour, M., Chaubet, F., Roudesli, M.S. and Maaroufi, R.M. (2009) Anticoagulant activity of a sulfated polysaccharide from the green alga *Arthrospira platensis*. *Biochimica et Biophysica Acta* **1790**, 1377-1381.
- Maness, P., Yu, J., Eckert, C. and Ghirardi, M. (2009) Photobiological hydrogen production – prospects and challenges efforts to scale up the capacity of green algae and cyanobacteria to use sunlight to convert water into hydrogen gas for energy use. *Microbe* **4**, 275–280.
- Mata, T.M., Martins, A.A. and Caetano, N.S. (2010) Microalgae for biodiesel production and other applications: A review. *Renewable and Sustainable Energy Reviews* **14**, 217-232.
- Milano, J., Ong, H.C., Masjuki, H.H., Chong, W.T., Lam, M.K., Loh, P.K. and Vellayan, V. (2016) Microalgae biofuels as an alternative to fossil fuel for power generation. *Renewable and Sustainable Energy Reviews* **58**, 180-197.
- Mubarak, M., Shaija, A. and Suchithra, T.V. (2015) A review on the extraction of lipid from microalgae for biodiesel production. *Algal Research* **7**, 117-123.

- Murff, H.J. and Edwards, T.L. (2014) Endogenous production of long-chain polyunsaturated fatty acids and metabolic disease risk. *Current Cardiovascular Risk Reports* **8**.
- Navarro, F., Forján, E., Vázquez, M., Montero, Z., Bermejo, E., Castaño, M.Á., Toimil, A., Chagüaceda, E., García-Sevillano, M.Á., Sánchez, M., Domínguez, M.J., Pásaro, R., Garbayo, I., Vílchez, C. and Vega, J.M. (2016) Microalgae as a safe food source for animals: nutritional characteristics of the acidophilic microalga *Coccomyxa onubensis*. *Food & Nutrition Research* **60**, 30472.
- Ohnishi, H. and Saito, Y. (2013) Eicosapentaenoic acid (EPA) reduces cardiovascular events-relationship with the EPA:arachidonic acid ratio. *Journal of Atherosclerosis and Thrombosis* **20**, 861-877.
- Perez-Garcia, O., Escalante, F.M., de-Bashan, L.E. and Bashan, Y. (2011) Heterotrophic cultures of microalgae: metabolism and potential products. *Water Research* **45**, 11-36.
- Posten, C. (2009) Design principles of photo-bioreactors for cultivation of microalgae. *Engineering in Life Sciences* **9**, 165-177.
- Royal Society of London (2009) Reaping the benefits: Science and the sustainable intensification of global agriculture.
- Rwehumbiza, V.M., Vennapusa, R.R., Gavara, P.R., Fernández-Lahore, H.M., Al-Karablieh, N., Ullrich, M.S. and Thomsen, C. (2014) Potential of fibrous adsorbents for the binding and characterization of *Porphyridium purpureum* bioactive polysaccharides. *Journal of Chemical Technology & Biotechnology* **89**, 65-72.
- Sanjeeva, K.K.A., Fernando, I.P.S., Samarakoon, K.W., Lakmal, H.H.C., Kim, E.-A., Kwon, O.N., Dilshara, M.G., Lee, J.-B. and Jeon, Y.-J. (2016) Anti-inflammatory and anti-cancer activities of sterol rich fraction of cultured marine microalga *Nannochloropsis oculata*. *Algae* **31**, 277-287.
- Santana, A., Jesus, S., Larrayoz, M.A. and Filho, R.M. (2012) Supercritical carbon dioxide extraction of algal lipids for the biodiesel production. *Procedia Engineering* **42**, 1755-1761.
- Sathasivam, R. and Ki, J.S. (2018) A review of the biological activities of microalgal carotenoids and their potential use in healthcare and cosmetic industries. *Marine Drugs* **16**.
- Sheih, I.C., Wu, T.K. and Fang, T.J. (2009) Antioxidant properties of a new antioxidative peptide from algae protein waste hydrolysate in different oxidation systems. *Bioresource Technology* **100**, 3419-3425.

- Shene, C., Chisti, Y., Vergara, D., Burgos-Diaz, C., Rubilar, M. and Bustamante, M. (2016) Production of eicosapentaenoic acid by *Nannochloropsis oculata*: Effects of carbon dioxide and glycerol. *Journal of Biotechnology* **239**, 47-56.
- Singh, K., Kaloni, D., Gaur, S., Kushwaha, S. and Mathur, G. (2017) Current research and perspectives on microalgae-derived biodiesel. *Biofuels*.
- Slade, R. and Bauen, A. (2013) Micro-algae cultivation for biofuels: Cost, energy balance, environmental impacts and future prospects. *Biomass Bioenergy*. **53**, 29-38.
- Spolaore, P., Joannis-Cassan, C., Duran, E. and Isambert, A. (2006) Commercial applications of microalgae. *Journal of Bioscience and Bioengineering* **101**, 87-96.
- Steinrucken, P., Prestegard, S.K., de Vree, J.H., Storesund, J.E., Pree, B., Mjos, S.A. and Erga, S.R. (2018) Comparing EPA production and fatty acid profiles of three *Phaeodactylum tricornutum* strains under western Norwegian climate conditions. *Algal Research* **30**, 11-22.
- Thomsen, C., Rill, S. and Thomsen, L. (2012) Case study with temperature controlled outdoor PBR system in Bremen. In: Posten, C, Walter C, editors. *Microalgal biotechnology: integration and economy, Chapter 4*. Berlin, Boston: De Gruyter **74-77**.
- Torzillo, G. and Chini Zittelli, G. (2015) Tubular photobioreactors. In: *Algal Biorefineries: Volume 2: Products and Refinery Design* (Prokop, A., Bajpai, R.K. and Zappi, M.E. eds), pp. 187-212. Cham: Springer International Publishing.
- Vaz, B.d.S., Moreira, J.B., Morais, M.G.d. and Costa, J.A.V. (2016) Microalgae as a new source of bioactive compounds in food supplements. *Current Opinion in Food Science* **7**, 73-77.
- Wang, B., Lan, C.Q. and Horsman, M. (2012) Closed photobioreactors for production of microalgal biomasses. *Biotechnology Advances* **30**, 904-912.
- Wang, S., Hakeem Said, I., Thorstenson, C., Thomsen, C., Ullrich, M.S., Kuhnert, N. and Thomsen, L. (2018) Pilot-scale production of antibacterial substances by the marine diatom *Phaeodactylum tricornutum* Bohlin. *Algal Research* **32**, 113-120.
- Wang, X. and Zhang, X. (2013) Separation, antitumor activities, and encapsulation of polypeptide from *Chlorella pyrenoidosa*. *Biotechnology Progress* **29**, 681-687.
- Xia, S., Wang, K., Wan, L., Li, A., Hu, Q. and Zhang, C. (2013) Production, characterization, and antioxidant activity of fucoxanthin from the marine diatom *Odontella aurita*. *Marine Drugs* **11**, 2667-2681.

Zhan, J., Rong, J. and Wang, Q. (2017) Mixotrophic cultivation, a preferable microalgae cultivation mode for biomass/bioenergy production, and bioremediation, advances and prospect. *International Journal of Hydrogen Energy* **42**, 8505-8517.

2. Aims of the Ph.D. study

Given to the fact that microalgae could serve as a reservoir of bioactive compounds, the study was designed to discover novel bioactive compounds from marine microalgae. The selection of appropriate species was the first step in each project. The methods of identification and quantification of the target compounds were established subsequently. Optimal conditions were determined to induce maximum productivity of the high-value bioactive substance. Last but not least, the performance of production was estimated in vertical bag PBRs to assess the viability of large-scale production. The cultivation of *P. tricornutum* in **Chapter 3** was carried out in a closed PBR with a volume of 3,000 L. The next step would be the cultivation of the algae in PBRs with a volume up to $2\text{-}50 \times 10^3$ L. The three projects in this thesis with different target products were performed with the aims mentioned above.

Due to the abuse of antibiotics, more and more bacteria strains evolved tolerance to antibiotics. Therefore, the development of alternatives to antibiotics became urgent for humans. Moreover, the prohibited use of antibiotics in animal feed in Europe also necessitates the alternatives. For this reason, the **objective** of **Chapter 3** was to discover alternatives to antibiotics from marine microalgae. The cellular extract of *P. tricornutum* exhibited antibacterial effect against *Bacillus subtilis* in preliminary experiment. Thus, *P. tricornutum* was chosen as the candidate to purify and identify the antibacterial compounds. Furthermore, we expected to achieve continuous cultivation of *P. tricornutum* in pilot-scale vertical bag PBRs and established the methods to purify and identify antibacterial compounds. Besides, the antibacterial effects of the obtained substances were compared with a commercial antibacterial product and antibiotics. Their inhibitory effect against pathogenic *Vibrio* species was also estimated by determining the minimal inhibitory concentrations. The attempt of increasing the production of the target compounds was performed by the induction of phytohormones and phytotoxin.

Fucoxanthin as an accessory pigment in photosystems of brown algae and diatom is known for potent bioactive effects and health benefits, such as anti-oxidative and anti-obesity effects. Brown algae as the current feedstock for fucoxanthin production accumulate much less fucoxanthin in

biomass compared to marine diatoms (Xia et al., 2013). Hence, the **objective** of **Chapter 4** was to select the best diatom producing the highest fucoxanthin productivity. Subsequently, light conditions were optimized by a “Design of Experiment” method. The application of LED light in inducing fucoxanthin synthesis was assessed. The fucoxanthin productivity of the diatom in a modified bag PBR towards large-scale production was measured. The regulatory mechanism of fucoxanthin synthesis was dissected by the comparative proteomic analyses of diatoms grown under favorable and unfavorable conditions.

Nitrogen starvation has been proved to be an effective way to induce lipid accumulation in algae and generate phenotypic differences for the study of lipogenesis (Zhu et al., 2016). Therefore, in **Chapter 5**, the **objective** was to elucidate the regulatory and mediatory mechanisms of lipid accumulation induced by nitrogen starvation in two species of oleaginous algae. *Scenedesmus* sp. belongs to Chlorophyceae while *C. closterium* is a benthic diatom (Bacillariophyceae). Algae cultured in bag PBRs were exposed to nitrogen starvation. A time-series lipidomic analysis was conducted to both algae by a time of flight MicrOTOF Focus mass spectrometer. The changes in glycerolipids were determined at the molecular level in both species along with the changes in growth kinetics, total lipids and fatty acids profiles at different time points during nitrogen starvation.

2.1 Reference

Xia, S., Wang, K., Wan, L., Li, A., Hu, Q. and Zhang, C. (2013) Production, characterization, and antioxidant activity of fucoxanthin from the marine diatom *Odontella aurita*. *Marine Drugs* **11**, 2667-2681.

Zhu, L.D., Li, Z.H. and Hiltunen, E. (2016) Strategies for lipid production improvement in microalgae as a biodiesel feedstock. *BioMed Research International*, 8792548.

**3 Pilot-scale production of antibacterial substances by the marine diatom
Phaeodactylum tricornutum Bohlin**

Manuscript was published in *Algal Research* **32** (2018), 113-120.

<https://doi.org/10.1016/j.algal.2018.03.014>

Song Wang^{1*}, Inamullah Hakeem Said², Candice Thorstenson², Claudia Thomsen³, Matthias S. Ullrich², Nikolai Kuhnert², Laurenz Thomsen¹

¹Department of Physics and Earth Sciences, Jacobs University Bremen, Campus Ring 1, 28759 Bremen, Germany

²Department of Life Science and Chemistry, Jacobs University Bremen, Campus Ring 1, 28759 Bremen, Germany

³Phytolutions GmbH, Campus Ring 1, 28759 Bremen, Germany.

*Corresponding author: Song Wang, s.wang@jacobs-university.de

3.1 Abstract

The production and extraction of antibacterial substances from *Phaeodactylum tricornerutum* biomass were tested on a pilot scale in a photo-bioreactor greenhouse installation. Using column chromatography two antibacterial active fractions were obtained from the algal biomass: a pure fraction of eicosapentaenoic acid (EPA) and a potentially new antibacterial substance(s) (identified as fraction B) produced by *P. tricornerutum*. Both fractions exhibited antibacterial activities against three human pathogens: *Vibrio vulnificus*, *V. parahaemolyticus*, and *V. cholerae*. Minimal inhibitory concentrations against *Bacillus subtilis* of active fractions and one antibacterial commercial product were determined revealing a higher antibacterial activity of EPA in comparison to the commercial product. Consequently, EPA as well as the raw algal biomass with both EPA and the fraction B compounds could be used as food additives and feeds in aquaculture, poultry, and livestock breeding. Two types of phytohormones, methyl jasmonate and salicylic acid, as well as one phytotoxin, coronatine, were tested for induction of the defense system of *P. tricornerutum*. However, only a minor change in the fatty acids profile and antibacterial effects of the treated cultures indicated that *P. tricornerutum* must employ another strategy to regulate its antibacterial defense system.

Keywords: Pilot-scale; Antibacterial substance; Eicosapentaenoic acid; Pathogen; Inducibility

3.2 Introduction

Microalgae are ubiquitously distributed and have the ability to adapt to various environmental factors such as temperature, salinity, moisture, photo-oxidation and ultra-violet (UV) light (Duong et al., 2015; Tandeau de Marsac and Houmard, 1993). Due to their high growth rate, ease of cultivation, and production of diverse bioactive substances, microalgae have been proposed as additives for feedstock, medicines, cosmetic products or biodiesel production (Hu et al., 2008; Kay, 1991; Shannon and Abu-Ghannam, 2016). The amount of novel marine natural compounds identified is increasing with > 1300 reported in 2014 (Blunt et al., 2016). Hence, microalgae, especially marine diatoms, have great potential in the search for novel bioactive secondary metabolites (Daniel, 2016; Kellam and Walker, 1989; Singh, 2005).

The marine pennate diatom *Phaeodactylum tricornerutum* Bohlin (genome sequence available) has been used as a model organism in biochemical, physiological and genetic studies of marine diatoms (Bowler et al., 2008; Jallet et al., 2016). The eicosapentaenoic acid (EPA) fraction from the methanol/water extract of *P. tricornerutum* has proved to be antibacterial against *Staphylococcus aureus* (Desbois et al., 2009). Different morphotypes of *P. tricornerutum* exhibit different antibacterial effects against marine bacteria and potential human and animal pathogens, with the antibacterial substances being identified as (9Z)-hexadecenoic acid and (6Z, 9Z, 12Z)-hexadecatrienoic acid and eicosapentaenoic acid (EPA) (Desbois et al., 2008).

The concerted biosynthesis and accumulation of phytohormones such as methyl jasmonate (MeJA), salicylic acid (SA) and ethylene play a crucial role in signaling plants to produce antimicrobial substances. The signaling mechanism of these phytohormones has been well studied in plants (Han, 2017; Reymond and Farmer, 1998; Xie et al., 1998). However, insufficient research has focused on the interaction between marine phytoplankton and bacteria (Amin et al., 2015). Interactions between algae and bacteria, dominated by the exchange of signaling molecules, substantially impact primary production and nutrient cycling in marine ecology (Seymour et al., 2017). Therefore, the search for signaling compounds that regulate antibacterial compound production in *P. tricornerutum*, as a model organism, is of great importance. Ultimately, more knowledge on this may also shed light on the evolution of plant-like immunity in the marine environment. The synthesis of secondary metabolites in the marine brown algae, *Laminaria digitate*, is induced by arachidonic acid and MeJA (Küpper et al., 2009). Furthermore, the addition of arachidonic acid was reported to have altered the fatty acid profile and the level of hydroxylated fatty acid derivatives. In contrast to brown algae, the defense systems and their induction in marine diatoms has not been as well studied. Antibiotic discovery is not very frequent these days, although there is an extreme need for new antimicrobials for clinical use and animal feed. Considering this fact, the aims of this study were to identify the antimicrobial substances, especially against human and animal pathogenic *Vibrio* species from *P. tricornerutum* biomass, to compare their efficacy with that of a commercial natural antibiotic substitute for animal feed production and to induce stress by phytohormones for increased production of such substances.

3.3 Materials and Methods

3.3.1 Microalgal species and cultivation conditions

Phaeodactylum tricornerutum was purchased from the Culture Collection of Algae (EPSAG), Goettingen University, Germany [<http://www.uni-goettingen.de/en/45175.html>]. *P. tricornerutum* stock culture was maintained in f/2 artificial seawater medium without silicates (Guillard, 1975). All chemical reagents were purchased from AppliChem (AppliChem GmbH, Darmstadt, Germany). Artificial seawater was prepared, filtrated using 0.2 µm filter cups (Merck Chemicals GmbH, Darmstadt, Germany), and autoclaved. Stock culture was cultivated in an incubator with light intensity of 50 µmol/s/m², and the temperature was maintained at 20 °C. *P. tricornerutum* was inoculated in 30-L phytobag photo-bioreactor, developed by Phytolutions GmbH (IP-rights patented), as the starter culture for the pilot plant with continuous 30-L/min air supply through a tube and light by 58W fluorescence lamps (Osram, Munich, Germany) at 75 µmol/s/m².

3.3.2 Photo-bioreactor (PBR)

The PBR was composed of four major components (**Fig. 1**). Twenty specially-designed polyethylene (PE) phytobags (4-meter long and 1.5-meter high, volume 150 L each) were connected to a circulation system driven by a peristaltic pump (Axflow, London, United Kingdom). A heat exchange system was integrated into the circulation system, which is designed for winter or summer production to maintain the temperature in a suitable range for growth of *P. tricornerutum* (between 18 and 24 °C). Aeration was provided by an air pump coupled to micro-bubble air tubes in the bottom of each PE bags. Carbon dioxide supply for pH control was achieved by an automatic valve, which was opened when the pH in algal solution exceeded the threshold of 7.8 as measured by a pH sensor. The pilot plant was located at a greenhouse at 8°39'1" E and 53°9'53" N in the OceanLab facility of Jacobs University Bremen, Germany under natural abiotic conditions. Thus, environmental conditions such as light and temperature in the PBR fluctuated on a regular basis.

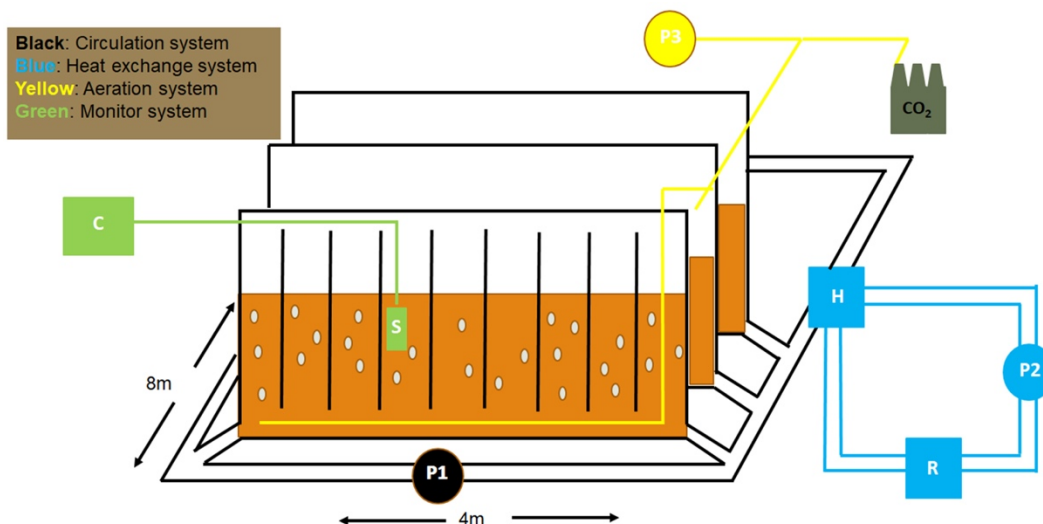


Figure 1. Sketch of the pilot plant. P1: Main pump in circulation system; P2: Pump in heat exchange system; H: heat exchanger; R: cooling/heating water reservoir; P3: air pump; S: temperature and pH sensors; C: control of sensors; CO₂: CO₂ bottles.

3.3.3 Growth kinetics and biomass productivity

Algal growth was monitored daily by measuring the culture's optical density at 750 nm with a spectrophotometer (Biochrom, Cambridge, United Kingdom). A calibration curve reflecting the correlation of OD₇₅₀ value (Brembu et al., 2017) and dry biomass concentration (g/L) was generated to calculate the biomass productivity (g/L/d) (**Fig. S1**). Biomass concentration was determined by filtering 10 mL of the algal solution on microfiber GF/F 47 mm filter (Whatman, Maidstone, United Kingdom), drying of the filter in an oven at 60 °C for 24 h, and subsequent weighing (Zhu and Lee, 1997).

3.3.4 Preparation of crude extract of *P. tricornutum*

After lyophilization using an Alpha 1-2 LD plus lyophilizer (Christ, Osterode, Germany), 6 g of dry biomass was mixed with 72 mL 100% methanol for 10 min and subsequently centrifuged at 1512 g. This step was repeated twice and the three supernatants were collected after centrifugation. The supernatant was evaporated by a rotary evaporator (Heidolph, Schwabach, Germany)

equipped with a PC500 vacuum pump (Vacuubrand, Wertheim, Germany) at 90 mbar and 40 °C. Crude extracts were stored at -20 °C for later chromatography.

3.3.5 Flash column and thin-layer chromatography

Column chromatography was performed using silica gel 60 (0.040-0.063 mm). Ethyl acetate (boiling point of 77 °C) and petroleum ether (boiling point range of 40-60 °C) were used as a mobile phase for column chromatography. Purification was achieved with the flash column chromatography under gradient linearly increasing elution using ethyl acetate and petroleum ether (0:100-25:75, EtOAc/pet ether). Thin-layer chromatography (TLC) was carried out for the antimicrobial active fractions using silica gel 60 F254 pre-coated plates and visualized under UV irradiation (254 nm). A total of 27 different fractions of 25 mL each were collected; which ended up with 14 fractions after TLC (designated as A-N). All fractions were dried by a rotary evaporator, resuspended in 500 µL DMSO, and examined for antibacterial activity in three replicates.

3.3.6 Disc diffusive assay and minimal inhibitory concentration (MIC)

Bacillus subtilis was streaked onto Lysogeny broth (LB) agar plates, which were subsequently incubated at 28 °C for 24 h. Bacterial colonies were picked, resuspended in LB broth and diluted to an OD₆₀₀ of 0.1. The bacterial solution was uniformly spread onto the LB agar plates using sterile glass beads. 7 mm GF/F filters (Whatman, Maidstone, United Kingdom) were put onto the LB agar plates seeded with the bacteria. 30 µL of each column chromatography fraction were pipetted onto the filters with an equivalent volume of dimethylsulfoxide (DMSO) as a negative control. After 24 h of incubation at 28 °C, the diameters of inhibition zone were measured by photography and subsequent analysis using ImageJ (<https://imagej.nih.gov/ij/>) to assess the antibacterial activity. Active chromatography fractions were subjected to mass spectroscopy. The susceptibility of six strains of potentially human-pathogenic *Vibrio* species to the active chromatography fractions was assessed in the same way but on Marine Broth (MB) agar plates (5g peptone, 1g yeast extract, 0.1 g FePO₄, 750 mL filter-sterilized North Sea water, 250 mL distilled water, 12 g agar, pH 7.6). The MICs against *B. subtilis* of two active fractions, EPA standard (marine-sourced, ≥98.5%, Sigma Aldrich, St. Louis, USA), a commercial antibacterial substance,

and two antibiotics were determined in 96-well plates, in duplicates, with the antibiotics, ampicillin and gentamycin, used as positive controls.

3.3.7 Electro spray Ionization-Tandem Mass Spectrometry (ESI-MSn) and micro Time of Flight Mass Spectrometry (ESI-microTOF).

The Ion-trap mass spectrometer fitted with an ESI source (Bruker Daltonics HCT Ultra, Bremen, Germany) operating in full scan auto MSn (tandem MS in series) mode to obtain fragment ions. Tandem mass spectra were acquired in Auto/Manual-MSn mode (smart fragmentation) using a ramping of the collision energy. Maximum fragmentation amplitude was fixed to 1 Volt. MS operating conditions (negative mode) were optimized with a capillary temperature of 365 °C, a dry gas flow rate of 10 L/min, and a nebulizer pressure 60 psi. The high-resolution mass was obtained using a Bruker Daltonics micro-TOF spectrometer using the negative electrospray ionization mode (ESI). The sample was injected at 200 uL/h flow rate and subjected to negative Ion ionization mode by keeping the mass window between 50 and 4000 *m/z*.

3.3.8 Quantification of EPA productivity of *P. tricornutum* biomass by fatty acid methyl esterification (FAME)

A modified gravimetric and FAME method was employed for total lipid content and fatty acid profile analysis (Bligh and Dyer, 1959; Mustafai, 2015). Approximately 30 mg of dry biomass was weighed into 10-mL glass screw tubes. Lipid was extracted with 6 mL methanol: chloroform (2:1) solvent using a magnetic stirrer at 250 rpm for 2 h. The organic phase was transferred into a new glass screw tube and 1.2 mL of 0.9% NaCl was added to each tube. After 10 min of incubation, two phases formed and the bottom organic phase was subsequently transferred to a new batch of pre-weighed tubes by syringe. The organic solvent was evaporated under nitrogen. Total lipids were calculated and maintained at -20 °C for methyl esterification. Total lipids were dissolved in 0.5 mL of chloroform. A 10 M KOH solution, 700 µL, and 5.3 mL of methanol were added to the vial and the lipids were incubated at 55 °C in a water bath with a stirrer in the glass tubes stirring for 1 h. All samples were cooled down to room temperature. Next, 580 µL of 12 M H₂SO₄ was added followed by incubation at 55 °C in a water bath with a stirrer for 1 h. Hexane, 1 mL, was

added after the samples cooled down to room temperature. Samples were vortexed and centrifuged at 1512 g for 5 min. The hexane phase (0.5 mL) was transferred to vials and stored at 4 °C. FAME was analyzed by Gas Chromatography (Shimadzu, Kyoto, Japan) integrated with a Flame Ionization Detector (FID). The GC program was developed by (Mustafai, 2015). The correlation curve was made by a gradient of EPA standards subjected to the same method.

3.3.9 Preparation of phytohormones and synthesis of coronatine to potentially induce the production of antimicrobial compounds.

Methyl jasmonate (MeJA) and salicylic acid (SA) were purchased from Sigma Aldrich (Sigma Aldrich, St. Louis, USA). Coronatine (COR) was isolated from the culture supernatant of the bacterium, *Pseudomonas syringae* pv. *glycinea* PG4180 wild type (WT). The COR-deficient mutant PG4180.D4 (D4) served as a negative control. After 48 h of incubation at 28 °C on LB agar plates, *P. syringae* WT and D4 single colonies were inoculated in 20 mL of HSC medium and cultivated at 18 °C and shaking at 250 rpm for 72 h (Palmer and Bender, 1993). Aliquots of 10 mL of WT and D4 were then inoculated into 1 L flasks filled with 400 mL of HSC medium to yield an initial OD₆₀₀ value of 0.02. Flasks were shaken at 18 °C and 250 rpm for five days until bacteria reached stationary phase. A slightly modified extraction protocol was used according to (Palmer and Bender, 1993). In brief, bacterial cells were removed by centrifugation (10,976 g, 10 min, 4 °C), and the culture supernatant was filtrated through 0.2 mm pore size filters to obtain a cell-free supernatant. Aliquots of 22.5 mL of supernatant were filled into 50 mL Falcon tubes. 30 µL of 6 M HCl was added to lower the pH to a range between 1-2. Equal volumes (22.5 mL) of ethyl acetate were added for extraction. Falcon tubes were shaken at 37 °C at 250 rpm for 30 min. This extraction procedure was repeated three times and the upper ethyl acetate fractions collected for evaporation. Evaporation was conducted by a rotary evaporator at 250 rpm, 30 °C, and 90 mbar. Ultrapure water was added to re-suspend the dried pellet containing the compounds. The resuspension solutions were kept at 4 °C, of which 30 µL was diluted 10-fold with water containing 0.05% trifluoroacetic acid (TFA) and filtrated through a 0.2-µm pore size filter before being subjected to High-Performance Liquid Chromatography (HPLC) Ultimate 3000 (Thermo Fisher, Waltham, United States) for quantification. The HPLC protocol was conducted according to (Palmer and Bender, 1993). A COR standard, Sigma Aldrich, was used to make a calibration curve

to estimate the concentration of COR in ethyl acetate extracts. The chromatograms of COR standard, extracts of WT and D4 are included in the supplementary materials (**Fig. S2**).

3.3.10 Induction of synthesis of antibacterial substance(s) in *P. tricornutum* and antibacterial effects analysis

The phytohormones, MeJA and SA, as well as the phytotoxin COR were supplemented to *P. tricornutum* cultures grown in 650-mL cell culture flasks at 20 °C, 75 mmol/s/m² to elicit an increased production of antibacterial compounds when the algal cultures reached mid-exponential growth phase. The two final concentrations of MeJA and SA, respectively, were 10 mg/L and 100 mg/L. The two final concentrations of COR were 0.5 mg/L and 5 mg/L. The same concentrations of ethyl acetate extract from the supernatant of D4 cultures were used as negative control. After treatments for 72 h, algal cells were harvested by centrifugation at 1512 g for 10 min. Total lipid content and fatty acid profiles were analyzed by the same methods in **2.8**. Methanolic extracts of treated biomass (approximately 100 mg), resuspended in DMSO, were tested by disc diffusive assay (DDA) to estimate the antibacterial effect. Each treatment was carried out in duplicate.

3.4 Results and Discussion

3.4.1 Algal growth kinetics and productivity

During a total of 19 days of recycled production, 4.63 kg of *P. tricornutum* dry biomass was produced (**Fig. 2**) with 1000 L of additional salt water supplemented to compensate for the loss of liquid from centrifugation. Thereby, a productivity of 7.62 g/m²/d dry biomass was achieved. As universally acknowledged, the biggest challenges for microalgae production are low productivity and high costs (Santos-Ballardo et al., 2016). *P. tricornutum* has been investigated numerous times, while most of these previous studies were performed at laboratory scale with flasks and bottles. Previously, 4.0 g/m²/d and 2.0 g/m²/d average productivities of *P. tricornutum* have been acquired in semi-continuous and batch mode cultivation, respectively (Veloso et al., 1991). Even after three recycling processes neither a slowdown in growth rate nor a burst of grazers occurred (**Fig. 2**). In a previous study using a specific type of 56 L glass tube PBR, a productivity of 13.1 g/m²/d was

yielded, with 13.33-fold and 7.2-fold NaNO_3 and NaH_2PO_4 consumption, respectively (Benavides et al., 2013). Water consumption contributes a significant portion of the production costs (Farooq et al., 2015). It has been estimated that 1 kg dry biomass production consumes one ton of water (Guieysse et al., 2013). In the current study, 4 t of seawater water was consumed to produce 4.63 kg dry biomass, which reduced water consumption to 0.86 t for 1 kg dry biomass production.

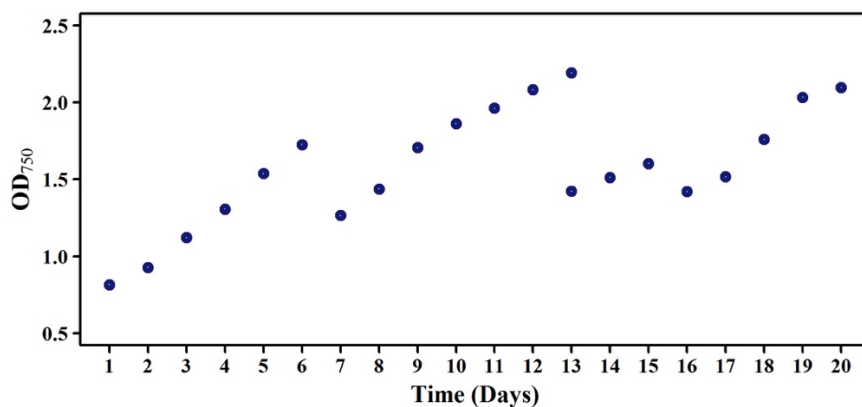


Figure 2. Growth kinetics of *P. tricornutum* in pilot plant. On Day 7, 2500 L algal solution was harvested by centrifugation. 2000 L solution after centrifugation was recycled with f/2 nutrients and 500 L fresh salt water compensating for the loss of salt water during centrifugation. On Day 13, 2500 L algal solution was harvested, of which 2000 L solution was recycled with f/2 nutrients. On Day 16, 500 L fresh salt water and f/2 nutrients was supplemented. On Day 20, all the algae were harvested. Data shown as mean \pm SD, n = 3.

3.4.2 Activity guided fractionation

To isolate and characterize bioactive compounds responsible for the antibacterial activity of algal extracts, a bioactivity-guided fractionation procedure was applied (mentioned in materials and methods 2.6). The obtained fractions, which showed similar compositions as judged by R_f values, were combined and concentrated to carry out a disc diffusion assay with *B. subtilis*. From these fractions, two highly active fractions termed B and J were identified (**Fig. 3**). Both active fractions were directly analyzed by ESI-MS in negative ion mode.

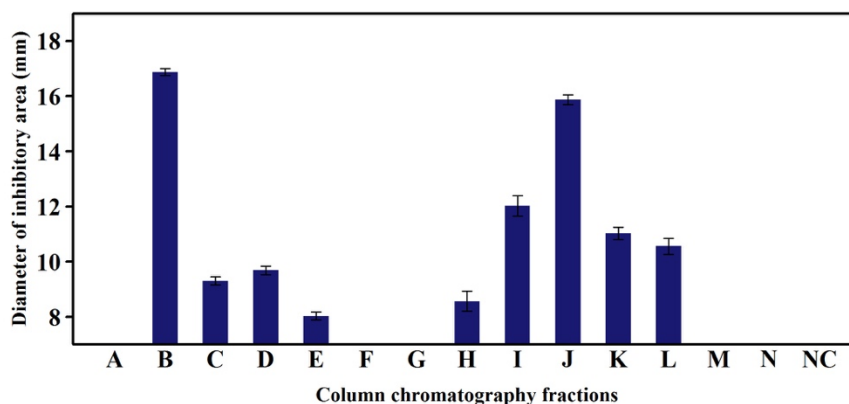


Figure 3. Inhibitory area of fractions from column chromatography. Nine fractions showed antibacterial activities against the test bacteria *B. subtilis*, of which two major peaks occurred. The total fourteen fractions were labelled as A-N based on the order of collected column fractions; NC: negative control. Data shown as mean \pm SD, $n = 3$.

High-resolution mass spectrometry suggested the molecular formula of $C_{20}H_{30}O_2$ with m/z at 301.2289 $[M-H]^-$ (**Fig. 4a**). The subsequent tandem MS fragment of 301 $[M-H]^-$ is giving a m/z 283 $[M-H]^-$ with the loss of water, m/z 257 $[M-H]^-$ with the loss of CO_2 and m/z 203 $[M-H]^-$ (**Fig. 4b**). These data are in full agreement with the Ω -3 polyunsaturated fatty acid EPA (Desbois et al., 2008). Further comparison with an EPA standard fully confirmed the identity of the antibacterial substance. If compared to previous work using RP-HPLC for active compound isolation (Desbois et al., 2008), we could demonstrate that a less demanding separation method yields sizeable quantities of the active compound in satisfactory yield and purity.

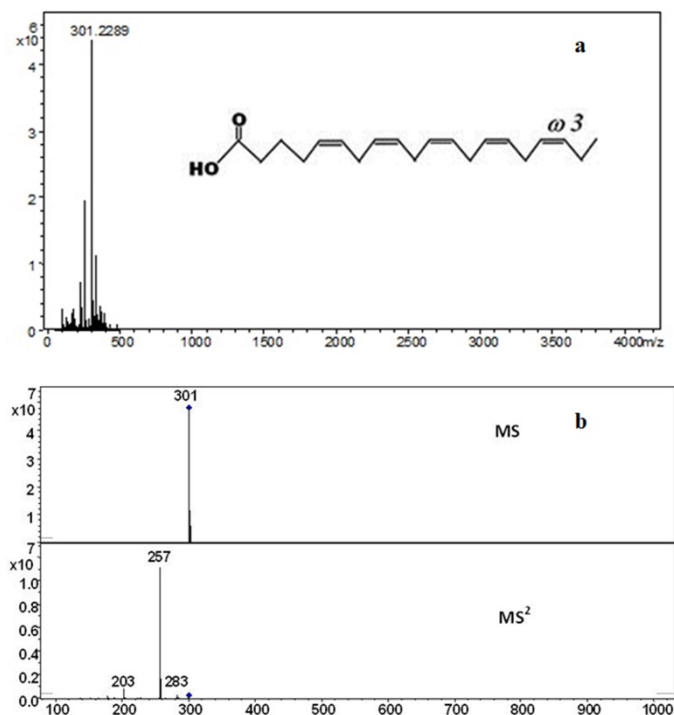


Figure 4. a: High resolution MS spectra of fraction J. Fraction J contains EPA at m/z 301.2289; **b: Tandem MS spectra of EPA at m/z 301 in negative Ion mode.**

The second bioactive fraction was shown to contain several currently inseparable compounds with m/z values at 175, 217, 265, 385, 417 and 509 in the negative ion mode. The molecular formulae for these natural products were assigned by high-resolution mass spectrometry, which is mentioned in **Table 1**. Tandem MS data were inconclusive and did not allow further structure elucidation. Further purification to a single compound level is required to fully characterize the antibacterial compounds. *P. tricornutum* produced at least two different antibacterial compounds.

Table 1: Possible hit candidates for secondary metabolites detected in fraction B

Measured m/z	Theoretical m/z	Error in ppm	Molecular Formula
217.0962	217.0974	3.5	C ₁₀ H ₁₇ O ₅
241.0871	241.0887	4.5	C ₁₁ H ₁₃ O ₆
265.1280	265.1305	8.5	C ₁₅ H ₂₁ O ₄
417.1802	417.1817	4.1	C ₂₀ H ₂₈ O ₉
509.1777	509.1757	6.8	C ₂₇ H ₂₅ O ₁₀

The EPA content of the produced biomass was $3.68 \pm 0.08\%$ of dry weight, which led to a productivity of $0.28 \text{ g/m}^2/\text{d}$. In a different panel photo-bioreactor (40 L), the highest EPA content (2.67% of dry weight) was achieved under nitrogen starvation during spring, while highest EPA productivity ($0.38 \text{ g/m}^2/\text{d}$ of dry weight) was achieved under nitrogen-replete conditions with a nitrogen consumption of 193.7 mg/L (Rodolfi et al., 2017). It may be concluded that with a nutrient-replete medium and extended cultivation, biomass and EPA productivity as observed in this study could be substantially enhanced and cost may thereby be reduced in the future.

P. tricornutum was considered as an EPA-rich species. It has been reported that one strain *P. tricornutum* that can grow in freshwater accumulated as much as 40% EPA of the total fatty acids at low sodium chloride concentration (0-1%). Urea was assessed as the best nitrogen source compared to ammonium and nitrate and resulted in a 30% EPA content of the total fatty acids (Yongmanitchai and Ward, 1991). EPA has been reported to be of great importance in defense reactions against grazing by zooplankton (Jüttner, 2001), but was also recommended as a food additive to lower the risk for cardiovascular diseases (Jump et al., 2012) demonstrating the high versatility of this algal compound.

Variable bacteriostatic effects of different free fatty acids and their derivatives had previously been determined to indicate that their *cis*-double bonds may raise the inhibitory effect when combined with another double bond (Kabara et al., 1972). The antibacterial effect displayed by EPA may be

attributed to the five *cis* double bonds in its structure. It has been noted before that the bacteriostatic effect of linoleic acid was due to increased permeability of bacterial membrane (Greenway and Dyke, 1979). Additionally, it had been shown that long-chain free fatty acids inhibited bacterial growth by reducing the activity of one key enzyme for fatty acid biosynthesis (Zheng et al., 2005). Currently, the mechanism of how EPA inhibits bacterial growth is not well understood, prompting further investigations, which is our utmost future focus.

3.4.3 Antibacterial activity against potentially human pathogenic *Vibrio vulnificus*, *Vibrio cholerae*, and *Vibrio parahaemolyticus*

To further explore the observed antibacterial activity against gram-negative bacteria described previously, both active fractions (J and B), were tested against different potentially pathogenic *Vibrio* species. *Vibrio* are widely disseminated throughout the marine environment, and 13 out of 130 *Vibrio* species are considered to be pathogenic to humans (Ramamurthy et al., 2014) with *V. vulnificus*, *V. parahaemolyticus*, and *V. cholerae* possibly inflicting severe infection, primarily through consumption of contaminated seafood (European Commission, 2001). Both *P. tricornutum* methanolic fractions (J and B) led to the formation of clear inhibitory zones for six tested *Vibrio* environmental isolates with a similar trend (**Fig. 5**). The susceptibility of three isolates for both active fractions B and J was lower in case of *Vibrio parahaemolyticus* as compared to *Vibrio cholerae* and *Vibrio vulnificus*. Fraction B was more active when compared to the fraction containing EPA (J). However, the conclusion that the active compounds in fraction B are more efficient than EPA cannot be drawn at this time, since fraction B constitutes a mixture of compounds with unknown molarity.

Previously, one fraction from the methanolic extract of the diatom *Skeletonema costatum* inhibited the growth of *Vibrio cholerae* (Daniel, 2016), but the bioactive compound was not purified. The antibiotic susceptibility of 141 *V. vulnificus* and 184 *V. cholerae* strains from German Bight and clinical settings were profiled in another study with *V. vulnificus* proven to be resistant to aminoglycosides and *V. cholerae* tolerant to amino-penicillins and aminoglycosides (Bier et al., 2015). The presence of carbapenemase in four *V. cholerae* strains caused great concern (Bier et al., 2015). Carbapenemase is capable of hydrolyzing Carbapenems, which are the antibiotics

featuring the widest antibacterial spectrum (Nordmann et al., 2012). Given our preliminary results above, the natural biomass of *P. tricornutum* as aquaculture feed possesses great potential to replace conventional antibiotics and reduce aquaculture animal and human infection risks.

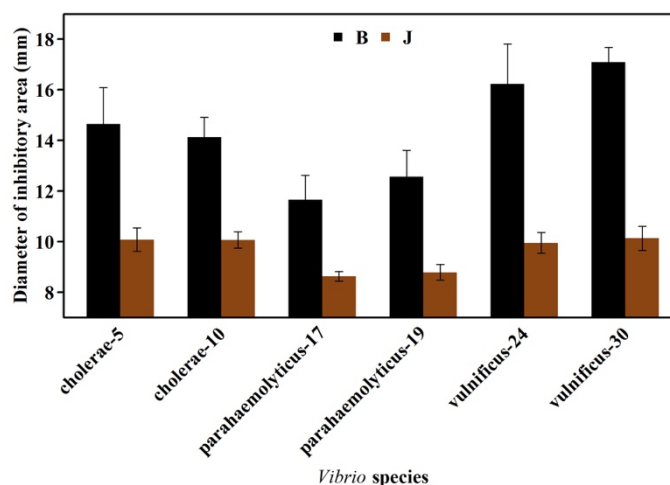


Figure 5. Disc diffusive assay of two active fractions against human and animal pathogens—two strains from each of the 3 *Vibrio* species. Fraction J: Antibacterial column chromatography fraction assigned as eicosapentaenoic acid; B: Antibacterial column chromatography unknown compounds fraction. Data shown as mean \pm SD, n = 3.

3.4.4 Comparison of minimum inhibitory concentration of fraction B and J (eicosapentaenoic acid) with eicosapentaenoic acid standard, a commercial antimicrobial product

The antibacterial effects of fraction B and J (EPA) were compared to those of an EPA standard, to a commercial antibacterial product, and to two commonly used antibiotics, ampicillin and gentamycin (Table 2). The MIC of fraction J (EPA) against *B. subtilis* was 18.4 $\mu\text{g/mL}$, which is comparable to that of the EPA standard (15.6 $\mu\text{g/mL}$). Interestingly, this fraction and pure EPA are 7-8-times more efficient against *B. subtilis* if compared to the commercial product. The two conventional antibiotics are 600-fold and 150-fold more efficient than fraction J (by concentration). The MIC of fraction B with its unknown bioactive compounds is 17-fold less effective when compared to fraction J (Table 2).

Table 2. Minimal inhibitory concentration of fraction B, J, EPA standard, one commercial product and two antibiotics

	B	J	EPA	CP	Amp	Gen
MIC ($\mu\text{g/mL}$)	307.500	18.438	15.625	125	0.031	0.125

B: Antibacterial column chromatography fraction; J: Antibacterial column chromatography fraction assigned as eicosapentaenoic acid; EPA: Eicosapentaenoic acid standard; CP: Commercial antibacterial product; Amp: Ampicillin; Gen: Gentamycin; Experiments were carried out in three replicates. Data shown as mean \pm SD (zero), n = 3.

The antibacterial effect of fraction J (EPA) is 7-times more potent than the commercially available product. A bacteriostatic effect against *B. subtilis* using 1 g of ampicillin, could be in theory substituted with EPA from 16.3 kg of *P. tricornutum* dry biomass or with 4 kg of the pure commercial product. In turn, one gram of gentamycin could be substituted by 4 kg of *P. tricornutum* dry biomass or 1 kg the commercial product, respectively. With the combination of the antibacterial compound(s) in fraction B and EPA, the weight of dry biomass to substitute antibiotics will be further reduced, when the antibacterial compound(s) in fraction B will be identified and quantified. Consequently, EPA as well as the raw algal biomass with both EPA and the fraction B compounds could be used as food additives and feeds in aquaculture, poultry, and livestock breeding. The supplementation of antibiotics in animal feed to prevent disease is strictly forbidden (European Commission, 2005). Therefore, microalgal biomass as replacement of antibiotics had been examined previously. For instance, 1% *Chlorella vulgaris* biomass supplementation in broiler chickens diet is beneficiary to the immune characteristics of chickens, compared to the diet with the antibiotic virginiamycin (Kang et al., 2013). Apart from prevention of bacterial infection, *P. tricornutum*, as food supplementation, led to the best performance of omega-3 long-chain poly unsaturated fatty acid enhancement in the egg yolk of hens, as compared to supplementation with *Nannochloropsis oculata* and *Chlorella fusca* (Lemahieu et al., 2013). In addition, a reddish color of the yolk was observed in yolk produced by chickens fed with *P.*

tricornutum-supplemented feed, suggesting the potential of *P. tricornutum* as a natural colorant (Lemahieu et al., 2013).

3.4.5 Inducibility of the defense system of *P. tricornutum*.

Most of the interspecies interaction knowledge comes from the terrestrial environment, e.g., rhizosphere, on the contrary, it was difficult to find a stable analog in the ocean (Amin et al., 2012). Therefore, it needed to be tested whether the known inducers of higher plant defense mechanisms could play a role in inducing synthesis of bioactive compounds in *P. tricornutum*. The bacterial phytotoxin, COR, has been proved potent in eliciting the accumulation of secondary metabolites in *Taxus media* (Onrubia et al., 2013) prompting us to comparatively study the potential effects of MeJA, SA, and COR on the synthesis of *P. tricornutum* bioactive compounds. SA and MeJA at the higher concentration (100 mg/L) led to 17% and 11.4% increase in total lipid content, respectively, compared to an uninduced control (**Fig. 6a**). An elevated level of lipid content was previously determined after 72 h of treatment with MeJA in *Scenedesmus incrassulatus* at optimal (20 °C) and higher temperatures (25, 30, and 36 °C) (Christov et al., 2001), which is in accordance with the present study. Concerning the fatty acid profiles, especially EPA content, no notable changes were found (**Fig. 6b**). A similar result was previously demonstrated for *Laminaria digitate* with MeJA (Küpper et al., 2009). On the contrary, a variety of free fatty acids were increased in *Laminaria digitate* by arachidonic acid (Küpper et al., 2009). Different fatty acid profiles of *Scenedesmus Incrassulatus* induced by MeJA were noted at lower and higher temperature, compared to the optimal temperature. These differences were suggested to be green algae adaptations to adverse temperature conditions (Christov et al., 2001). No pronounced increase displayed from each treatment suggested that the active substance in fraction B was not affected by all the inducers used in this study (**Fig. S3**). In the current study, *P. tricornutum* was grown under optimal conditions. Hence the regulatory effects of molecules such MeJA, SA and COR possibly required in hostile environments might not have been needed to induce bioactive compound syntheses. In consequence, additional studies with a different experimental set up (e.g., environmental stress and adapted phytobag PBR-design) is needed to elucidate any phytohormonal regulation in the herein tested microalgae.

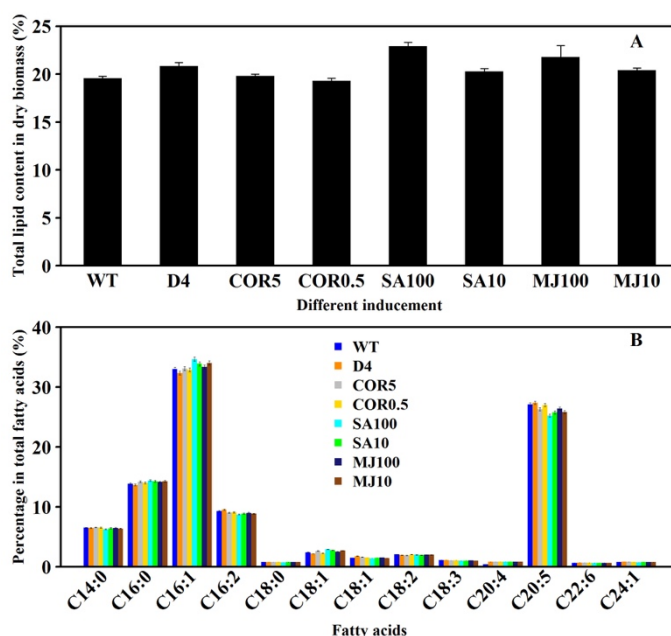


Figure 6. a: Total lipid content (% of dry weight); b: fatty acid profiles (% of total free fatty acid) of dry biomass after 72 h inducement at the end of the exponential phase. D4 mutant as the negative control for coronatine treatment, wild type (WT) for MeJA and SA treatment. WT represents wild type without treatment; D4 coronatine-free treatment; C5 coronatine at 5 mg/L; C0.5 coronatine at 0.5 mg/L; SA100 SA at 100 mg/L; SA10 SA at 10 mg/L; MJ100 MJ at 100 mg/L; MJ10 MJ at 10 mg/L. Data shown as mean \pm SD, n = 2

3.5 Conclusions

Two independent antibacterial fractions were obtained from *P. tricornerutum* biomass. One could be identified as EPA while the other fraction might contain several secondary algal metabolites. Both active fractions displayed an inhibitory effect against potential pathogenic *Vibrio* species. The antibacterial effect of the substances showed superiority over one commercial antimicrobial product indicating the potential of *P. tricornerutum* biomass as a supplement in animal feeds. No noticeable changes were observed in fatty acid profiles when inducers of the plant defense system were applied, indicating that the proper conditions for an induction of bioactive compound synthesis remains to be elucidated.

Acknowledgement

The authors would like to thank Jiemin Du for the assistance in disc diffusive assays, Annika Moje and Diana Sirbu for help in fatty acid analysis method, and Nina L. Böttcher for excellent support in the COR extraction. The work was financially supported by Phytolutions GmbH. The Ph.D. stipend for Song Wang was funded by China Scholarship Council.

Authors' contributions

Song Wang, Inamullah Hakeem Said, Matthias S. Ullrich and Laurenz Thomsen designed the experiment. Song Wang cultivated algal biomass in the pilot plant, tested the fractions from column chromatography and determined the MICs of active fractions against *Bacillus subtilis*. Inamullah Hakeem Said identified the antibacterial substances by mass spectrometry. Candice Thorstenson carried out the disc diffusive assays against *Vibrio* species. Song Wang and Inamullah Hakeem Said drafted the article. Candice Thorstenson, Claudia Thomsen, Matthias S. Ullrich, Nikolai Kuhnert and Laurenz Thomsen gave critical reviews. All the authors made contributions to the interpretation of data and approved the final manuscript. Song Wang is responsible for the integrity of the work as a whole.

3.6 Reference

- Amin, S.A., Hmelo, L.R., van Tol, H.M., Durham, B.P., Carlson, L.T., Heal, K.R., Morales, R.L., Berthiaume, C.T., Parker, M.S., Djunaedi, B., Ingalls, A.E., Parsek, M.R., Moran, M.A. and Armbrust, E.V. (2015) Interaction and signalling between a cosmopolitan phytoplankton and associated bacteria. *Nature* **522**, 98-101.
- Amin, S.A., Parker, M.S. and Armbrust, E.V. (2012) Interactions between diatoms and bacteria. *Microbiology and Molecular Biology Reviews* **76**, 667-684.
- Benavides, A.M.S., Torzillo, G., Kopecky, J. and Masojídek, J. (2013) Productivity and biochemical composition of *Phaeodactylum tricornutum* (Bacillariophyceae) cultures grown outdoors in tubular photobioreactors and open ponds. *Biomass Bioenergy* **54**, 115-122.
- Bier, N., Schwartz, K., Guerra, B. and Strauch, E. (2015) Survey on antimicrobial resistance patterns in *Vibrio vulnificus* and *Vibrio cholerae* non-O1/non-O139 in Germany reveals carbapenemase-producing *Vibrio cholerae* in coastal waters. *Frontiers in microbiology* **6**, 1179.
- Bligh, E.G. and Dyer, W.J. (1959) A rapid method of total lipid extraction and purification. *Canadian Journal of Biochemistry and Physiology* **37**, 911-917.
- Blunt, J.W., Copp, B.R., Keyzers, R.A., Munro, M.H. and Prinsep, M.R. (2016) Marine natural products. *Natural Product Reports* **33**, 382-431.
- Bowler, C., Allen, A.E., Badger, J.H., Grimwood, J., Jabbari, K., Kuo, A., Maheswari, U., Martens, C., Maumus, F., Otilar, R.P., Rayko, E., Salamov, A., Vandepoele, K., Beszteri, B., Gruber, A., Heijde, M., Katinka, M., Mock, T., Valentin, K., Verret, F., Berges, J.A., Brownlee, C., Cadoret, J.P., Chiovitti, A., Choi, C.J., Coesel, S., De Martino, A., Detter, J.C., Durkin, C., Falciatore, A., Fournet, J., Haruta, M., Huysman, M.J., Jenkins, B.D., Jiroutova, K., Jorgensen, R.E., Joubert, Y., Kaplan, A., Kroger, N., Kroth, P.G., La Roche, J., Lindquist, E., Lommer, M., Martin-Jezequel, V., Lopez, P.J., Lucas, S., Mangogna, M., McGinnis, K., Medlin, L.K., Montsant, A., Oudot-Le Secq, M.P., Napoli, C., Obornik, M., Parker, M.S., Petit, J.L., Porcel, B.M., Poulsen, N., Robison, M., Rychlewski, L., Ryneerson, T.A., Schmutz, J., Shapiro, H., Siaut, M., Stanley, M., Sussman, M.R., Taylor, A.R., Vardi, A., von Dassow, P., Vyverman, W., Willis, A., Wyrwicz, L.S., Rokhsar, D.S., Weissenbach,

- J., Armbrust, E.V., Green, B.R., Van de Peer, Y. and Grigoriev, I.V. (2008) The *Phaeodactylum* genome reveals the evolutionary history of diatom genomes. *Nature* **456**, 239-244.
- Brembu, T., Chauton, M.S., Winge, P., Bones, A.M. and Vadstein, O. (2017) Dynamic responses to silicon in *Thalassiosira pseudonana* - Identification, characterisation and classification of signature genes and their corresponding protein motifs. *Scientific Reports* **7**, 4865.
- Christov, C., Pouneva, I., Bozhkova, M., Toncheva, T. and Fournadzieva, S. (2001) Influence of temperature and methyl jasmonate on *Scenedesmus Incrassulatus*. *Biologia Plantarum* **44**, 367-371.
- Daniel, R. (2016) Antibacterial activity of the marine diatom *Skeletonema costatum* against selected human pathogens. *International Journal of Current Pharmaceutical Research* **7**, 233-236.
- Desbois, A.P., Lebl, T., Yan, L. and Smith, V.J. (2008) Isolation and structural characterisation of two antibacterial free fatty acids from the marine diatom, *Phaeodactylum tricornutum*. *Applied Microbiology and Biotechnology* **81**, 755-764.
- Desbois, A.P., Mearns-Spragg, A. and Smith, V.J. (2009) A fatty acid from the diatom *Phaeodactylum tricornutum* is antibacterial against diverse bacteria including multi-resistant *Staphylococcus aureus* (MRSA). *Marine Biotechnology (NY)* **11**, 45-52.
- Duong, V.T., Ahmed, F., Thomas-Hall, S.R., Quigley, S., Nowak, E. and Schenk, P.M. (2015) High protein- and high lipid-producing microalgae from northern australia as potential feedstock for animal feed and biodiesel. *Frontiers in Bioengineering and Biotechnology* **3**, 53.
- European Commission (2001) Opinion of the Scientific Committee on veterinary measures relating to public health on *Vibrio vulnificus* and *Vibrio parahaemolyticus*. *European Commission*.
- European Commission (2005) Ban on antibiotics as growth promoters in animal feed enters into effect Ban on antibiotics as growth promoters in animal feed enters into effect. *European Commission*, IP/05/1687.
- Farooq, W., Suh, W.I., Park, M.S. and Yang, J.W. (2015) Water use and its recycling in microalgae cultivation for biofuel application. *Bioresource Technology* **184**, 73-81.

- Greenway, D.L. and Dyke, K.G. (1979) Mechanism of the inhibitory action of linoleic acid on the growth of *Staphylococcus aureus*. *Journal of general microbiology* **115**, 233-245.
- Guieysse, B., Bechet, Q. and Shilton, A. (2013) Variability and uncertainty in water demand and water footprint assessments of fresh algae cultivation based on case studies from five climatic regions. *Bioresource Technology* **128**, 317-323.
- Guillard, R.R.L. (1975) Culture of phytoplankton for feeding marine invertebrates. In: *Culture of Marine Invertebrates Animals* (Smith, W.L. and Chanley, M.H. eds), pp. 26-60. New York, USA: Plenum Press.
- Han, G.Z. (2017) Evolution of jasmonate biosynthesis and signaling mechanisms. *Journal of Experimental Botany* **68**, 1323-1331.
- Hu, Q., Sommerfeld, M., Jarvis, E., Ghirardi, M., Posewitz, M., Seibert, M. and Darzins, A. (2008) Microalgal triacylglycerols as feedstocks for biofuel production: perspectives and advances. *Plant Journal* **54**, 621-639.
- Jallet, D., Caballero, M.A., Gallina, A.A., Youngblood, M. and Peers, G. (2016) Photosynthetic physiology and biomass partitioning in the model diatom *Phaeodactylum tricornutum* grown in a sinusoidal light regime. *Algal Research* **18**, 51-60.
- Jump, D.B., Depner, C.M. and Tripathy, S. (2012) Omega-3 fatty acid supplementation and cardiovascular disease. *Journal of Lipid Research* **53**, 2525-2545.
- Jüttner, F. (2001) Liberation of 5,8,11,14,17-eicosapentaenoic acid and other polyunsaturated fatty acids from lipids as a grazer defense reaction in epilithic diatom biofilms. *Journal of Phycology* **37**, 744-755.
- Kabara, J.J., Swieczkowski, D.M., Conley, A.J. and Truant, J.P. (1972) Fatty acids and derivatives as antimicrobial agents. *Antimicrobial Agents and Chemotherapy* **2**, 23-28.
- Kang, H.K., Salim, H.M., Akter, N., Kim, D.W., Kim, J.H., Bang, H.T., Kim, M.J., Na, J.C., Hwangbo, J., Choi, H.C. and Suh, O.S. (2013) Effect of various forms of dietary *Chlorella* supplementation on growth performance, immune characteristics, and intestinal microflora population of broiler chickens. *Journal of Applied Poultry Research* **22**, 100-108.
- Kay, R.A. (1991) Microalgae as food and supplement. *Critical Reviews in Food Science and Nutrition* **30**, 555-573.
- Kellam, S.J. and Walker, J.M. (1989) Antibacterial activity from marine microalgae in laboratory culture. *British Phycological Journal* **24**, 191-194.

- Küpper, F.C., Gaquerel, E., Cosse, A., Adas, F., Peters, A.F., Muller, D.G., Kloareg, B., Salaun, J.P. and Potin, P. (2009) Free Fatty Acids and Methyl Jasmonate Trigger Defense Reactions in *Laminaria digitata*. *Plant and Cell Physiology* **50**, 789-800.
- Lemahieu, C., Bruneel, C., Termote-Verhalle, R., Muylaert, K., Buyse, J. and Foubert, I. (2013) Impact of feed supplementation with different omega-3 rich microalgae species on enrichment of eggs of laying hens. *Food Chemistry* **141**, 4051-4059.
- Mustafai, M. (2015) Correlation studies of Cocoa FAMES. *Bachelor thesis of Jacobs University Bremen, Germany*.
- Nordmann, P., Dortet, L. and Poirel, L. (2012) Carbapenem resistance in Enterobacteriaceae: here is the storm! *Trends in Molecular Medicine* **18**, 263-272.
- Onrubia, M., Moyano, E., Bonfill, M., Cusido, R.M., Goossens, A. and Palazon, J. (2013) Coronatine, a more powerful elicitor for inducing taxane biosynthesis in *Taxus media* cell cultures than methyl jasmonate. *Journal of plant physiology* **170**, 211-219.
- Palmer, D.A. and Bender, C.L. (1993) Effects of environmental and nutritional factors on production of the polyketide phytotoxin coronatine by *Pseudomonas syringae* pv. *Glycinea*. *Applied and Environmental Microbiology* **59**, 1619-1626.
- Ramamurthy, T., Chowdhury, G., Pazhani, G.P. and Shinoda, S. (2014) *Vibrio fluvialis*: an emerging human pathogen. *Frontiers in microbiology* **5**, 91.
- Reymond, P. and Farmer, E.E. (1998) Jasmonate and salicylate as global signals for defense gene expression. *Current Opinion in Plant Biology* **1**, 404-411.
- Rodolfi, L., Biondi, N., Guccione, A., Bassi, N., D'Ottavio, M., Arganaraz, G. and Tredici, M.R. (2017) Oil and eicosapentaenoic acid production by the diatom *Phaeodactylum tricornutum* cultivated outdoors in Green Wall Panel (GWP(R)) reactors. *Biotechnology and Bioengineering* **114**, 2204-2210.
- Santos-Ballardo, D.U., Rendon-Unceta Mdel, C., Rossi, S., Vazquez-Gomez, R., Hernandez-Verdugo, S. and Valdez-Ortiz, A. (2016) Effects of outdoor cultures on the growth and lipid production of *Phaeodactylum tricornutum* using closed photobioreactors. *World Journal of Microbiology and Biotechnology* **32**, 128.
- Seymour, J.R., Amin, S.A., Raina, J.B. and Stocker, R. (2017) Zooming in on the phycosphere: the ecological interface for phytoplankton-bacteria relationships. *Nature Microbiology* **30**, 17065.

- Shannon, E. and Abu-Ghannam, N. (2016) Antibacterial Derivatives of Marine Algae: An Overview of Pharmacological Mechanisms and Applications. *Marine Drugs* **14**, 81.
- Singh, S., Kate, B.N., Banerjee, U.C. (2005) Bioactive compounds from cyanobacteria and microalgae: an overview. *Critical Reviews in Biotechnology* **25**, 73-95.
- Tandeau de Marsac, N. and Houmard, J. (1993) Adaptation of cyanobacteria to environmental stimuli: new steps towards molecular mechanisms. *FEMS Microbiology Reviews* **104**, 119-190.
- Veloso, V., Reis, A., Gouveia, L., Fernandes, H.L., Empis, J.A. and Novais, J.M. (1991) Lipid production by *Phaeodactylum tricornutum*. *Bioresource Technology* **38**, 115-119.
- Xie, D.X., Feys, B.F., James, S., Nieto-Rostro, M. and Turner, J.G. (1998) COI1: an *Arabidopsis* gene required for jasmonate-regulated defense and fertility. *Science* **280**, 1091-1094.
- Yongmanitchai, W. and Ward, O. (1991) Growth and omega-3 fatty acid production by the *Phaeodactylum tricornutum* under different culture conditions. *Applied and Environmental Microbiology* **57**, 419-425.
- Zheng, C.J., Yoo, J.S., Lee, T.G., Cho, H.Y., Kim, Y.H. and Kim, W.G. (2005) Fatty acid synthesis is a target for antibacterial activity of unsaturated fatty acids. *FEBS Letters* **579**, 5157-5162.
- Zhu, C.J. and Lee, Y.K. (1997) Determination of biomass dry weight of marine microalgae. *Journal of Applied Phycology* **9**, 189-194.

3.7 Supplementary material

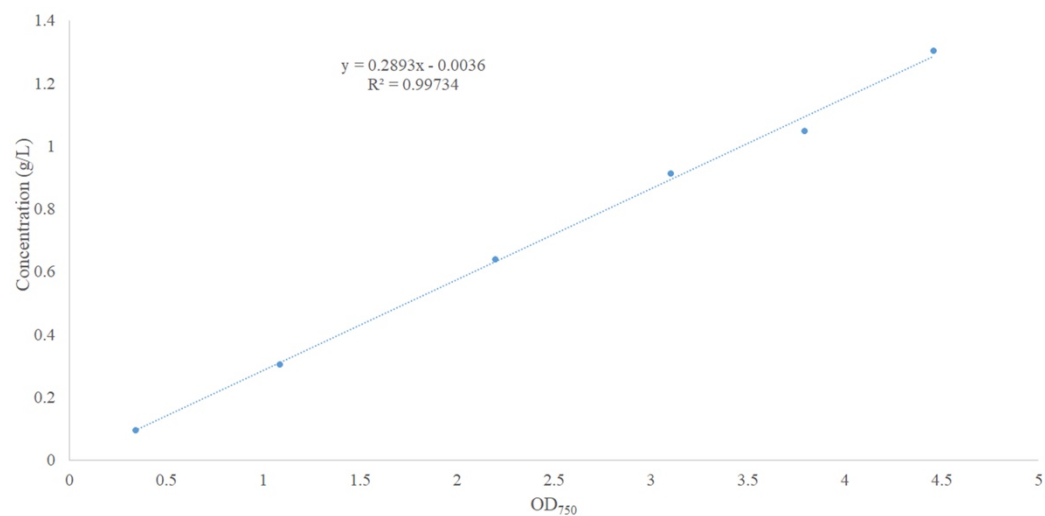


Figure S1. Correlation curve between OD₇₅₀ value and dry biomass concentration (g/L).

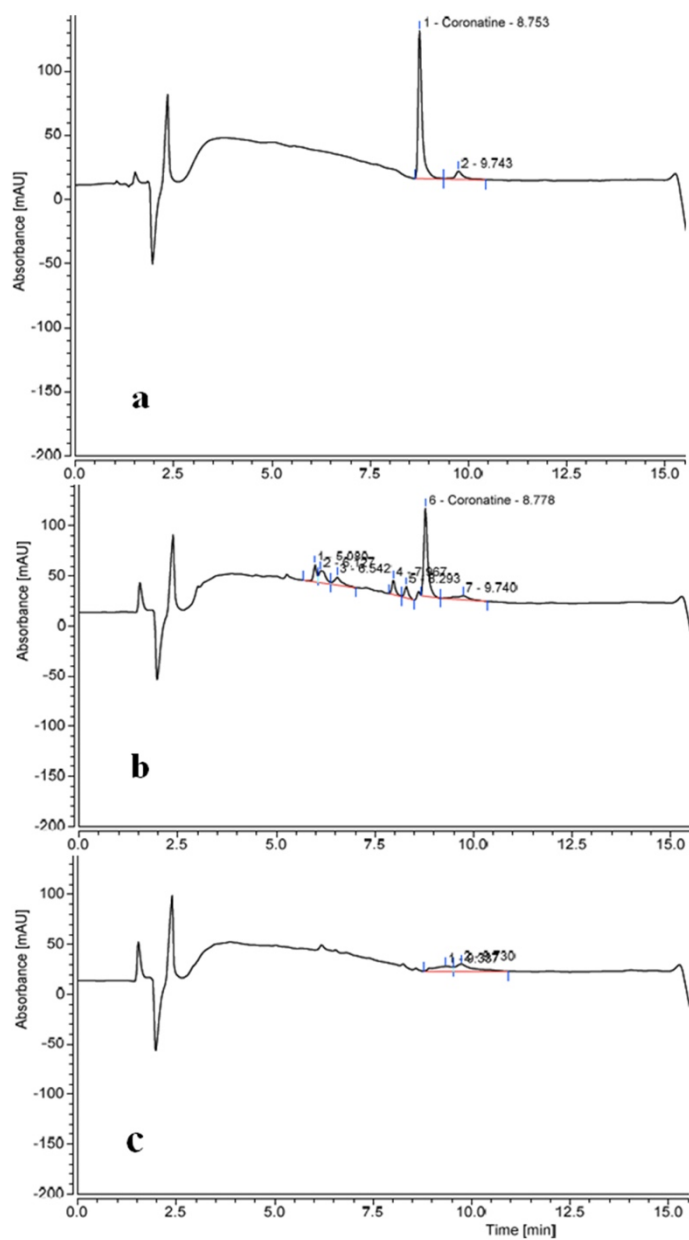


Figure S2. Chromatograms of a: COR standard; b: extracts of *P. syringae* WT; c: extracts of *P. syringae* D4

4 Changes in the fucoxanthin production and protein profiles in *Cylindrotheca closterium* in response to blue light-emitting diode light

Manuscript was published in *Microbial Cell Factories* **17** (2018):110

<https://doi.org/10.1186/s12934-018-0957-0>

Song Wang^{1*}, Sujit K. Verma², Inamullah Hakeem Said², Laurenz Thomsen¹, Matthias S. Ullrich², Nikolai Kuhnert²

¹Department of Physics and Earth Sciences, Jacobs University Bremen, Campus Ring 1, 28759 Bremen, Germany

²Department of Life Science and Chemistry, Jacobs University Bremen, Campus Ring 1, 28759 Bremen, Germany

*Corresponding author: Song Wang, s.wang@jacobs-university.de,

This article is distributed under the terms of the Creative Commons Attribution 4.0 International License (<http://creativecommons.org/licenses/by/4.0/>). Changes in the structure were made to keep the consistency of the thesis.

4.1 Abstract

Marine diatoms have a higher fucoxanthin content in comparison to macroalgae. Fucoxanthin features many potent bioactive properties, particularly anti-obesity properties. Despite the great potential for harvesting larger amounts of fucoxanthin, the impacts of light quality (light source, intensity, and photoperiod) on fucoxanthin production and the essential proteins involved in fucoxanthin biosynthesis in marine diatoms remain unclear.

In the present study, *Cylindrotheca closterium* was selected from four different species of diatoms based on its high fucoxanthin content and productivity. Optimal light conditions (light source, intensity, and regime) were determined by a “Design of Experiment” approach (software MODDE Pro 11 was used). The model indicated that an 18/6 light/darkness regime increased fucoxanthin productivity remarkably as opposed to a 12/12 or 24/0 regime. Eventually, blue light-emitting diode light, as an alternative to fluorescent light, at 100 $\mu\text{mol}/\text{m}^2/\text{s}$ and 18/6 light/darkness regime yielded maximum fucoxanthin productivity and minimal energy consumption. The fucoxanthin production of *C. closterium* under the predicted optimal light conditions was assessed both in bottle and bag photobioreactors (PBRs). The high fucoxanthin content (25.5 mg/g) obtained from bag PBRs demonstrated the feasibility of large-scale production. The proteomes of *C. closterium* under the most favorable and unfavorable fucoxanthin biosynthesis light/darkness regimes (18/6 and 24/0 respectively) were compared to identify the essential proteins associated with fucoxanthin accumulation by matrix-assisted laser desorption/ionization-time of flight-mass spectrometry. Six proteins that were up-regulated in the 18/6 regime but down-regulated in the 24/0 were identified as important chloroplastic proteins involved in photosynthesis, energy metabolism, and cellular processes.

Blue light-emitting diode light at 100 $\mu\text{mol}/\text{m}^2/\text{s}$ and 18/6 light/darkness regime induced maximum fucoxanthin productivity in *C. closterium* and minimized energy consumption. The high fucoxanthin production in the bag photobioreactor under optimal light conditions demonstrated the possibility of commercialization. Proteomics suggests that fucoxanthin biosynthesis is intimately associated with the photosynthetic efficiency of the diatom, providing another technical and bioengineering outlook on fucoxanthin enhancement.

Keywords: Diatom; Fucoxanthin; Photobioreactor; Proteomics; Photosynthesis

4.2 Introduction

Diatoms (Bacillariophyta) are ubiquitously distributed in aquatic ecosystems and contribute up to 20% of the global primary production (organic compounds produced from CO₂) (Malviya et al., 2016). Thus diatoms constitute an important autotrophic functional group in the marine food web (Armbrust, 2009). Diatoms, besides their ecological and geochemical functions, are receiving increasing attention because of their potential use in biodiesel production (Valenzuela et al., 2013) and for pharmaceutical purposes (Kuppusamy et al., 2017). Furthermore, diatoms are abundant in bioactive metabolites such as antibacterial polyunsaturated fatty acids, i.e. eicosapentaenoic acid (Wang et al., 2018), and photosynthetic accessory pigments, such as fucoxanthin, both of which have been heavily investigated over the last several decades (Kuczynska et al., 2015). Previously, we identified and purified the benthic diatom, *Cylindrotheca closterium*, which showed outstanding characteristics in growth and lipid content (Wang et al., 2015). Its additional characteristic of rapid sedimentation became beneficial for reducing the harvesting cost.

Fucoxanthin is a major carotenoid in diatom and brown algae. It accounts for more than one-tenth of the total carotenoid production in nature (Peng et al., 2011) and serves as a light-harvesting pigment (Kuczynska et al., 2015). In diatoms, fucoxanthin is primarily bound to chlorophyll a/c and forms a fucoxanthin-chlorophyll a/c protein complex (FCP), which functions as the light-harvesting complex associated with both photosystem I (Veith et al., 2009) and II (Nagao et al., 2014). Along with pigments of the xanthophyll cycle, FCPs also participate in the formation of non-photochemical quenching to avoid photo-oxidation (Lavaud et al., 2003). Fucoxanthin exhibits several potent bioactivities, including anti-obesity properties, and is consequently available in various nutritional supplements (Woo et al., 2010). The most common dietary source of fucoxanthin is brown algae in Japanese cuisine, such as in Miso soups. Commercial production of fucoxanthin mainly derives from macroalgae, such as *Laminaria japonica*, *Eisenia bicyclis*, *Undaria pinnatifida* and *Hijikia fusiformis*. These macroalgae are known to have a low fucoxanthin content (Xia et al., 2013). Microalgae, on the other hand, with two-magnitude greater

fucoxanthin content, are more promising for fucoxanthin production. Nevertheless, only a few species of marine diatoms such as *Phaeodactylum tricornutum* (Kim et al., 2012), *Odontella aurita* (Xia et al., 2013) and *Cyclotella cryptica* (Guo et al., 2016) have been studied for their commercial feasibility in fucoxanthin production.

The biosynthesis of diatom carotenoids is profoundly affected by the quality of the light (Beuzenberg et al., 2016). Yet, the impact of light quality (light source, intensity, and photoperiod) on fucoxanthin production remains unclear. Light-emitting diode (LED) has been considered as the ideal artificial light source due to its advantages like long life-span, low heat generation, low energy consumption, and narrow light emission spectrum suited specifically for the high-value bioactive compound production (Glemser et al., 2016). Most importantly, LED light is now available at various wavelength ranges, allowing for the exploitation of photo-stimulation in natural product biosynthesis (Schulze et al., 2014). The induction of specific pigments (astaxanthin in *Haematococcus pluvialis* and β -carotene in *Dunaliella salina*) by specific LED light (Katsuda et al., 2004) has already been demonstrated in principle, however never applied to a natural product of commercial and medicinal interest like fucoxanthin. Red & blue and blue LED were chosen in the present experiment since fucoxanthin mainly absorbs blue light, and red mixed with blue light is beneficial for photosynthesis (Kuczynska et al., 2015).

With more genomic and transcriptional data available from diatoms, diatom adaptation to different environments has been well understood on the molecular level. Advances in proteomics have led to a better understanding of the diatom's proteome response to environmental changes (Muhseen et al., 2015). Matrix-assisted laser desorption/ionization-time of flight-mass spectrometry (MALDI-TOF-MS) based proteomic analysis in green algae, *Haematococcus lacustris*, found proteins related to an increase of astaxanthin production under nutrient and illumination stress were up-regulated (Tran et al., 2009). Proteomic approaches have also been used to show increased lipid biosynthesis under darkness stress (Bai et al., 2016) and high light acclimation strategy (Dong et al., 2016) in diatoms. Therefore, in our current study, a proteomic study was employed to identify the essential proteins involved in fucoxanthin biosynthesis in the diatom *C. closterium*.

Cylindrotheca closterium was selected from four species of diatoms as the best candidate for fucoxanthin production. An experimental model was constructed to determine the optimal light conditions (light source, intensity, and regime), leading to the highest fucoxanthin productivity while consuming the lowest amount of energy. The effects of optimal light conditions for fucoxanthin production were confirmed in bottle PBRs and, for commercialization purpose, tested in bag PBRs with continuous and flashing light. Finally, key enzymes related to fucoxanthin biosynthesis, differentially expressed under herein tested conditions, were analyzed by a proteomics approach to understand the cellular basis for the observed phenotypic changes in fucoxanthin synthesis and to predict further optimization strategies for fucoxanthin production in this model diatom.

4.3 Materials and Methods

4.3.1 Microalgae species and culture conditions

Cylindrotheca closterium and *Amphora* sp. were provided by the culture collection of the Laboratory of Applied Microalgae Biology of the Ocean University of China. *P. triornutum* was ordered from the Culture Collection of Algae at Gottingen University. *T. weissflogii* was provided by the microbiology laboratory of Jacobs University Bremen. Stock cultures were maintained at photosynthetically active radiation (PAR) of 45 $\mu\text{mol}/\text{m}^2/\text{s}$, 12/12 light/darkness cycle and 20 °C in f/2 medium (Guillard, 1975). Algae in bottle and bag PBRs were cultured in f medium.

4.3.2 Equipment

Flexible LED RGB stripes with LED 5030 were purchased from LE (Hannover, Germany). Fluorescent lamps (L 58W/840) were purchased from Osram (Munich, Germany). PAR was measured with the photosynthetic yield analyzer MINI-PAM from Heinz Walz (Effeltrich, Germany). Energy consumption of illumination was measured by an energy consumption meter from Hugo Brennenstuhl GmbH (Tübingen, Germany). The spectra of fluorescent light and LED light were determined by one CCD spectrometer from Mightex (California, United States).

4.3.3 Experimental design

Cylindrotheca closterium, *Amphora* sp., *P. tricornutum* and *T. weissflogii* were all pre-cultured to exponential phase before inoculation. Pre-cultures were diluted into bottle PBRs (in triplicates) with 800 mL of f medium to yield an initial optical density value of 0.1 at 750 nm. All cultures were kept at 20 ± 1 °C and a 12/12 light/darkness regime by fluorescent light of $80 \mu\text{mol}/\text{m}^2/\text{s}$. The cultures were screened for highest fucoxanthin productivity to optimize light conditions.

An experimental model regarding optimal light conditions was designed, and results were analyzed by the “Design of Experiment” software MODDE Pro 11 (Sartorius, Gottingen, Germany). The purpose of “Design of Experiment” approach was to develop a rational and efficient way to estimate the effects of variables by running the minimum number of experiments. Three illuminative variables (light source, intensity, and regime) were evaluated by response factors (fucoxanthin content, fucoxanthin productivity, and energy consumption). With the objective of optimization, a quadratic model comprised of 20 runs of experiments with three center points was built (**Table 1**). Algae in every treatment received of a total illumination period of 72 h before harvesting. The accuracy and validity of the predicted optimal light conditions were confirmed with experiments in bottle PBRs. Furthermore, the feasibility of large-scale production was tested in bag PBRs (patented by Phytolutions GmbH, Bremen, Germany) as a prototype (**Fig. S4**), of which the robustness and expandability had been tested in large-scale production in the field (Thomsen et al., 2012). Illumination of two bag PBRs with a volume of 20 L was provided by LED plates mounted with four LED stripes lit continuously or flashing at 1Hz with a duty cycle of 50%. The protein of *C. closterium* cultured under 18/6 or 24/0 blue LED light regime at $100 \mu\text{mol}/\text{m}^2/\text{s}$ (with triplicates) was evaluated by a proteomics approach to potentially elucidate the mechanism of light-induced fucoxanthin biosynthesis in this diatom.

Table 1. Experiments recommended by “Design of Experiment” software

Experiment No.	Light intensity ($\mu\text{mol}/\text{m}^2/\text{s}$)	Light regime (h/h light/darkness)	Light source
1	50	12/12	Fluorescent
2	100	12/12	Fluorescent
3	75	18/6	Fluorescent
4	50	24/0	Fluorescent
5	100	24/0	Fluorescent
6	50	12/12	Blue
7	100	12/12	Blue
8	75	18/6	Blue
9	50	24/0	Blue
10	100	24/0	Blue
11	50	12/12	R & B
12	75	12/12	R & B
13	100	12/12	R & B
14	50	18/6	R & B
15	100	18/6	R & B
16	50	24/0	R & B
17	75	24/0	R & B
18	75	18/6	R & B
19	75	18/6	R & B
20	75	18/6	R & B

Fluorescent: fluorescent light; blue: blue LED light; R & B: red & blue LED light. Experiment **No.18-20** are center points.

4.3.4 Measurement of growth kinetics, biomass productivity, and specific growth rate

The growth kinetics of the diatoms in the screening experiment were monitored daily by determining the dry biomass concentration (mg/L) with a gravimetric method. Algal suspension

(30 mL) was filtered onto pre-weighed 47 mm Whatman GF/F filters (Maidstone, United Kingdom) and algae rinsed by ultrapure water to remove the salts. The obtained filters were dried in an oven for 24 hours at 60 °C and then weighed subsequently to calculate the dry biomass concentration (mg/L). Biomass productivity (P) was calculated with the following equation: $P = (X_t - X_0)/(t - t_0)$ (Hempel et al., 2012) and specific growth rate (μ) was calculated with the equation: $\mu = (\ln X_t - \ln X_0)/(t - t_0)$ (Liao et al., 2018), in which X_t and X_0 represent the dry biomass concentration on time points t and t_0 respectively. Since the inoculum for bag PBRs is cultivated in bottle PBRs, the initial concentration (X_0) was calculated by the correlation curve between cell number and dry biomass in bottle PBRs with an $R^2 = 0.99635$. Cell concentration in bottle PBRs was determined with a cell counting chamber from Paul Marienfeld GmbH (Lauda-Königshofen, Germany).

4.3.5 Fucoxanthin extraction, identification, and quantification

Volumes of 30 mL algal suspension were harvested by centrifugation at 3000 x g at 16 °C for 5 min. Algae biomass was rinsed twice with ultrapure water to remove seawater. Samples were stored at -20 °C and subsequently lyophilized for 24 h. Pre-weighed samples were extracted by vortexing with sterile glass beads for 15 min in methanol. The extraction procedure was then repeated. Methanolic extracts were combined, diluted 1 to 20 and filtered through 0.2 μm pore size filters before quantification by high-performance liquid chromatography (HPLC). Every step was performed in a dim environment due to the light sensitivity of fucoxanthin. The fucoxanthin content of all samples was analyzed by a Thermo Fisher Ultimate 3000 HPLC, (Waltham, United States) equipped with a C18 reverse-phase column. The mobile phase consisted of acetonitrile, methanol, and water (70:25:5) with 50 mg/L ammonia acetate. A standard calibration curve ($R^2 = 0.9999$) was made by taking five points between the range of 0.25 and 0.5 $\mu\text{g/mL}$ with fucoxanthin standards dissolved in methanol (Sigma Aldrich, Darmstadt, Germany). Samples were diluted 10-20 times to the range of the calibration curve, and 50 μL of each sample was injected into the HPLC. Absorbance was recorded at 445 nm (Kim et al., 2012). Fucoxanthin productivity was calculated by multiplying fucoxanthin content with biomass productivity.

4.3.6 Protein extraction using SDS-DTT buffer

Protein extraction was performed according to a previously described method (Kumari et al., 2016) with minor modifications. Dried biomass (50 µg) was incubated in 5 mL of SDS-DTT buffer for 10 min at 80 °C to activate the protein extraction and then left rotating at 40 °C for 2 h. After 2 h, the samples were centrifuged at 3220 x g for 20 min at room temperature. Then the protein-containing supernatant was collected. Ice-cold acetone was used to precipitate the protein from the supernatant. The precipitate was incubated at -20 °C overnight. On the next day, the samples were centrifuged at 16,000 x g for 20 min at 4 °C in a bench top 5415R centrifuge (Eppendorf, Hamburg, Germany), and the pellet was re-suspended in 50 mM Tris-HCl buffer (pH of 8.0). The acetone precipitation of the protein was repeated twice. Subsequently, the protein pellet was either re-solubilized in 1 mL of 50 mM Tris-HCl, pH 8.0, and then directly used in SDS-PAGE analysis or was re-solubilized in 1 mL of rehydration buffer (2 M thiourea, 6 M urea, 16.2×10^{-3} M 3-[(3-Cholamidopropyl) dimethyl ammonio]-1-propane sulphonate, 25.9×10^{-3} M DTT) supplemented with ampholytes (BioRad, Munich, Germany) according to manufacturer's specification and used for 2D-PAGE analysis.

4.3.7 Determination of protein concentration

The protein content of extracted algal protein solutions was assessed using the Bicinchoninic Acid (BCA) method (Smith et al., 1985). The BCA kit was purchased from Thermo-Fischer (Schwerte, Germany). The protein concentrations were measured in triplicates according to the provided protocol.

4.3.8 Sodium dodecyl sulfate-polyacrylamide gel electrophoresis (SDS-PAGE)

The extracted algal proteins were separated according to their molecular weight using SDS-PAGE. The protein sample (30 µg) was mixed with 6 x sample buffer (5 µL) (Laemmli, 1970) containing bromophenol blue as tracking dye. The mixture was heated at 95 °C for 5 min and loaded onto SDS-PAGE gels (83 mm × 65 mm × 1 mm) containing 12.5% (w/v) acrylamide. The SDS-PAGE gels were run in the Mini-PROTEAN Tetra cell system from BioRad. Electrophoresis was done at

130 V for 90 min. The resulting gel was stained with Coomassie® Blue [45% (v/v) methanol, 10% acetic acid, 2.93×10^{-3} M Coomassie® Brilliant Blue G-250] for 20 min and further treated with a de-staining solution [10% (v/v) acetic acid, 5% (v/v) 2-propanol] overnight with gentle shaking.

4.3.9 Two-dimensional protein gel electrophoresis

Two-dimensional (2D) gel electrophoresis of algal proteins was performed by isoelectric focusing and subsequent SDS-PAGE. For this, 120 µg of protein were applied to immobilized pH gradient (IPG) strips (7 cm, pH 3-10; Bio-Rad) by soaking for 16 h at room temperature. Isoelectric focusing was carried out on a Bio-Rad Protean® i12TM IEF Cell (50 V, 70 min; 150 V, 20 min; 300 V, 15 min; gradient to 600 V, 10 min; 600 V, 15 min; gradient to 1500 V, 10 min; 1500 V, 30 min; gradient to 3000 V, 20 min; 3000 V, 210 min; pause on 50 V). Next, IPG strips were equilibrated for 15 min in 6.48×10^{-2} M DTT and 0.216 M iodoacetamide solution dissolved in equilibration buffer [6 M urea, 30% (w/v) glycerol, 69.2×10^{-3} M SDS in 0.05 M Tris-HCl buffer, pH 8.8] at room temperature. Molecular weight separation was conducted on a Bio-Rad Mini-Protean® Tetra System (50 mV, 10 min; 110 mV further on) via a 12.5% polyacrylamide gel. The molecular weight of the proteins was assessed by their visual mobilization in polyacrylamide gel and the predicted weight of the amino-acid sequence. The resulting gel was stained and de-stained as described above.

4.3.10 In-gel protein digestion

Protein spots of interest were excised from the SDS polyacrylamide gels, chopped into small pieces, and washed twice for 15 min in 100 µL of 0.05 M ammonium bicarbonate buffer, containing 50% acetonitrile (ACN) (v/v). Gel pieces were then dehydrated by the addition of 500 µL ACN and incubated at room temperature (RT) for 10 min. After decanting and a short air-drying, samples were supplemented with trypsin digestion buffer as previously established (Shevchenko et al., 2006). The tryptic digest was carried out at 37 °C overnight. On the next day, the sample was directly used for MALDI-TOF-MS analyses.

4.3.11 MALDI-TOF-MS analyses of proteins

For spectrometric identification of peptide patterns, 1 μL of protein digest solution was mixed with the same volume of α -Cyano-4-hydroxycinnamic acid solution (prepared in 85% ACN, 15% H_2O , 0.1% trifluoroacetic acid and 0.001 M ammonium dihydrogen phosphate), and spotted on a MTB AnchorChip target with an anchor diameter of 600 μm (Bruker Daltonics, Bremen, Germany). Spots were left for drying followed by an additional spotting of 1 μL of 2, 5-dihydroxybenzoic acid. After further drying the samples were subsequently submitted to an Auto flex II TOF/TOF mass spectrometer (Bruker Daltonics), which was used with standard parameters [acquisition range 500-4000 Da; S/N = 6, in specific cases 3; error range 50 ppm; allowed miss cleavages = 1; potential modifications ‘Oxidation (M)’]. Peptide masses derived from trypsin auto-digestion were used for calibration (842.50940; 1045.56370; 1713.80840; 1774.89750; 2083.00960; 2211.10400; 2283.18020 Da). Raw data were processed with Flex Analysis, version 3.0 (Bruker Daltonics). Protein identification was carried out using the Mascot search engine (Perkins et al., 1999), using the Bio-tools software, version 3.1 (Bruker Daltonics). Mass lists were searched against the NCBI database (Sayers et al., 2009). The restricting taxonomy frame for the search was set to “other eukaryotes” in the NCBI database, and the Mascot score probability was set at $p < 0.05$. Due to this setting, the significance threshold for a score was set between 70 and 80 (Perkins et al., 1999). Oxidation of methionine [‘Oxidation (M)’] was selected as variable modification. For fixed modifications, carbamidomethyl (C) was selected. The mass error for tryptic peptide identification was set at 50 ppm, and the measurements were done in positive ion mode.

4.3.12 Data analysis

The significance of variance was analyzed by analysis of variance (ANOVA) single factor analysis ($p < 0.05$) in Microsoft Office Excel.

4.4 Results

4.4.1 Screening for species with highest fucoxanthin production

Four species of diatoms were cultured in bottle PBRs under the same abiotic conditions with growth monitored daily. As seen in the growth curves (**Fig. 1A**), *C. closterium* showed a considerable advantage in maximum biomass accumulation over the other three species of diatoms ($p < 0.05$). The specific growth rate of *C. closterium* (**Fig. 1B**) was significantly higher than that of the other three species ($p < 0.05$), while no significant difference was found among the other three species. *C. closterium* accumulated the highest fucoxanthin content (21 mg/g in bottle PBRs) at the end of cultivation (**Fig. 1C**), which is 1-2-time higher when compared to *Phaeodactylum tricornutum*, *Amphora* sp., and *Thalassiosira weissflogii*. Among all four species, *T. weissflogii* produced the lowest fucoxanthin content (10 mg/g). Notably, the fucoxanthin productivity of *C. closterium* reached as high as 1.1 mg/L/day under 12/12 light/darkness cycle, which was 2-3-time more than *P. tricornutum*, *Amphora* sp. and *T. weissflogii* (**Fig. 1C**). Therefore, *C. closterium* was selected to optimize the light conditions in the next step.

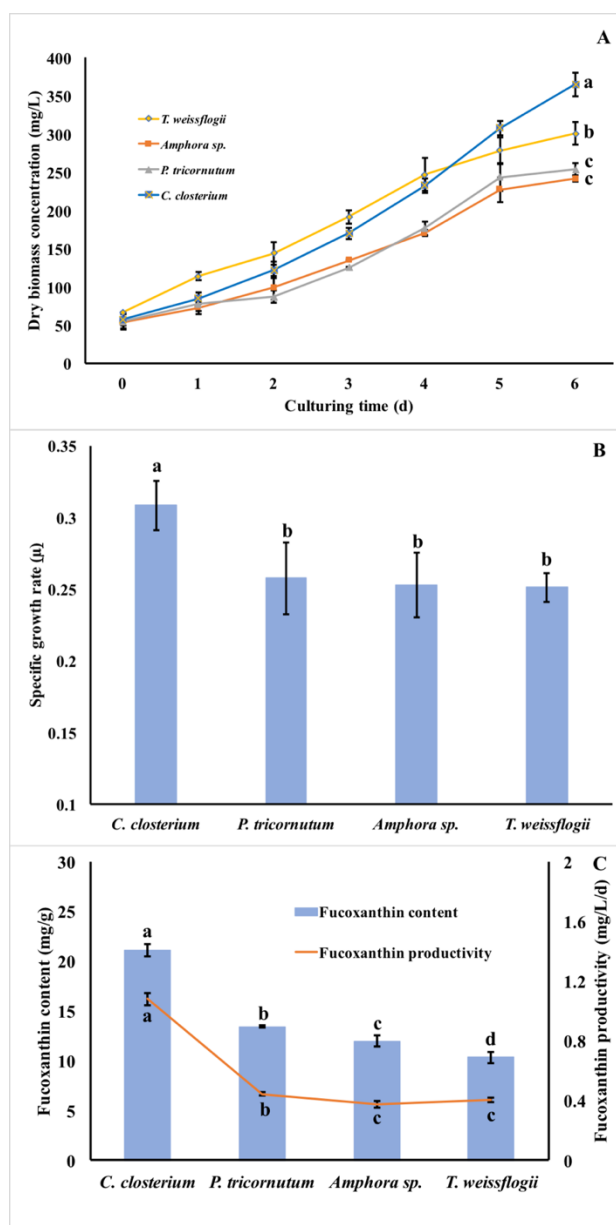


Figure 1: Screening of four diatom candidates. (A) Growth kinetics were monitored daily; (B) specific growth rate; (C) fucoxanthin content (column) and productivity (line) based on the dry biomass accumulation was quantified after a 6-day cultivation. The structure of fucoxanthin was inserted. Results are shown as mean \pm SD, $n = 3$. Lowercase letters indicate statistical differences, which was analyzed by ANOVA single-factor test with an alpha value of 0.05.

4.4.2 Predictions by “Design of Experiment” software

For optimization of fucoxanthin productivity in *C. closterium*, a “Design of Experiment” approach by software MODDE Pro 11 (<https://umetrics.com/product/modde-pro>) was chosen. Fucoxanthin content (mg/g), productivity (mg/L/day) and power input (W) were chosen as the response parameters for the predictive model. A total amount of 20 experiments led to prediction plots shown in **Fig. 2** with a 95% confidence interval. When the relation between a predicted response and a light condition was discussed in each panel (A-H) individually, the other two light variables were maintained under the set constant light conditions (blue LED light at 100 $\mu\text{mol}/\text{m}^2/\text{s}$ and 18/6 light regime). To the best of our knowledge, this study, for the first time, systematically compared the use of LED light to the equivalent fluorescent light. With 95% confidence interval overlapped, no difference was found between fluorescent light and the two types of LED lights with respect to fucoxanthin content, as illustrated in **Fig. 2A** at 100 $\mu\text{mol}/\text{m}^2/\text{s}$ and 18/6 light regime, though different spectra of light were emitted by the three different light sources. As indicated in **Fig. 3**, fluorescent light (grey line in **Fig. 3**), compared to the two different kinds of LED light, generated broader light spectra with multiple peaks between 400-410, 430-440, 480-500, and 530-630 nm with a higher percentage of red light (600-660 nm). There is no difference found in fucoxanthin content by increasing the photosynthetic active radiation (PAR) of blue LED light from 50 to 100 $\mu\text{mol}/\text{m}^2/\text{s}$ at 18/6 light regime (**Fig. 2B**) with the confidence interval overlapped. A photoperiod of 24 h substantially suppresses the accumulation of fucoxanthin content with blue LED light at 100 $\mu\text{mol}/\text{m}^2/\text{s}$, whereas 12/12 and 18/6 illumination cycles were favorable for fucoxanthin synthesis in *C. closterium* (**Fig. 2C**). For fucoxanthin productivity, both biomass accumulation and fucoxanthin content were taken into consideration. Fluorescent light exposure does not generate higher productivity as compared to exposures with two types of LED light (**Fig. 2D**) at 100 $\mu\text{mol}/\text{m}^2/\text{s}$ and 18/6 light regime. Blue LED light at 100 $\mu\text{mol}/\text{m}^2/\text{s}$ led to more fucoxanthin productivity than 50 $\mu\text{mol}/\text{m}^2/\text{s}$ but not 75 $\mu\text{mol}/\text{m}^2/\text{s}$ (**Fig. 2E**) under 18/6 light cycle. As indicated in **Fig. 2F**, blue LED light under 18/6 light regime increased fucoxanthin productivity remarkably as opposed to a 12/12 or 24/0 regime at 100 $\mu\text{mol}/\text{m}^2/\text{s}$. A response surface plot revealing the relation between fucoxanthin productivity, the light intensity and regime of blue LED light is provided in the supplementary material (**Fig. S1**). According to the prediction in **Fig. 2G**, the illumination by the blue LED light could save half or even three-fourths of the power input

compared to red & blue LED or fluorescent light, respectively, at the given constant light conditions. More power (50%) was needed to generate $100 \mu\text{mol}/\text{m}^2/\text{s}$ than $50 \mu\text{mol}/\text{m}^2/\text{s}$ of blue LED light (**Fig. 2H**). Since illumination durations (72 h) were the same under different light regimes, no difference was observed in power input between different photoperiods with blue LED light (**Fig. 2I**). Blue LED, with one-quarter of the power input, could produce comparable fucoxanthin productivity to fluorescent light at $100 \mu\text{mol}/\text{m}^2/\text{s}$ and an 18/6 light regime. Consequently, optimal light conditions (blue LED light at a light intensity of $100 \mu\text{mol}/\text{m}^2/\text{s}$ and an 18/6 light/darkness cycle) were predicted to produce a maximum fucoxanthin production of 1.9 mg/L/day and a fucoxanthin content of 24.5 mg/g in dry weight under the minimum energy demand of 0.055 kWh/L/day.

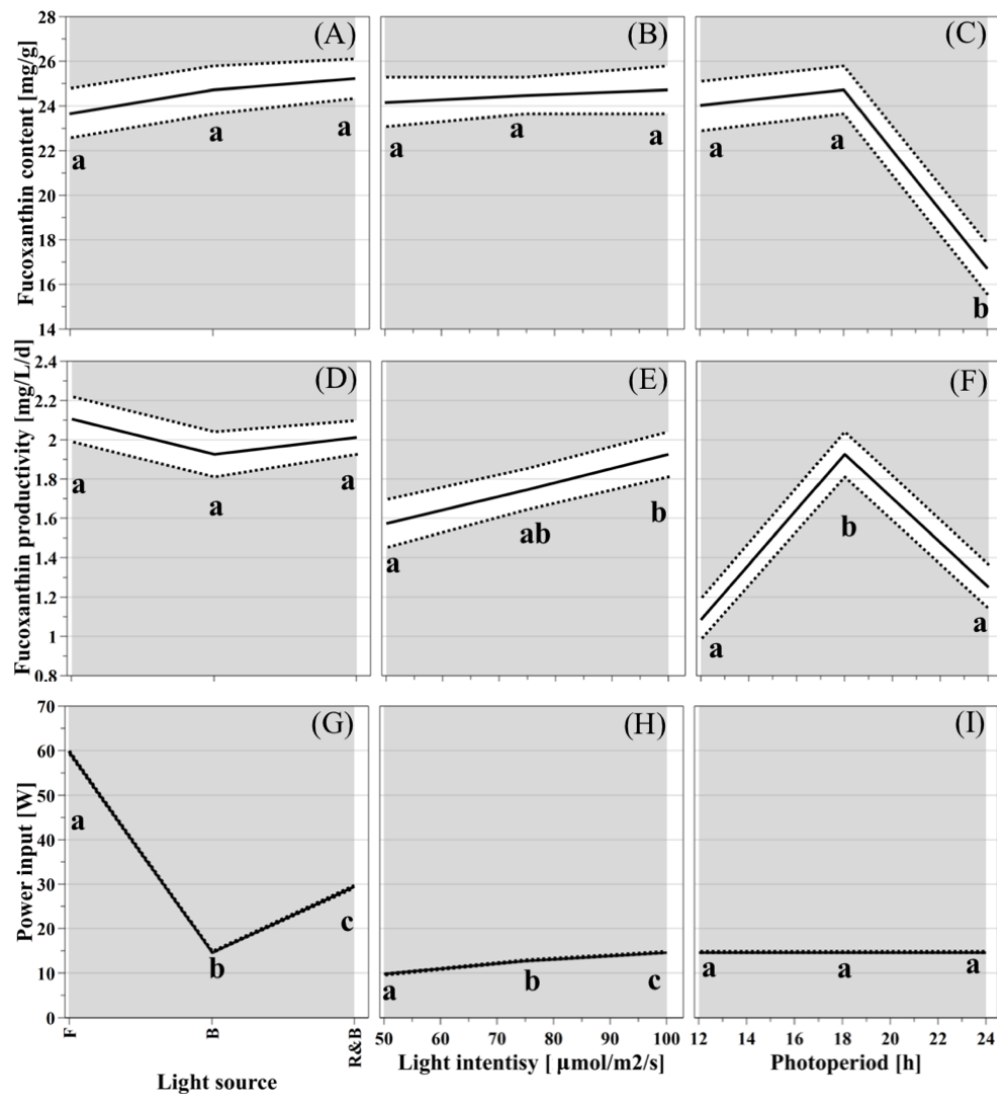


Figure 2: The prediction plots of “Design of Experiment”. The solid line represents the predicted value, while the dashed line represents the upper and lower limits of the confidential interval (95%). A, D and G: The predicted responses of fucoxanthin content, fucoxanthin productivity and power input to light source, respectively, at $100 \mu\text{mol}/\text{m}^2/\text{s}$ and 18/6 light regime; B, E and H: the predicted responses of fucoxanthin content, fucoxanthin productivity and power input to light intensity, respectively, at 18/6 light regime with blue LED light; C, F and I: The predicted response of fucoxanthin content, fucoxanthin productivity and power input to light regime, respectively, at $100 \mu\text{mol}/\text{m}^2/\text{s}$ with blue LED light. Lowercase letters indicate statistical differences.

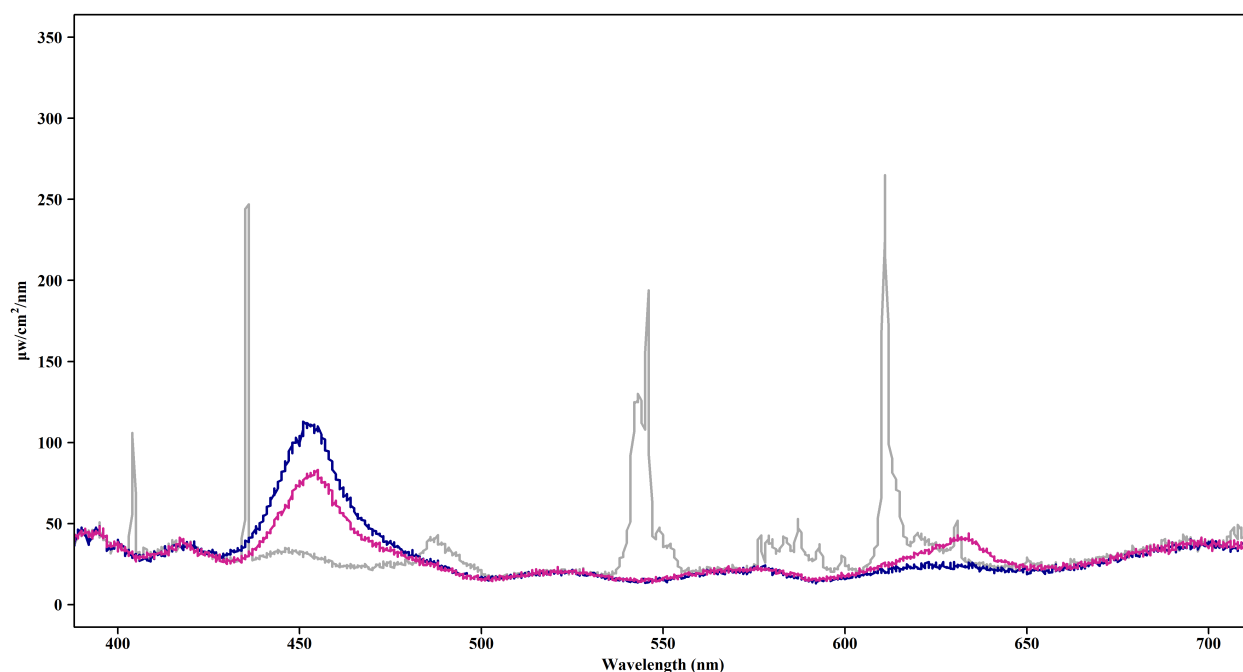


Figure 3: Spectra of fluorescent light, blue and red mixed with blue LED light. Grey line: fluorescent light; blue line: blue LED light; purple line: red & blue LED light.

4.4.3 Test for large-scale production in bag PBRs

The predicted outcome of the optimal combination of light variables was validated in the bottle PBRs and bag PBRs (**Fig. 4**). The biomass productivity during 4 days cultivation was found to be 76 mg/L/day in bottle PBRs versus 57 and 41 mg/L/day in bag PBRs under constant light and flashing light respectively. This decreased biomass productivity in the bags PBRs may have been caused by a lower ratio of the aeration flow rate versus volume and light penetration rate of blue LED light in bag PBRs. A fucoxanthin content of 23.6 mg/g and productivity of 1.8 mg/L/day was obtained in the bottle PBRs (**Fig. 4**). These actual values were close to the predicted values of 24.5 mg/g content and 1.9 mg/L/day productivity of fucoxanthin thus proving the reliability and validity of the experimental matrix. The fucoxanthin content and fucoxanthin productivity in bag PBRs with continuous illumination during daytime reached 25.5 mg/g (an increase of 8%) and 1.4 mg/L/day (22% less), as compared to the respective values from the bottle PBRs (**Fig. 4**). Flashing light cultivation mode only needed half the energy consumption of continuous light cultivation,

however, a noticeable decrease was observed in fucoxanthin productivity, which only reached 64% of the fucoxanthin productivity in continuous illumination (**Fig. 4**).

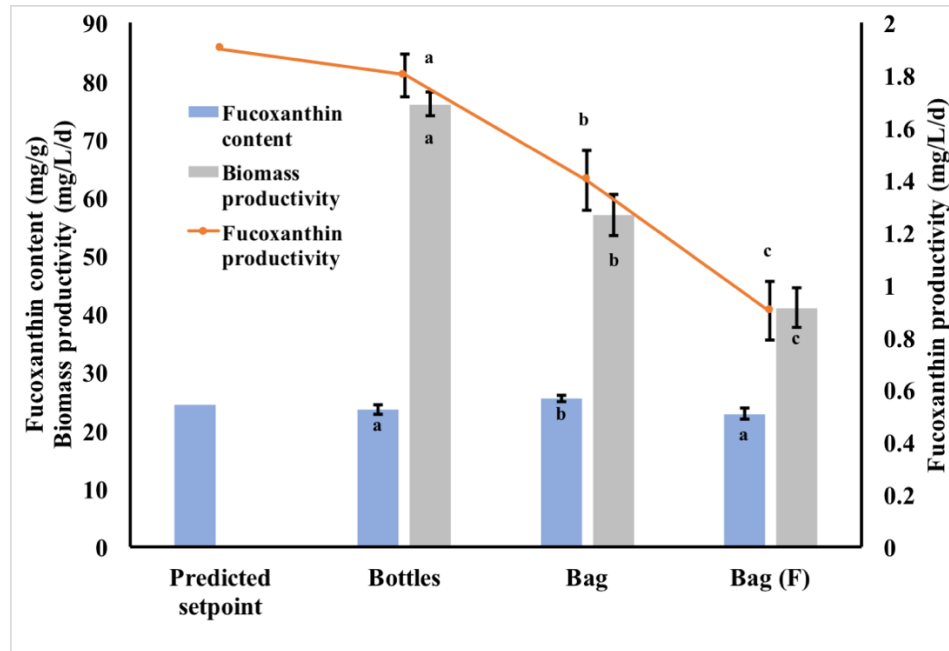


Figure 4: Confirmation of optimal light condition in bottle and bag PBRs. Fucoxanthin content and biomass productivity are represented by columns and productivity by line. Data was shown in mean \pm SD, $n = 3$. Lowercase letters indicate statistical differences, which was analyzed by an ANOVA single-factor test with an alpha value of 0.05.

4.4.4 Protein content and sodium dodecyl sulfate-polyacrylamide gel electrophoresis analyses using sodium dodecyl sulphate–dithiothreitol buffer

In diatoms, fucoxanthin is primarily bound to proteins to form an FCP complex, and it would be scientifically interesting to investigate the changes in protein profiles in response to light period changes. A proteomics study was conducted to get a deeper insight and hence, proteins were extracted from algal biomass. To obtain optimal amounts of cellular protein extracts, several methods were compared. The determined values of proteins extracted from *C. closterium* using conventional methods are shown in **Fig. S2**. Different extraction buffers led to different yields of solubilized proteins with the sodium dodecyl sulphate–dithiothreitol (SDS-DTT) buffer extraction yielding 2.5- to 5-time more extracted proteins as compared to the Tris buffer-based, pH 8.0 (buffer control) and the water-based (control) extraction methods (**Fig. S2**). Additionally, the yield of the SDS-DTT buffer extraction showed a 1.5- to 2-time rise as compared to the yield obtained by the methods using homogenization or ultra-sonication (**Fig. S2**). SDS-DTT buffer and the chemical method showed similar extractability of the solubilized proteins from *C. closterium*. However, we proceeded with SDS-DTT buffer as it yielded better protein extractability and already had been established successfully for protein extraction from higher plants such as *Theobroma cacao* (Kumari et al., 2016) (Kumari et al., 2018).

To assess the overall quality of the proteins extracted from *C. closterium*, sodium dodecyl sulfate-polyacrylamide gel electrophoresis (SDS-PAGE) analysis was conducted (**Fig. 5**). The SDS-PAGE profiles of the extracted proteins showed high-intensity protein bands at 15, 17, 19, 25, 45, and 55-kDa (**Fig. 5B**). Furthermore, the SDS-PAGE analysis demonstrated that high yields of proteins could be obtained from dry biomass, and indicated that the used protein quantification data (**Fig 5A**) are reliable indicators for total protein amount.

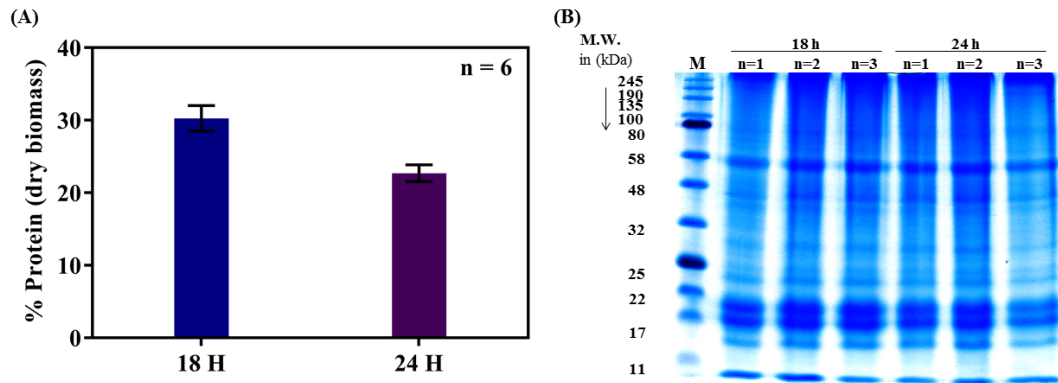


Fig. 5: Quantification and visualization of proteins by Bradford assay and SDS-PAGE analysis. (A) Total proteins were extracted from the marine diatom *Cylindrotheca closterium* for 18 h and 24 h using SDS-DTT buffer and were quantified using BCA as percentage protein of dried biomass. Bovine serum albumin was used as a standard for calibration, and the absorbance was measured at 562 nm. Measurements were done in triplicates and repeated twice. **(B)** The protein fractions were separated on 12.5% polyacrylamide gels and stained with Coomassie G-250. Standard protein markers were run for molecular mass determination. The three samples (n=1, n=2, and n=3) were biological replicates both for the 18 h and 24 h sample.

4.4.5 Protein annotation via MALDI-TOF-MS analyses

Proteins extracted from biomass samples from 18 h and 24 h were subjected to two-dimensional polyacrylamide gel electrophoresis (2D-PAGE) analysis (**Fig. 6**), which separates protein both by molecular weight and isoelectric point (pI). Electrophoresis revealed well-resolved protein spots with little streaking. Most of the extracted proteins appeared to be acidic with pIs between pH 3 and 5. The 2D-PAGE of the 18 h sample (**Fig. 6A**) showed higher-intensity and well-resolved protein spots as compared to the 24 h sample (**Fig. 6B**). Subsequently, protein spot excision and proteolytic cleavage followed by MALDI-TOF mass spectrometry showed that out of the 9 well-resolved spots (marked with red circles in **Fig. 6**), three of the peptide mass fingerprints (spot no. 5, 8 and 9) revealed poor spectra with low intensities and could not be attributed to known protein sequences in the database. The remaining six protein spots were identified with high confidence following database searches and exhibited high intensity peptide mass fingerprint spectra attributable to proteins from the diatom *C. closterium* (**Fig. 6**). The protein spot numbers, matching accession numbers (NCBI and Uniprot), corresponding protein names with predicted functions and the experimental and theoretical molecular weights and pIs for each protein are summarized in **Table S1**. All six highly expressed proteins from the two *C. closterium* cultures were critical chloroplast proteins, most of which are directly involved in photosynthesis. In terms of their predicted functions, protein spot no. 1 and 6 were assigned to the smaller and the larger subunit of the enzyme ribulose-1,5-biphosphate carboxylase/oxygenase (RuBisCO) based on their peptide fragment patterns (**Fig. S3**). Spot no. 4 was identified as the RuBisCO operon transcription regulator. Spot no. 2 and 3 were assigned to the chloroplastic ATP synthase subunits b and a, respectively. Finally, protein spot no. 7 displayed a peptide fragment pattern indicative of the ATP-dependent zinc metalloprotease, FtsH.

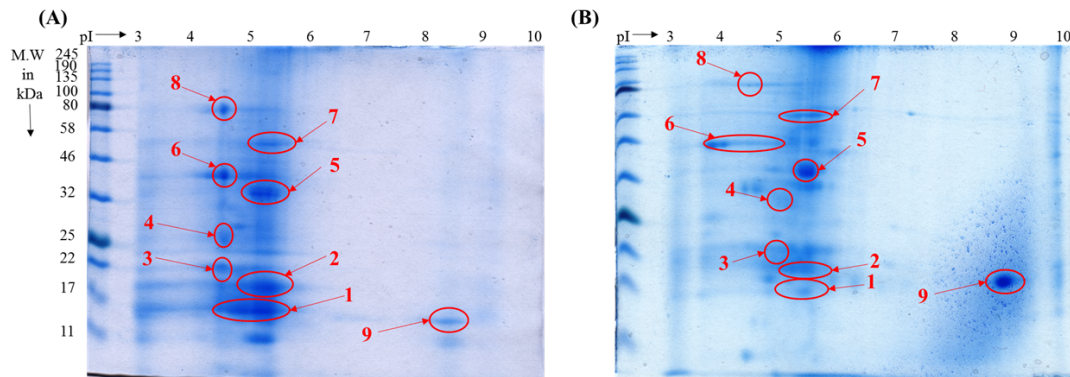


Fig. 6: *Cylindrotheca closterium* protein visualization by two-dimensional gel electrophoresis. Total proteins were extracted from the marine diatom *Cylindrotheca closterium* from 18 h (A), and 24 h (B) dried biomass samples using SDS-DTT buffer. Sample proteins (120 μ g) were loaded per gel, and standard protein markers were run on each gel for molecular mass determination. A total of 9 proteins were excised and subjected to MALDI-TOF-MS analyses, out of which only six were identified with high confidence and attributed to *C. closterium*.

4.5 Discussion

4.5.1 Screening for species with the highest fucoxanthin production

It was previously reported that one strain of the *C. closterium*, cultivated in f/2 medium in the presence of antioxidant agents accumulated approximately 10 mg/g of fucoxanthin in dry biomass after a 17-day cultivation (Erdoğan et al., 2016), which corresponds to only half of the accumulated fucoxanthin content obtained in this experiment. This difference could be attributed to the differences in the growth stage of the algal cultures during fucoxanthin collection. The fucoxanthin content of the marine diatom *Odontella aurita* decreased after reaching the late exponential phase under 100 μ mol photons/m²/s (Xia et al., 2013). For this reason, in our study, *C. closterium* was harvested during the late exponential phase and, as a result, synthesized remarkably higher fucoxanthin content, further highlighting the importance of harvesting time. *P. tricornutum* and *O. aurita*, exhibited high fucoxanthin productivity of approximately 0.2 mg/L/day under autotrophic cultivation (Guo et al., 2016), which by contrast is more than five times lower than the *C. closterium* culture selected in this study. Another high fucoxanthin-containing *P. tricornutum*

(42.8 mg/g maximum specific fucoxanthin content) was reported previously (McClure et al., 2018), but the actual specific fucoxanthin productivity (0.64 mg/L/day) was reported to be only 60% of that of *C. closterium* from this study. Furthermore, *C. closterium*, under calm water without aeration, rapidly settles to the bottom of the bioreactor because of its benthic characteristics (Kingston, 2009), which is beneficial for lowering dewatering costs during downstream harvesting processes. Consequently, *C. closterium* could serve as an excellent candidate for future mass fucoxanthin production.

4.5.2 Predictions by “Design of Experiment” software

The application of “Design of Experiment” approach significantly increased the efficiency of experimentation. The prediction of fucoxanthin content (**Fig. 2A-C**) indicated no remarkable increase of fucoxanthin was induced by sole blue light at the same photosynthetic PAR and light/darkness cycle, though fucoxanthin prefers visible blue light (Kuczynska et al., 2015). We propose that the high light intensity caused a significant reduction of fucoxanthin content due to photo-inhibition, as was demonstrated in the marine diatom *O. aurita*, where the fucoxanthin content dropped significantly under 300 $\mu\text{mol}/\text{m}^2/\text{s}$ as compared to 100 $\mu\text{mol}/\text{m}^2/\text{s}$ light intensity (Xia et al., 2013). This agreed with the prediction of our model, where a light intensity of 100 $\mu\text{mol}/\text{m}^2/\text{s}$ induced more fucoxanthin synthesis in *C. closterium* with blue LED light at an 18/6 regime. From the prediction of fucoxanthin productivity (**Fig. 2D-F**), it can be concluded that the photoperiod, not the light type nor light intensity, is the most influential parameter for optimal fucoxanthin biosynthesis in the present experimental matrix. Blue LED light, due to its low energy consumption (one-quarter of the power for fluorescent light), at 100 $\mu\text{mol}/\text{m}^2/\text{s}$ and an 18/6 light/darkness cycle was predicted to maximize fucoxanthin productivity and minimize energy consumption.

4.5.3 Test for large-scale production in bag PBRs

The performance of fucoxanthin production in both bottle and bag PBRs suggested that *C. closterium* in the present study is one of the highest fucoxanthin-producing strains so far tested in bioreactors, compared to the fucoxanthin-producing algae listed in a previous study (Petrushkina

et al., 2017). In *P. tricornutum*, fucoxanthin productivity in panel PBRs with f/2 medium was found to be 0.72 mg/L/day (McClure et al., 2018), which is half of the productivity of *C. closterium*, and 2.16 mg/L/day, in tenfold f/2 medium at 150 $\mu\text{mol}/\text{m}^2/\text{s}$ with five times more nitrogen consumption than in our study (McClure et al., 2018). The low nitrogen consumption and energy demand (0.07 kWh/L/day including both illumination and aeration) used in our study will significantly reduce the cost of cultivation. The decrease of fucoxanthin productivity by flashing light could be that the flashing light mode is only beneficial to photosynthesis and secondary metabolites production with an excess amount of PAR to avoid the induction of photo-inhibition. PAR was not high enough to trigger severe photo-inhibition and degradation of fucoxanthin in this study. Considering that 64% of the fucoxanthin productivity was generated by using 50% energy consumption, the efficiency of light absorption was higher in flashing light cultivation. In the future, flashing LED light with a higher PAR will be tested. Ultimately, advantages such as the high expandability, low cost, ease of construction, and high energy efficiency make bag PBRs outcompete panel and column PBRs in large-scale algal plant construction.

4.5.4 Protein annotation via MALDI-TOF-MS analyses

RuBisCO is a hexadecamer complex of 550 kDa, consisting of eight larger (50-55 kDa) and eight smaller (12-15 kDa) subunits (ChemgaPedia), found in all higher plants, algae, and cyanobacteria. RuBisCO is involved in converting atmospheric carbon dioxide into energy-rich organic molecules, such as glucose, by all photosynthetic organisms (Dhingra et al., 2004). In the red algae *Cyanidioschyzon merolae*, chloroplasts can autonomously activate the RuBisCO operon transcription regulator, which controls the expression of RuBisCO genes (Kusano and Sugawara, 1993) in response to the activation of photosynthesis during the dark-light shift (Minoda et al., 2010). In that study, incubation of *C. merolae* for 16 h in the dark (8:16 h light/darkness) led to an increase of RuBisCO. A similar trend was observed in this study (spot no. 1 and 6) in **Fig. 6**. The *C. closterium* RuBisCO operon transcription regulator was expressed in the 18 h illumination sample, possibly due to a dark period of 6 h, and was down-regulated under the permanent light as seen in the form of the 25-kDa protein bands (spot no. 4) in **Fig. 6**.

Chloroplastic ATP synthase is involved in energy conservation in the form of ATP, and therefore is a critical component of the proton channel and plays a direct role in the translocation of protons across the membrane (Clement et al., 2017; Kamikawa et al., 2015). The absence of a dark period (24 h illumination) might have led to a down-regulation of energy generation proteins such as ATP synthase, as reported previously (Feng et al., 2015) and as seen in our study, where both subunits (17 and 19 kDa) were more expressed in the 18 h illumination sample as compared to permanent illumination sample (spot no.2 and 3) in **Fig. 6**. We speculate that the turnover of photosynthesis between light-dependent and light-independent phase was disturbed by the 24 h photoperiod. In the light-independent phase of photosynthesis, the down-regulation of RuBisCO and ATP synthase reduces CO₂ fixation, NADPH consumption, and energy (in the form of ADP) turnover back to the reaction center of photo-systems in the light-dependent phase (Sysoeva et al., 2010). This reduction results in an ultimate overload of electron transportation and photo-oxidation in photosystems. For diatoms, it has previously been observed that the protein-bound diadinoxanthin cycle pigments participate in a mechanism of non-photochemical quenching (Kuczynska et al., 2015).

ATP-dependent zinc metalloprotease, FtsH, belongs to the family of ATP-dependent proteases and is localized in the chloroplast (Marbach et al., 2001). Like in most photosynthetic organisms, in *Chlamydomonas* spp, FtsH was demonstrated to play a vital role in diverse protein degradation and maturation mechanisms, degradation of the photo-system (PS) II reaction center D1 protein, regulation of cytochrome b6 levels, and as a molecular chaperone involved in protein assembly (Szyszka-Mroz et al., 2015). The down-regulation of FtsH during permanent illumination in this study may indicate that there was an induction of photo-inhibition in *C. closterium* (spot no.7 in **Fig 6**). Since the PS II, and particularly its D1 protein, in the reaction center is subject to photo-damage, the efficiency of photosynthesis depends on the restoration of this photo-system. This repair consists of the degradation of damaged D1 protein by FtsH and re-assembly of the PS II with de-novo synthesized D1 protein (Krynická et al., 2015) (Campbell et al., 2013). Consequently, a repressed repair rate of PS II during 24 h illumination could have led to a reduction of fucoxanthin content as the antenna in the form of fucoxanthin-chlorophyll a/c complexes in PS II.

In this experiment, the differently expressed proteins under an 18/6 (favorable for fucoxanthin synthesis) and a 24/0 (least favorable) light regime were determined. These differentially expressed proteins were found to be key enzymes involved in photosynthesis, but not in the de novo fucoxanthin biosynthesis. In conclusion, fucoxanthin content is intimately correlated with photosynthetic efficiency and could be further induced by an increased turnover rate between light-dependent and independent reactions. Furthermore, this work provides a novel perspective for rational, genetic engineering of fucoxanthin where future investigations could focus on the essential genes of photosynthesis, as well as the genes along the de novo fucoxanthin biosynthesis pathway.

4.6 Conclusions

Due to its excellent growth performance and fucoxanthin productivity, the marine diatom *C. closterium*, was selected for optimizing illumination conditions using an experimental matrix design, where blue LED light, as an alternative to fluorescent light, induced maximum fucoxanthin productivity and minimum energy consumption at 100 $\mu\text{mol}/\text{m}^2/\text{s}$ and an 18/6 light/darkness cycle. Fucoxanthin productivities of 1.8 and 1.4 mg/L/day were achieved in bottle and bag PABs, respectively, with the highest fucoxanthin content of 25.5 mg/g attained in bag PBRs, which may be suitable devices for follow-up, large-scale production. Proteins induced by LED light illumination were identified by MALDI-TOF-MS. Convincingly, the up-regulation of key proteins involved in photosynthesis, energy conservation, and PS II repair mechanisms under 18 h illumination may have resulted in a higher photosynthetic efficiency as compared to permanent illumination (24 h). Our results shed valuable light on fucoxanthin regulation by photosynthesis in diatoms. Fucoxanthin, aside from the de novo biosynthesis, also correlates with photosynthetic efficiency. To further increase the fucoxanthin production, future investigations should focus on the augmentation of photosynthetic efficiency, for example, the increase of the bio-availability of CO_2 and over-expression of the photosynthetic-related genes.

Acknowledgement

The authors appreciate the excellent assistance of Neha Kumari in the protein analysis and Jiemin Du and Annika Moje in fucoxanthin quantification, Dr. Vladislav Jovanov and Prof. Veit Wagner in spectrometer analysis and Sven Klüber in PBR construction. We are grateful for the effort from Candice Thorstenson for polishing the language.

Authors' contributions

Song Wang performed the experiment, interpreted the data and drafted the manuscript. Sujit K. Verma carried out the proteomics experiment with Song Wang and wrote part of the manuscript. Inamullah Hakeem Said established the fucoxanthin quantification method with Song Wang and reviewed the manuscript. Laurenz Thomsen, Matthias S. Ullrich, and Nikolai Kuhnert supervised the experiment, reviewed and gave critical comments on the manuscript.

4.7 Reference

- Armbrust, E.V. (2009) The life of diatoms in the world's oceans. *Nature* **459**, 185-192.
- Bai, X., Song, H., Lavoie, M., Zhu, K., Su, Y., Ye, H., Chen, S., Fu, Z. and Qian, H. (2016) Proteomic analyses bring new insights into the effect of a dark stress on lipid biosynthesis in *Phaeodactylum tricornutum*. *Scientific Reports* **6**, 25494.
- Beuzenberg, V., Goodwin, E.O., Puddick, J., Romanazzi, D., Adams, S.L. and Packer, M.A. (2016) Optimising conditions for growth and xanthophyll production in continuous culture of *Tisochrysis lutea* using photobioreactor arrays and central composite design experiments. *New Zealand Journal of Botany*, 64-78
- Campbell, D.A., Hossain, Z., Cockshutt, A.M., Zhaxybayeva, O., Wu, H. and Li, G. (2013) Photosystem II protein clearance and FtsH function in the diatom *Thalassiosira pseudonana*. *Photosynthesis Research* **115**, 43-54.
- ChemgaPedia
http://www.chemgapedia.de/vsengine/vlu/vsc/de/ch/8/bc/vlu/photosynthese/ps_dark.vlu/Page/vsc/de/ch/8/bc/stoffwechsel/photosynthese/rubisco4.vscml.html.
- Clement, R., Lignon, S., Mansuelle, P., Jensen, E., Pophillat, M., Lebrun, R., Denis, Y., Puppo, C., Maberly, S.C. and Gontero, B. (2017) Responses of the marine diatom *Thalassiosira pseudonana* to changes in CO₂ concentration: a proteomic approach. *Scientific Reports* **7**, 42333.
- Dhingra, A., Portis, A.R.J. and Daniell, H. (2004) Enhanced translation of a chloroplast-expressed RbcS gene restores small subunit levels and photosynthesis in nuclear RbcS antisense plants. *Proceedings of the National Academy of Sciences of the United States of America* **101**, 6315-6320.
- Dong, H.P., Dong, Y.L., Cui, L., Balamurugan, S., Gao, J., Lu, S.H. and Jiang, T. (2016) High light stress triggers distinct proteomic responses in the marine diatom *Thalassiosira pseudonana*. *BMC Genomics* **17**, 994.
- Erdoğan, A., Demirel, Z., Dalay, M.C. and Eroglu, A.E. (2016) Fucoxanthin content of *Cylindrotheca closterium* and its oxidative stress mediated enhancement. *Turkish Journal of Fisheries and Aquatic Sciences* **16**, 499-506.

- Feng, T.Y., Yang, Z.K., Zheng, J.W., Xie, Y., Li, D.W., Murugan, S.B., Yang, W.D., Liu, J.S. and Li, H.Y. (2015) Examination of metabolic responses to phosphorus limitation via proteomic analyses in the marine diatom *Phaeodactylum tricornutum*. *Scientific Reports* **5**, 10373.
- Glemser, M., Heining, M., Schmidt, J., Becker, A., Garbe, D., Buchholz, R. and Brück, T. (2016) Application of light-emitting diodes (LEDs) in cultivation of phototrophic microalgae-current state and perspectives. *Applied Microbiology and Biotechnology* **100**, 1077-1088.
- Guillard, R.R.L. (1975) Culture of phytoplankton for feeding marine invertebrates. In: *Culture of Marine Invertebrates Animals* (Smith, W.L. and Chanley, M.H. eds), pp. 26-60. New York, USA: Plenum Press.
- Guo, B., Liu, B., Yang, B., Sun, P., Lu, X., Liu, J. and Chen, F. (2016) Screening of diatom strains and characterization of *Cyclotella cryptica* as a potential fucoxanthin producer. *Marine Drugs* **14**, 125.
- Hempel, N., Petrick, I. and Behrendt, F. (2012) Biomass productivity and productivity of fatty acids and amino acids of microalgae strains as key characteristics of suitability for biodiesel production. *Journal of Applied Phycology* **24**, 1407-1418.
- Kamikawa, R., Tanifuji, G., Ishikawa, S.A., Ishii, K., Matsuno, Y., Onodera, N.T., Ishida, K., Hashimoto, T., Miyashita, H., Mayama, S. and Inagaki, Y. (2015) Proposal of a twin arginine translocator system-mediated constraint against loss of ATP synthase genes from nonphotosynthetic plastid genomes. *Molecular Biology and Evolution* **32**, 2598-2604.
- Katsuda, T., Lababpour, A., Shimahara, K. and Katoh, S. (2004) Astaxanthin production by *Haematococcus pluvialis* under illumination with LEDs. *Enzyme and Microbial Technology* **35**, 81-86.
- Kim, S.M., Jung, Y.J., Kwon, O.N., Cha, K.H., Um, B.H., Chung, D. and Pan, C.H. (2012) A potential commercial source of fucoxanthin extracted from the microalga *Phaeodactylum tricornutum*. *Applied Biochemistry and Biotechnology* **166**, 1843-1855.
- Kingston, M.B. (2009) Growth and motility of the diatom *Cylindrotheca closterium*: implications for commercial applications. *Journal of the North Carolina Academy of Science* **125**, 138-142.

- Krynická, V., Shao, S., Nixon, P.J. and Komenda, J. (2015) Accessibility controls selective degradation of photosystem II subunits by FtsH protease. *Nature Plants*, Article number: 15168.
- Kuczynska, P., Jemiola-Rzeminska, M. and Strzalka, K. (2015) Photosynthetic pigments in diatoms. *Marine Drugs* **13**, 5847-5481.
- Kumari, N., Grimbs, A., D'Souza, R.N., Verma, S.K., Corno, M., Kuhnert, N. and Ullrich, M.S. (2018) Origin and varietal based proteomic and peptidomic fingerprinting of *Theobroma cacao* in non-fermented and fermented cocoa beans. *Food Research International* **111**, 137-147.
- Kumari, N., Kofi, K.J., Grimbs, S., D'Souza, R.N., Kuhnert, N., Vrancken, G. and Ullrich, M.S. (2016) Biochemical fate of vicilin storage protein during fermentation and drying of cocoa beans. *Food Research International* **90**, 53-65.
- Kuppusamy, P., Soundharajana, I., Srigopalrama, S., Yusoffa, M.M., Maniamb, G.P., Govindanb, N. and Choia, K.C. (2017) Potential pharmaceutical and biomedical applications of Diatoms microalgae - An overview. *Indian Journal of Geo-Marine Sciences* **46**, 663-667.
- Kusano, T. and Sugawara, K. (1993) Specific binding of *Thiobacillus ferrooxidans* RbcR to the intergenic sequence between the *rbc* operon and the *rbcR* gene. *Journal of Bacteriology* **175**, 1019-1025.
- Laemmli, U.K. (1970) Cleavage of structural proteins during the assembly of the head of bacteriophage T4. *Nature* **227**, 680.
- Lavaud, J., Rousseau, B. and Etienne, A.L. (2003) Enrichment of the light-harvesting complex in diadinoxanthin and implications for the nonphotochemical fluorescence quenching in diatoms. *Biochemistry*. **42**, 5802-5808.
- Liao, Q., Chang, H.X., Fu, Q., Huang, Y., Xia, A., Zhu, X. and Zhong, N. (2018) Physiological-phased kinetic characteristics of microalgae *Chlorella vulgaris* growth and lipid synthesis considering synergistic effects of light, carbon and nutrients. *Bioresource Technology* **250**, 583-590.
- Malviya, S., Scalco, E., Audic, S., Vincent, F., Veluchamy, A., Poulain, J., Wincker, P., Iudicone, D., de Vargas, C., Bittner, L., Zingone, A. and Bowler, C. (2016) Insights into global

- diatom distribution and diversity in the world's ocean. *Proceedings of the National Academy of Sciences of the United States of America* **113**, E1516-1525.
- Marbach, P.A.S., Coelho, A.S.G. and Silva-Filho, M.C. (2001) Mitochondrial and chloroplast localization of FtsH-like proteins in sugarcane based on their phylogenetic profile. *Genetics and Molecular Biology* **24**, 183-190.
- McClure, D.D., Luiz, A., Gerber, B., Barton, G.W. and Kavanagh, J.M. (2018) An investigation into the effect of culture conditions on fucoxanthin production using the marine microalgae *Phaeodactylum tricornutum*. *Algal Research* **29**, 41-48.
- Minoda, A., Weber, A.P., Tanaka, K. and Miyagishima, S.Y. (2010) Nucleus-independent control of the rubisco operon by the plastid-encoded transcription factor Ycf30 in the red alga *Cyanidioschyzon merolae*. *Plant Physiology* **154**, 1532-1540.
- Muhseen, Z.T., Xiong, Q., Chen, Z. and Ge, F. (2015) Proteomics studies on stress responses in diatoms. *Proteomics* **15**, 3943-3953.
- Nagao, R., Yokono, M., Teshigahara, A., Akimoto, S. and Tomo, T. (2014) Light-harvesting ability of the fucoxanthin chlorophyll a/c-binding protein associated with photosystem II from the Diatom *Chaetoceros gracilis* as revealed by picosecond time-resolved fluorescence spectroscopy. *Journal of Physical Chemistry B* **118**, 5093-5100.
- Peng, J., Yuan, J.P., Wu, C.F. and Wang, J.H. (2011) Fucoxanthin, a marine carotenoid present in brown seaweeds and diatoms: metabolism and bioactivities relevant to human health. *Marine Drugs* **9**, 1806-1828.
- Perkins, D.N., Pappin, D.J., Creasy, D.M. and Cottrell, J.S. (1999) Probability-based protein identification by searching sequence databases using mass spectrometry data. *Electrophoresis* **20**, 3551-3567.
- Petrushkina, M., Gusev, E., Sorokin, B., Zotko, N., Mamaeva, A., Filimonova, A., Kulikovskiy, M., Maltsev, Y., Yampolsky, I., Guglya, E., Vinokurov, V., Namsaraev, Z. and Kuzmin, D. (2017) Fucoxanthin production by heterokont microalgae. *Algal Research* **24**, 387-393.
- Sayers, E.W., Barrett, T., Benson, D.A., Bryant, S.H., Canese, K., Chetvernin, V., Church, D.M., DiCuccio, M., Edgar, R., Federhen, S., Feolo, M., Geer, L.Y., Helmberg, W., Kapustin, Y., Landsman, D., Lipman, D.J., Madden, T.L., Maglott, D.R., Miller, V., Mizrachi, I., Ostell, J., Pruitt, K.D., Schuler, G.D., Sequeira, E., Sherry, S.T., Shumway, M., Sirotkin, K., Souvorov, A., Starchenko, G., Tatusova, T.A., Wagner, L., Yaschenko, E. and Ye, J. (2009)

- Database resources of the national center for biotechnology information. *Nucleic Acids Research* **37**, D5-15.
- Schulze, P.S., Barreira, L.A., Pereira, H.G., Perales, J.A. and Varela, J.C. (2014) Light emitting diodes (LEDs) applied to microalgal production. *Trends in Biotechnology* **32**, 422-430.
- Shevchenko, A., Tomas, H., Havlis, J., Olsen, J.V. and Mann, M. (2006) In-gel digestion for mass spectrometric characterization of proteins and proteomes. *Nature Protocols* **1**, 2856-2860.
- Smith, P.K., Krohn, R.I., Hermanson, G.T., Mallia, A.K., Gartner, F.H., Frovenzano, M.D., Fujimoto, E.K., Goeke, N.M., Olson, B.J. and Klenk, D.C. (1985) Measurement of protein using bicinchoninic acid. *Analytical Biochemistry* **150**, 76-85.
- Sysoeva, M.I., Markovskaya, E.F., Shibaeva, T.G. and (2010) Plants under continuous light- A review. *Plant stress* **4**, 5-17.
- Szyszkka-Mroz, B., Pittock, P., Ivanov, A.G., Lajoie, G. and Huner, N.P. (2015) The antarctic psychrophile *Chlamydomonas* sp. UWO 241 preferentially phosphorylates a photosystem I-cytochrome b6/f supercomplex. *Plant Physiology* **169**, 717-736.
- Thomsen, C., Rill, S. and Thomsen, L. (2012) Case study with temperature controlled outdoor PBR system in Bremen. In: Posten, C, Walter C, editors. *Microalgal biotechnology: integration and economy, Chapter 4*. Berlin, Boston: De Gruyter **74–77**.
- Tran, N.P., Park, J.K. and Lee, C.G. (2009) Proteomics analysis of proteins in green alga *Haematococcus lacustris* (Chlorophyceae) expressed under combined stress of nitrogen starvation and high irradiance. *Enzyme and Microbial Technology* **45**, 241-246.
- Valenzuela, J., Carlson, R.P., Gerlach, R., K., C., Peyton, B.M., Bothner, B. and Fields, M.W. (2013) Nutrient resupplementation arrests bio-oil accumulation in *Phaeodactylum tricorutum*. *Applied Microbiology and Biotechnology* **97**, 7049–7059.
- Veith, T., Brauns, J., Weisheit, W., Mittag, M. and Buchel, C. (2009) Identification of a specific fucoxanthin-chlorophyll protein in the light harvesting complex of photosystem I in the diatom *Cyclotella meneghiniana*. *Biochimica et Biophysica Acta* **1787**, 905-912.
- Wang, S., Hakeem Said, I., Thorstenson, C., Thomsen, C., Ullrich, M.S., Kuhnert, N. and Thomsen, L. (2018) Pilot-scale production of antibacterial substances by the marine diatom *Phaeodactylum tricorutum* Bohlin. *Algal Research* **32**, 113-120.

- Wang, S., Zhang, L., Yang, G., Zhu, B. and Pan, K. (2015) Purification of a diatom and its identification to *Cylindrotheca closterium*. *Journal of Ocean University of China* **14**, 357-361.
- Woo, M.N., Jeon, S.M., Kim, H.J., Lee, M.K., Shin, S.K., Shin, Y.C., Park, Y.B. and Choi, M.S. (2010) Fucoxanthin supplementation improves plasma and hepatic lipid metabolism and blood glucose concentration in high-fat fed C57BL/6N mice. *Chemico-Biological Interactions* **186**, 316-322.
- Xia, S., Wang, K., Wan, L., Li, A., Hu, Q. and Zhang, C. (2013) Production, characterization, and antioxidant activity of fucoxanthin from the marine diatom *Odontella aurita*. *Marine Drugs* **11**, 2667-2681.

4.8 Supplementary material

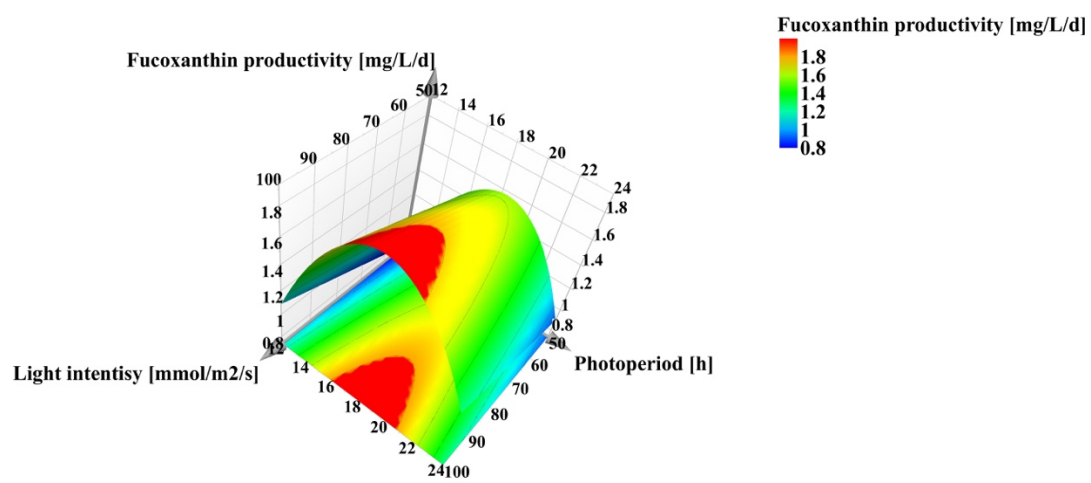


Figure S1. Surface response plot. It indicates relation between fucoxanthin productivity, light intensity and photoperiod with blue LED light.

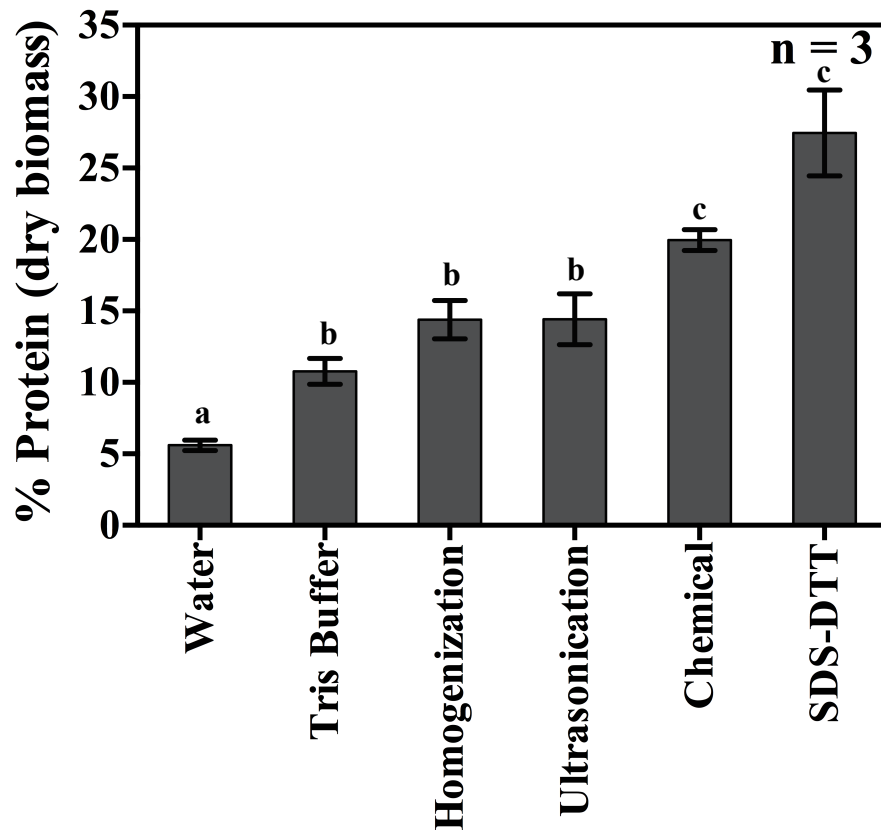


Figure S2: Quantification of proteins by Bradford assay (A). Total proteins were extracted from the marine diatom *Cylindrotheca closterium* using different extraction methodologies and were quantified using BCA as percentage protein of dried biomass. Bovine serum albumin was used as standard for calibration and the absorbance was measured at 562 nm. Measurements were done in triplicates. Lowercase letters indicate the statistical differences.

Ribulose-1,5-biphosphate carboxylase/oxygenase (RuBisCO), chloroplastic

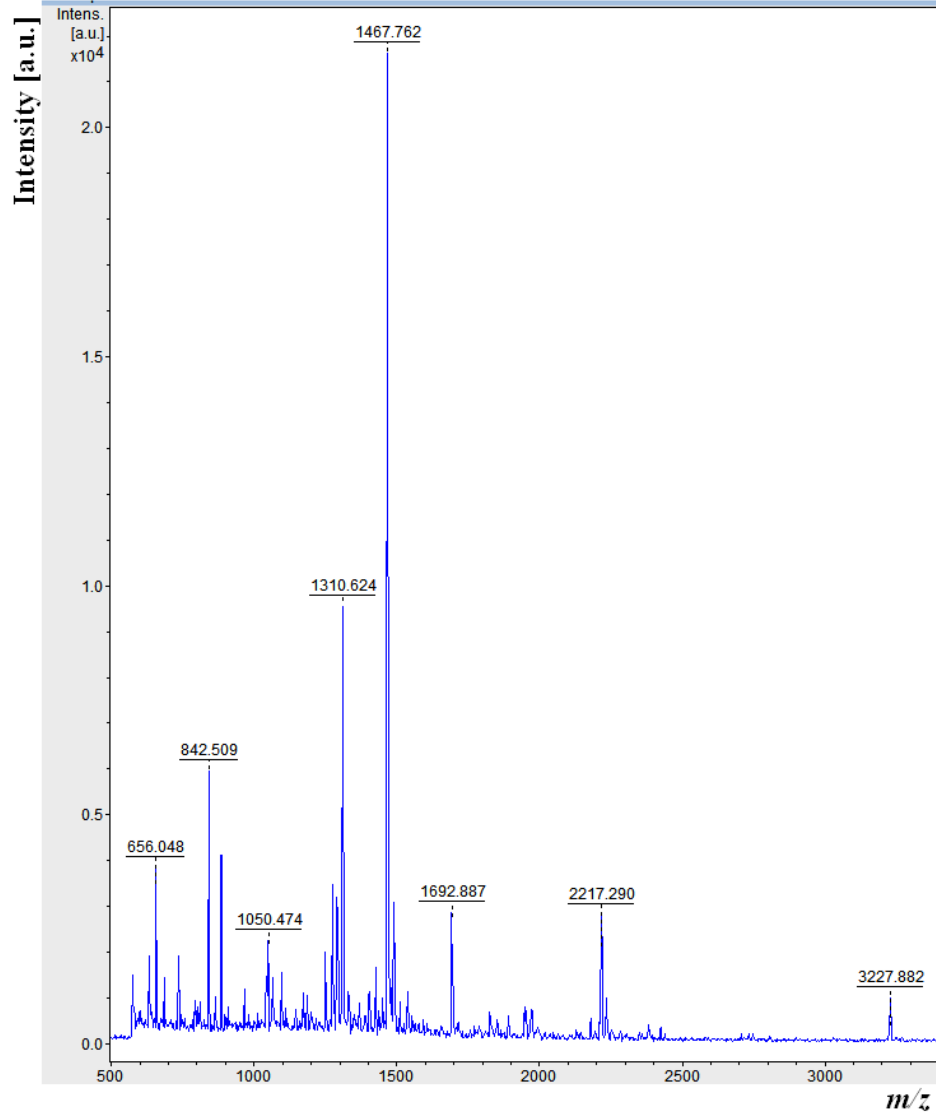


Figure S3: Peptide mass fingerprint mass spectra as observed by MALDI-TOF-MS analysis. MALDI-TOF-MS analysis of tryptically digested *Cylindrotheca closterium* protein spot. All prominent m/z ratio peaks from the MALDI MS spectra were subjected to MASCOT analysis and assigned to predicted peptide fragments of ribulose-1,5-biphosphate carboxylase/oxygenase (RuBisCO), chloroplastic.

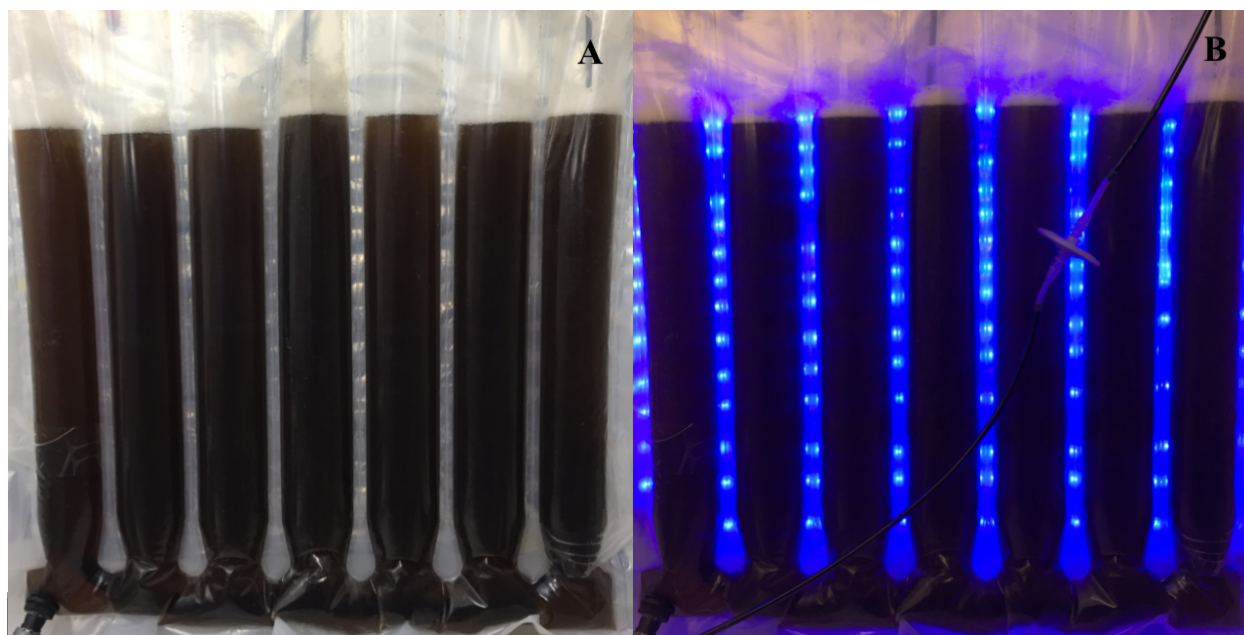


Figure S4: Bag photobioreactors with LED illumination. A: LED panel was off; B: blue LED light was applied to *Cylindrotheca closterium* cultivation.

Table S1: Summarized table for the proteins identified.

Spot ID	Accession No.	Accession No.	Annotation	Functional group	Experimental M.W. (kDa)/pI	Theoretical M.W. (kDa)/pI
	NCBI	UniProt				
1	YP_00902906 6.1	A0A023HC 89	Ribulose-1,5-biphosphate carboxylase/oxygenase (RuBisCO), small subunit	Photosynthesis	15/5.1	15.9/5.1
2	YP_00902907 3.1	A0A023HA Y6	ATP synthase subunit b, chloroplastic	Energy Metabolism	17/5.3	20.4/6.9
3	YP_00902907 0.1	A0A023HA H4	ATP synthase subunit a, chloroplastic	Energy Metabolism	19/4.5	26.9/4.5
4	YP_00902914 4.1	A0A023HA I9	RuBisCO operon transcription regulator	Photosynthesis	25/4.6	34.9/8.7
6	YP_00902906 7.1	A0A023HB P6	Ribulose-1,5-biphosphate carboxylase/oxygenase (RuBisCO), large subunit	Photosynthesis	45/4.5	54.0/6.1
7	YP_00902907 7.1	A0A023HB P8	ATP-dependent zinc metalloprotease FtsH	Cellular Functions	55/5.5	68.4/5.3

Spots, accession numbers (NCBI and Uniprot) and protein names with their functions and experimental M.W. and pI for each of the proteins identified by MALDI-TOF-MS studies.

5. Comparative lipidomic studies of *Scenedesmus* sp. (Chlorophyceae) and *Cylindrotheca closterium* (Bacillariophyceae) reveal their differences in lipid production under nitrogen starvation

Under revision by *Journal of Phycology*

Song Wang^{1*}, Diana Sirbu², Laurenz Thomsen¹, Nikolai Kuhnert², Matthias S. Ullrich², Claudia Thomsen³

¹ Department of Physics and Earth Sciences, Jacobs University Bremen, Campus Ring 1, 28759 Bremen, Germany

² Department of Life Science and Chemistry, Jacobs University Bremen, Campus Ring 1, 28759 Bremen, Germany

³ Phytolutions, iSeaMC GmbH, Campus Ring 1, Bremen, Germany

* Corresponding author: Song Wang, s.wang@jacobs-university.de

5.1 Abstract

Microalgae are a promising resource for highly sustainable production of various biomaterials (food, feed), high-value biochemicals or biofuels. However, factors influencing the valued lipid production from oleaginous algae require more investigation with detailed studies at the molecular level. This study elucidates the variations of lipid metabolites between a marine diatom (*Cylindrotheca closterium*) and a freshwater green alga (*Scenedesmus* sp.) under nitrogen starvation at the molecular level with a special emphasis on triacylglycerols using liquid chromatography-electrospray ionization mass spectrometry techniques. A comprehensive analysis of lipid biosynthesis was carried out by comparing the changes in total lipids, growth kinetics, fatty acids compositions, and glycerolipids profiles on the molecular level at different time points of nitrogen starvation. A total of sixty and seventy-two triacylglycerol molecules, along with many other polar lipids, were identified in *Scenedesmus* sp. and *C. closterium*, respectively providing the most abundant triacylglycerol profiles in these two species. During nitrogen starvation, more triacylglycerols of *Scenedesmus* sp. were synthesized by the “eukaryotic pathway” in the endoplasmic reticulum, whereas the increase of triacylglycerols in *C. closterium* after 96 h of nitrogen starvation was mainly contributed by the “prokaryotic pathway” in the chloroplast. The distinct responses of lipid synthesis to nitrogen starvation exhibited by the two species indicated different strategies of lipid accumulation, notably triacylglycerols, in green algae and diatoms. *Scenedesmus* sp. and *Cylindrotheca closterium* could serve as excellent candidates for mass production of biofuels or polyunsaturated fatty acids for nutraceutical purpose.

Keywords: Fatty acid, Glycolipids, HPLC-MS, Lipid, Lipidomics, Triacylglycerol

5.2 Introduction

One main challenge in algal biotechnology in the near future is the improvement of bio-refinery concepts for product extraction of high value and processing of the residual biomass for less valuable bulk products in feed, energy or chemicals (Chew et al., 2017). Microalgae are rich in high-value pigments, fatty acids, and other biomolecules and mostly have complete protein composition of high nutritious value (Becker, 2007; Yaakob et al., 2014). Algae encompass an

incredible diversity of lipids and fatty acids, the compositions of which vary significantly in different classes of algae (Harwood and Guschina, 2009). The lipids in algae can be classified into three groups: neutral lipids, glycolipids, and phospholipids accompanied by some betaine lipids (Kumari et al., 2013). Triacylglycerols (TAGs) as the most dominant form of neutral lipids are synthesized by algae in an adverse environment for the storage of carbon and energy, but the more physiological roles of TAGs have been unraveled (Hu et al., 2008; Solovchenko, 2012). Glycolipids predominated by monogalactosyldiacylglycerol (MGDG), digalactosyldiacylglycerol (DGDG) and sulfoquinovosyl diacylglycerol (SQDG) in algae are plastidial lipids, which are primarily present in the photosynthetic membrane, while phospholipids serve as the building blocks of the extra-plastidial membrane except for phosphatidylglycerol (PG) (da Costa et al., 2016; Kumari et al., 2013). Algal lipids as the feedstock for biodiesel production and polyunsaturated fatty acids have received extensive studies as summarized in previous reviews (Adarme-Vega et al., 2012; Faried et al., 2017).

However, high costs of algal biofuel production have, to date, prevented its widespread industrialization. Selection of algal species with an increased lipid content could cut down costs and thus make mass production more feasible (Chu, 2017). Stress strategies, such as the modifications of nutrient supply and environmental parameters, have already been successfully applied to algae cultivation to induce lipid synthesis (Benavente-Valdes et al., 2016). Among all stress induction approaches, nitrogen starvation has been the most thoroughly investigated one and has been found to cause an increase in lipid synthesis. For example, higher efficiency of lipid production in *Phaeodactylum tricorutum* was obtained when nitrogen availability was insufficient in media (Frada et al., 2013). Similarly, the biomass of the green algae *Neochloris oleoabundans* with higher lipid content was produced under nitrogen-depleted medium accompanied with the decrement of chlorophyll a (Li et al., 2008). It has been reported that the lipid content of *Scenedesmus obliquus* attained 22.4 % of the dry biomass by five-day nitrogen starvation (Ho et al., 2012). Besides, the different phenotypes induced by starvation offer an opportunity to study the lipid biosynthesis pathway in algae (Zhu et al., 2016).

Despite those interesting phenotypic observations, the lipid metabolisms of algae from different classes in response to nitrogen starvation are not well understood at the molecular level.

Comprehensive analyses of the changes in intact lipids, including neutral lipids and membrane lipids under nitrogen starvation have been carried out in model algae, such as *P. tricornutum* (Levitan et al., 2015), *Nannochloropsis oceanica* (Li et al., 2014), and *Chlamydomonas reinhardtii* (Yang et al., 2015). A recent study claimed that time-series lipidomes induced by nitrogen stress were studied for the first time in the non-model oleaginous species *Ettlia oleoabundans* (Matich et al., 2018). However, the knowledge of lipid metabolism under nitrogen starvation in other non-model oleaginous species remains unclear. The development of mass spectrometry-based methods enabled the comprehensive analysis of lipidome, of which shotgun lipidomics (Yang et al., 2015) and liquid chromatography-mass spectrometry (LC-MS) (Li et al., 2014; Matich et al., 2018) were used in the studies mentioned above. Combination of transcriptomic and lipidomic analyses in *N. oceanica* revealed that in a nitrogen-free medium the *de novo* fatty acid biosynthesis pathway was suppressed, but the pathway redirecting carbon flux from protein to lipid and carbohydrate was upregulated (Li et al., 2014). With the advance in RNA sequencing technology, the analysis of transcript abundance was successfully employed to elucidate the mechanism of lipogenesis in microalgae in response to nitrogen stress (Miller et al., 2010; Rismani-Yazdi et al., 2012). However, the metabolic and regulatory mechanisms of neutral lipids revealed at the transcript level should be confirmed by lipidomic analysis in various oleaginous species of commercial interest. This will eventually enable a rational manipulation of lipid biosynthesis for optimized biofuel production.

In the present study, detailed changes of lipids composition at the molecular level were determined with the HPLC-MS method, along with growth and fatty acids profile in response to nitrogen starvation in the freshwater green alga *Scenedesmus* sp. (Chlorophyceae) and the marine diatom *Cylindrotheca closterium* (Bacillariophyceae). *Scenedesmus* sp. was initially isolated from municipal sewage water. This organism is highly tolerant to heavy metals, organic pollutants, and wide thermal variation. Biofuel production coupled with wastewater treatment currently was considered as a promising approach to reduce the costs (Christenson and Sims, 2011). *C. closterium* showed a high growth rate and lipid content in our previous work, emerging as a promising candidate for biofuel and high-value pigment production (Wang et al., 2015) (Wang et al., 2018). Additionally, both algal species synthesize a wide array of poly-unsaturated fatty acids essential to human health such as α -linolenic acid by *Scenedesmus obliquus* (Makulla, 2000) and eicosapentaenoic acid by *C. closterium* (Wang et al., 2015). This study elucidates the variations of

lipid metabolites between a marine diatom and a freshwater green alga under nitrogen starvation at the molecular level with a particular emphasis on TAGs.

5.3 Materials and Methods

5.3.1 Algae and culture condition

Scenedesmus sp. was isolated from a sewage plant in Germany. *C. closterium* was provided as a courtesy of the algae collection in the Lab. of Applied Microalgae Biology of Ocean University of China, Qingdao, China. The stocks of *Scenedesmus* sp. and *C. closterium* were maintained in freshwater with Bold's Basal Medium (BBM) and seawater enriched with f/2 medium nutrients (Guillard, 1975), respectively, at 12 h/12 h light/darkness cycle and a light intensity of 40 $\mu\text{mol}/\text{m}^2/\text{s}$. Algae used in nitrogen starvation experiments were harvested from a culture in a bag photobioreactor (PBR) (Phytolutions, Bremen, Germany) at a light regime of 18 h /6 h light/darkness and a light intensity of 100 $\mu\text{mol}/\text{m}^2/\text{s}$. *C. closterium* in the bag PBR was cultured in f medium at $20\pm 1^\circ\text{C}$, whereas *Scenedesmus* sp. was grown in BBM at $25\pm 2^\circ\text{C}$. Algae reaching the late exponential phase after 4-day cultivation were harvested by centrifugation at 2,000 g. Cell pellets of *C. closterium* were rinsed with seawater three times to remove nitrogen, while pellets of *Scenedesmus* sp. were washed with ultra-pure water three times. The algae were re-suspended in nitrogen-free media in bottle PBRs at the same environmental parameters as for those of the bag PBRs. Algal biomass was harvested at 0 h, 12 h, 24 h, 48 h, and 96 h after inoculation with three biological replicates. Lyophilized dry biomass was subjected to lipid extraction. The growth performance was monitored by determining the cell concentrations daily using a cell-counting chamber.

5.3.2 Chemicals and agents

Gradient-grade ethanol was purchased from Merck (Darmstadt, Germany); isopropanol (Rotisolv® HPLC-grade), acetonitrile (Rotisolv® HPLC ultra gradient-grade), methanol (Rotisolv® HPLC ultra gradient-grade), chloroform (Rotisolv® HPLC-grade) and Tetra-dodecyl ammonium bromide were purchased from Carl Roth (Karlsruhe, Germany); dichloromethane 99,8% stabilized

with amylene for synthesis was purchased from Panreac AppliChem (Darmstadt, Germany); ammonium formate LC-MS Ultra and formic acid (puriss., $\geq 98\%$ (T) for mass spectrometry), potassium hydroxide (KOH), sulfuric acid (H_2SO_4), heptane (synthesis-grade) and potassium chloride (KCl) were ordered from Carl Roth (Karlsruhe, Germany); molecular sieves pellets (AW-300, 1.6 mm) and Spelco Supelco 37 component fatty acids methyl esterification (FAME) mix 1x1 mL were purchased from Sigma-Aldrich Chemie (Steinheim, Germany).

5.3.3 Total lipids extraction

Total lipids were extracted by a modified gravitational method. Approximately 100 mg of the sample was extracted with 9 mL of dichloromethane/methanol at the ratio of 1:1 in a glass vial. Extraction was assisted by a magnetic stirrer for 1 h at room temperature. The mixture was centrifuged at 3,000 g for 10 min. The extraction procedure was repeated once. The supernatant was combined in fresh vials. KCl solution (0.88%, 4.5 mL) was added to the combined supernatant. An organic and an aqueous phase were separated by centrifugation at 3,000 g for 5 min. The separation procedure was repeated once more with KCl solution. The organic phase (3 mL) was transferred to a pre-weighed test vial and evaporated by N_2 . Total lipids content was calculated by subtracting the mass of the empty vials from that of the vials with lipids. Chloroform was added to dissolve the lipids at a concentration of 5 mg/mL. The dissolved lipid samples were stored at $-20\text{ }^\circ\text{C}$ for further analysis.

5.3.4 Fatty acids methyl esterification preparation and measurement by gas chromatography

A total volume of 0.5 mL of the lipid extract, dissolved in chloroform, was transferred in a glass vial for fatty acid methyl ester (FAME) synthesis. KOH (10 N, 0.7 mL) and methanol (5.3 mL) were added to the extract, stirred continuously at $50\text{ }^\circ\text{C}$ for one hour. Subsequently, H_2SO_4 (24 N, 0.58 mL) was added after the samples were cooled down to room temperature. The samples were stirred continuously at $50\text{ }^\circ\text{C}$ for one hour. FAME was isolated with 2 mL heptane by vortex for 5 minutes and centrifugation at 3,000 g for 3 minutes. The aqueous phase was removed using molecular sieves. FAME was subjected to gas chromatography (GC)-flame ionization detector (FID) for analysis. A capillary column VF-5ms, 30 m x 0.25 mm with an injector temperature of

265 °C and the detector temperature of 300 °C was integrated to the GC. The GC used helium as a carrier gas at a flow rate of 40 mL/min. The split ratio was 1:50 with an injection volume of 1.0 µL. GC program started at 60 °C for 1 minute, followed by a second step of 17 °C/min temperature rate until 160 °C, a third step of 7 °C/min rate until 240 °C and a temperature rate of 5 °C/min until 300 °C with a hold time of 10 min. Fatty acids were assigned by Supelco 37 compounds fatty acid methyl ester (FAME) MIX standard and quantified by the calibration curves of the standard.

5.3.5 High-performance liquid chromatography

Lipids were fractionated by HPLC (Agilent 1100 series, Waldbronn, Germany) with our previously established method (Sirbu et al., 2018) to which slight modifications on elution gradient were applied. One column Pursuit XRs C18 (250 mm × 3 mm i.d., 5 µm particles) was integrated to the HPLC. The temperature of the column oven was set to 35 °C. Each extract was diluted at the ratio of 1:22 in chloroform/ethanol (1:1) with 3 µL of sample were injected. Solvent A consisted of acetonitrile with 0.01% formic acid and B of ethanol with 10 mmol/L ammonium formate and 0.01% formic acid. The mobile phase was applied through the column at a flow rate of 0.6 mL/min. The gradient elution program started with A/B (90/10%) increased linearly to A/B (65/35%) in 4 min; followed by a second linear increasing to solvent A/B (50/50%) in 16 min; a third linear increase to solvent A/B (37/63%) in 2 min; a fourth linear increase to solvent A/B (20/80%) in 23 min; a fifth step, linear increase to solvent B (100%) in 2 min; ending with isocratic elution at solvent B (100%) for 10 min. The column was equilibrated at A/B (90/10%) solvent for 10 min before reuse. Tetra-dodecyl ammonium bromide at the concentration of 0.0002 mg/mL, mass-to-charge (m/z) 690.7850, and retention time (rt) 4.5 min was used as internal standard.

5.3.6 High-resolution mass spectrometry

High-resolution masses were acquired by a time of flight MicrOTOF Focus MS (Bruker Daltonics, Bremen, Germany) fitted with an ESI source as the detector with the following parameter settings: capillary voltage of 4.5 kV; nebulizing gas pressure of 2 Ba drying gas flow rate of 10 L/min; drying gas temperature of 220 °C. ESI mass spectra were measured in the range of m/z 200–1200 in the positive ion mode. Internal calibration was achieved with 10 mL of 0.1 M sodium formate

solution injected through a six-port valve prior to each chromatographic run. Calibration was carried out by the enhanced quadratic mode.

5.3.7 Tandem mass spectrometry

LC-tandem MS was carried out by using an Ion-Trap detector in positive ion mode equipped with an ESI source (Bruker Daltonics, Bremen, Germany). The full scan mass spectra were recorded in the range m/z 200-1200 operating in positive ion mode. Capillary temperature was set to 350 °C, drying gas flow rate 10 L/min and nebulizer pressure 10 psi. Tandem mass spectra were acquired in Auto MSⁿ (smart fragmentation) using a ramping of the collision energy.

5.3.8 Statistical analysis

The individual lipid lists of the high-resolution masses were combined for peak matching and retention time (rt) alignment using a m/z tolerance of $\Delta m/z = 0.0001$ and a rt tolerance of 0.5 min for elution time <20 min and 1.0 min for an elution time ≥ 20 min. Extensive manual curation resulted in a set of 102 peaks for *C. closterium* and 93 peaks for *Scenedesmus* sp.. Lipid compounds could be uniquely assigned with m/z and rt tolerances of $\Delta m/z = 0.01$ and $\Delta rt = 0.8$ min. For further analyses, the peak areas were normalized to the peak area of the internal standard (Tetra-dodecyl ammonium bromide), and relative quantification was achieved for each identified compound. Heat maps, as graphical representations for visualizing attribute values by class in a two-way matrix, as well as principal component analyses (PCA) were performed by Orange software. Microsoft Office Excel 2016 was used to process data and perform ANOVA single-factor analysis.

5.4 Results

5.4.1 Total lipid content and growth kinetics under nitrogen starvation

Total lipids were determined gravimetrically following the dichloromethane extraction. As displayed in **Fig. 1A**, lipids content of 13 % in dry biomass were synthesized in *Scenedesmus* sp.

before nitrogen starvation. The total lipids content of *Scenedesmus* sp. reached the highest amounts after 96 h of nitrogen starvation, while no noticeable changes were observed between 0 h and 48 h ($p>0.05$). *C. closterium* could accumulate lipids content of 20 % in dry biomass before the onset of nitrogen starvation. Surprisingly, the lipids content of *C. closterium* decreased significantly after 12 h of nitrogen starvation ($p<0.05$) and maintained at this level until 48 h ($p>0.05$). *C. closterium* showed a remarkable increment of lipids between 48 and 96 h of starvation ($p<0.05$), while no significant differences were found between the total lipids amount between 0 h and 96 h ($p>0.05$). The growth kinetics (**Fig. 1B**) suggested that the cell concentration of *Scenedesmus* sp. is 5-fold higher than that of *C. closterium* before nitrogen starvation. Both *Scenedesmus* sp. and *C. closterium* continued to grow in nitrogen-free media. However, the trends of growth varied remarkably. After 24 h of nitrogen starvation, cell concentration of *Scenedesmus* sp. increased by approximately 12 %, whereas that of *C. closterium* increased by 64 % after 12 h, nearly doubled the concentration after 24 h and remained constant after 48 h.

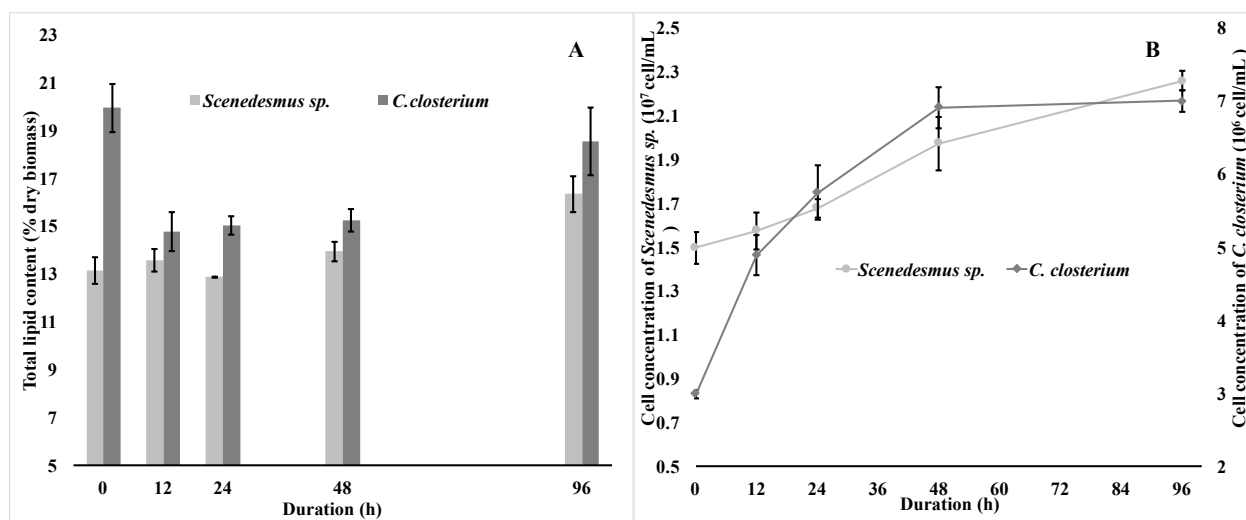


Figure 1. Total lipids and growth kinetics of *Scenedesmus* sp. and *C. closterium* under nitrogen starvation. Results are shown as means \pm SD ($n=3$), except the growth kinetics of *Scenedesmus* sp. ($n=4$).

5.4.2 Fatty acids profile under nitrogen starvation

FAME analyses of lipid extraction are shown in **Fig. 2**. It appeared that C16:3, C16:0 and C18:1 were the major fatty acids in *Scenedesmus* sp. with C18:1 being the most abundant one, and that long-chain fatty acids (>20 C) were present in a minor amount in the *Scenedesmus* sp. (**Fig. 2A & B**). Saturated fatty acids, such as C14:0, C16:0 and C18:0, increased significantly after 96 h of nitrogen starvation ($p < 0.05$) with C16:0 and C18:0 increasing approximately 4-folds and 9-folds, respectively. The monounsaturated fatty acids C20:1 increased by 3-folds at 96 h, while C18:1 only increased by 10 % at 96 h ($p < 0.05$). Polyunsaturated fatty acids, such as C16:3 and C18:3, and odd number fatty acids such as C15:0 and C17:0 decreased significantly after 96 h starvation with the exception of C18:2. C16:3 and C18:3 decreased by 67 % and 37 %, respectively at 96 h as compared to 0 h. After 96 h of nitrogen starvation C16:0 and C18:1 accounted for more than 70 % of the total fatty acids in *Scenedesmus* sp..

Five most abundant fatty acids (C14:0, C16:1, C16:0, C20:4 and C20:5) were synthesized by *C. closterium* with C16:1 and C16:0 as the most dominant fatty acids at 0 h (**Fig. 2C & D**). Under nitrogen starvation, a 26 % increase of the saturated fatty acid C14:0 occurred after 96 h, while C16:0 decreased within first 12 h and increased after 12 h, following the same tendency of total lipids amount. The remarkable increments of monounsaturated fatty acids C15:1 and C16:1 were observed at 96 h ($p < 0.05$). C20:4 and C20:5 reduced by 14 % and 19 % respectively at 96 h when compared to 0 h. The odd number saturated fatty acids (C15:0 and C17:0), rarely reported, followed a decreasing trend. At 96 h, the three dominant fatty acids—C16:1, C16:0 and C20:5 represented 67 % of the total fatty acids.

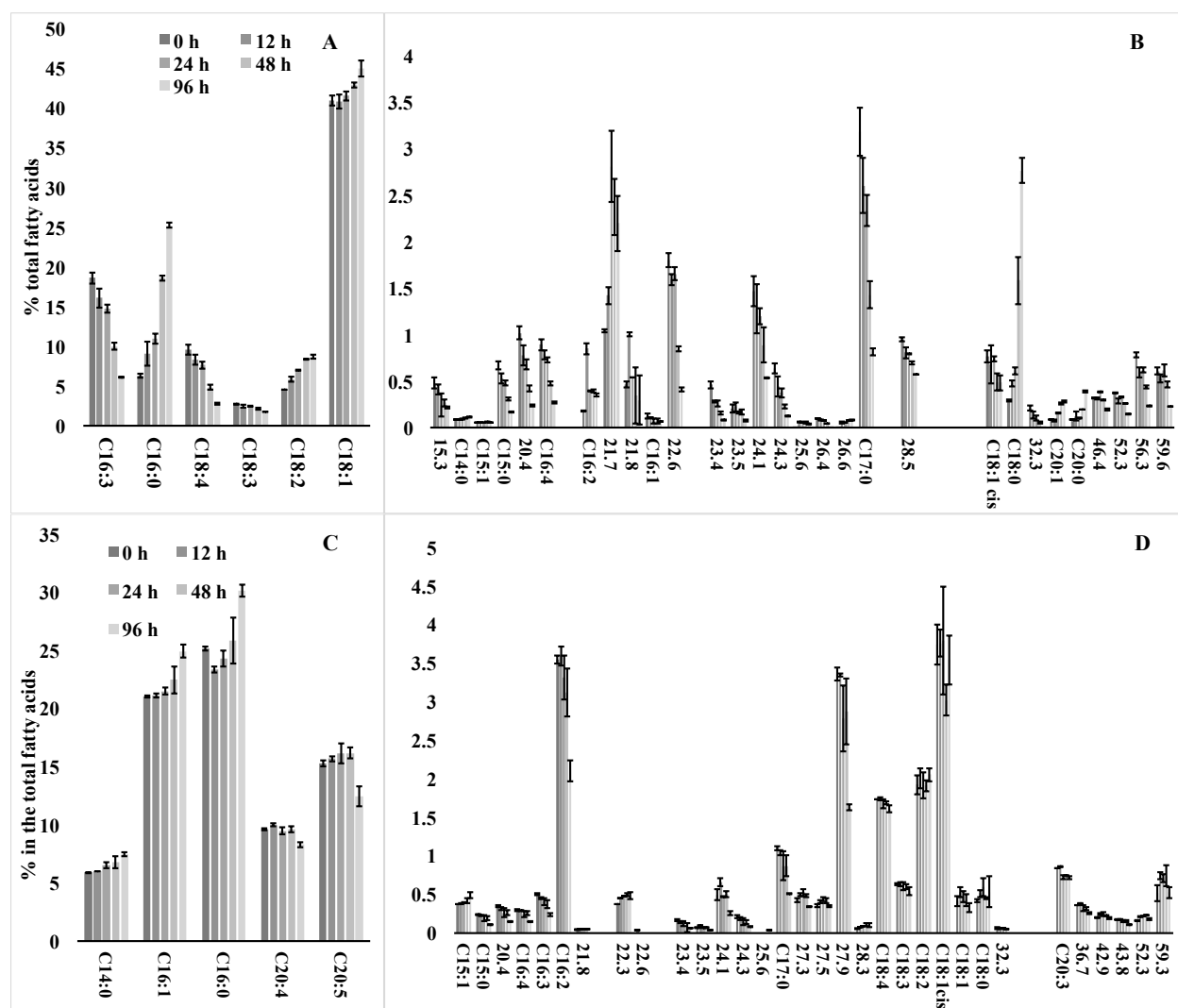


Figure 2. Fatty acids composition of *Scenedesmus* sp. and *C. closterium* under nitrogen starvation. A: Major fatty acids in *Scenedesmus* sp.; B: Minor fatty acids in *Scenedesmus* sp.; C: Major fatty acids in *C. closterium*; D: Minor fatty acids in *C. closterium*. Results are shown as means \pm SD (n=3). Compounds could not be assigned by standards were named by the retention time.

5.4.3 Relatively quantitative analysis of glycerolipids and pigments

Identification of lipid compounds was achieved by a high-resolution MicroTOF MS operating in positive mode. The study of the compound fragmentation was conducted in an Ion-Trap MS. Moreover, the tandem MS data were compared with fragmentation pathways in literature and the database LIPID MAPS (<http://www.lipidmaps.org>). For high-resolution MS, calculation of

molecular formula with mass error <4 ppm was accepted. Tandem MS data were interpreted as described by (Sirbu et al., 2018). Relative quantification of all the identified compounds was performed in positive ion mode with respect to an internal standard (Tetra-dodecyl ammonium bromide). Additionally, representative chromatograms and their two-dimensional maps at 0 and 96 h for each species are in the supplementary material (**Fig. S1 and S2**).

Through the development of lipidomics based on MS, much more knowledge could be attained on different groups of lipids in algae. Ninety-nine molecules (**Table S1**) were successfully annotated in the total lipids of *Scenedesmus* sp. and assigned to 9 classes: triacylglycerol (TAG) ≤ 3 double-bond, TAG > 3 double-bond, MGDG, DGDG, PG, diacylglycerol-N,N,N-trimethylhomoserine (DGTS), lyso-DGTS, phosphatidylethanolamine (PE) and pigments as indicated in **Fig. 3A & B**. Before the start of nitrogen starvation, TAG (≤ 3 and > 3 double-bond) and plastidial lipids (MGDG, DGDG, and PG) accounted for 1.8 % and 5.1 % of the dry biomass respectively. After 96 h of nitrogen starvation, the overall amount of TAG increased by more than 600 % in *Scenedesmus* sp.. TAG ≤ 3 and > 3 double-bonds increased by 4-folds and 28-folds respectively. Total TAGs accounted for 68 % and 11 % of the total lipids and biomass respectively at 96 h in *Scenedesmus* sp.. Pigments including chlorophyll a/b and pheophytin, decreased significantly by 75 % after 96 h, accompanied with the decrements of MGDG and PG. MGDG and PG decreased to approximately 33 % and 22 % respectively after 96 h. Another essential plastidial lipid DGDG reached the maximum at 48 h and dropped at 96 h. The concentration of DGDG at 48 and 96 h was 3 and 2 times higher than at 0 h, respectively. The plastidial membrane lipids (MGDG, DGDG, and PG) comprised 39 % of the total lipids at 0 h and dropped to 15 % at 96 h. DGTS, lyso-DGTS, and PE, as N-containing lipids, are crucial extra-plastidial membrane lipids. A significant decrease of DGTS and PE occurred at 12 and 24 h ($p < 0.05$), respectively, while lyso-DGTS first increased at 24 h and subsequently decreased until 48 h.

Ninety-two lipid molecules (**Table S2**) were identified in the *C. closterium*, which were allocated into 6 groups: TAG ≤ 3 and > 3 double-bond, MGDG, DGDG, sulfoquinovosyl diacylglycerol (SQDG) and pigments (**Fig. 3C & D**). The TAG (≤ 3 and > 3 double-bond) and plastidial lipids (MGDG, DGDG, and SQDG) represented 14 % and 2 % of the dry biomass respectively in *C. closterium* before being subjected to nitrogen-free media. Under nitrogen starvation, pigments

decreased to 35 % after 96 h when compared to 0 h. The abundance of both TAGs classes dramatically decreased during the first 12 hours ($p < 0.05$) and gradually increased afterwards. Total TAG content increased by 20 % at 96 h, with TAGs (> 3 double-bond) increasing by 49 %, but the increase of TAGs (≤ 3 double-bond) is not significant ($p > 0.05$). Total TAGs represented up to 90 % and 17 % of the total lipids and dry biomass at 96 h. Among the three plastidial membrane lipid classes (MGDG, DGDG, and SQDG), the dominant class was MGDG which decreased to 26 % at 96 h as compared to 0 h. Concurrently, DGDG dropped by 57 % at 96 h, while SQDG maintained constantly till 48 h and decreased significantly afterwards. Plastidial membrane lipids accounted for 10 % and 4 % of the total lipids at 0 and 96 h respectively.

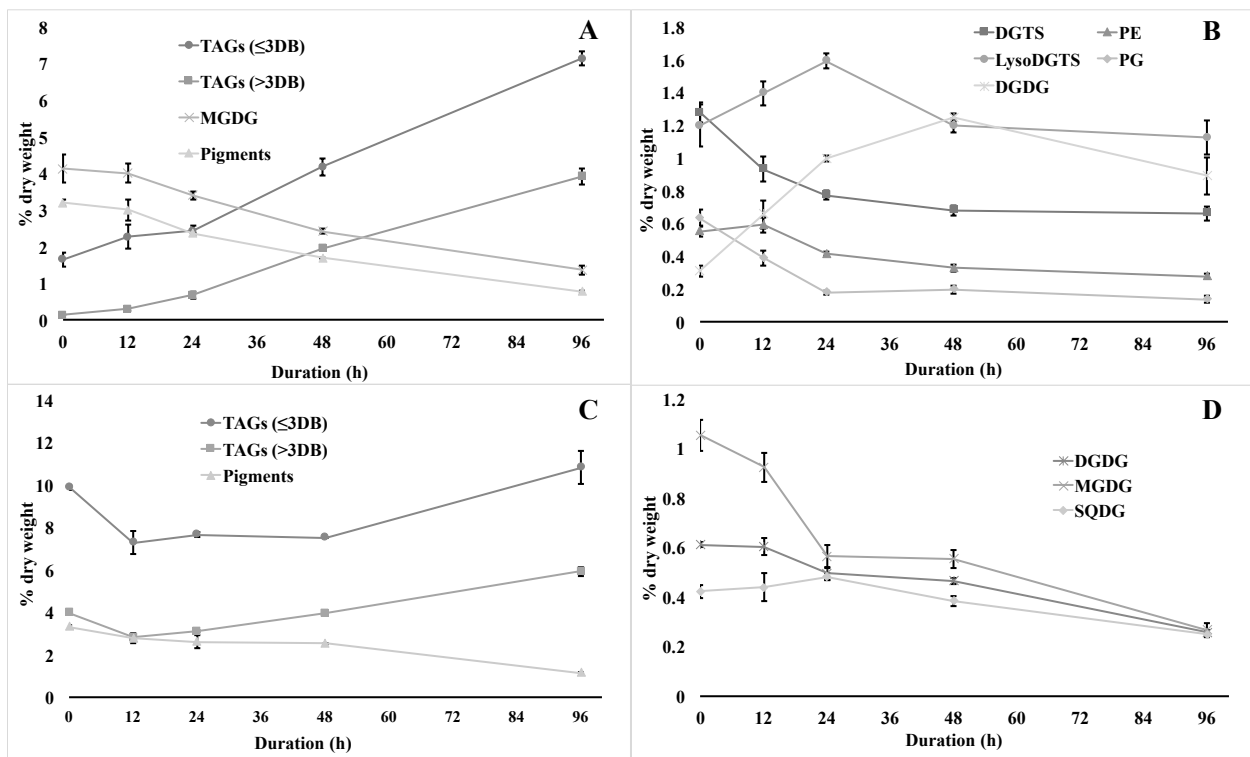


Figure 3. Changes of glycerolipids and pigments in *Scenedesmus* sp. and *C. closterium* under nitrogen starvation. A and B: Glycerolipids and pigments in *Scenedesmus* sp.; C and D: Glycerolipids and pigments in *C. closterium*. Results are shown as means \pm SD (n=3).

5.4.4 Lipid and pigment molecules alteration

PCA of LC-MS data of lipid extract recorded at different time points was performed for each of the two species based on the lipids and pigments identified (**Fig. 4**). PCA on the *Scenedesmus* sp. showed a clear separation of samples collected at each time series. The first principal component in the score plot is strongly correlated with the amount of TAG. Significant changes occurred after 12 h of nitrogen starvation in *Scenedesmus* sp.. In contrast, *C. closterium* did not show a clear separation between all the time series, but distinguishable changes of samples at 0 h and 96 h in comparison to the other 3 could be observed. Moreover, the grouping on the plots reflects the reproducibility of data and how close the samples are to each other in terms of the lipid profile.

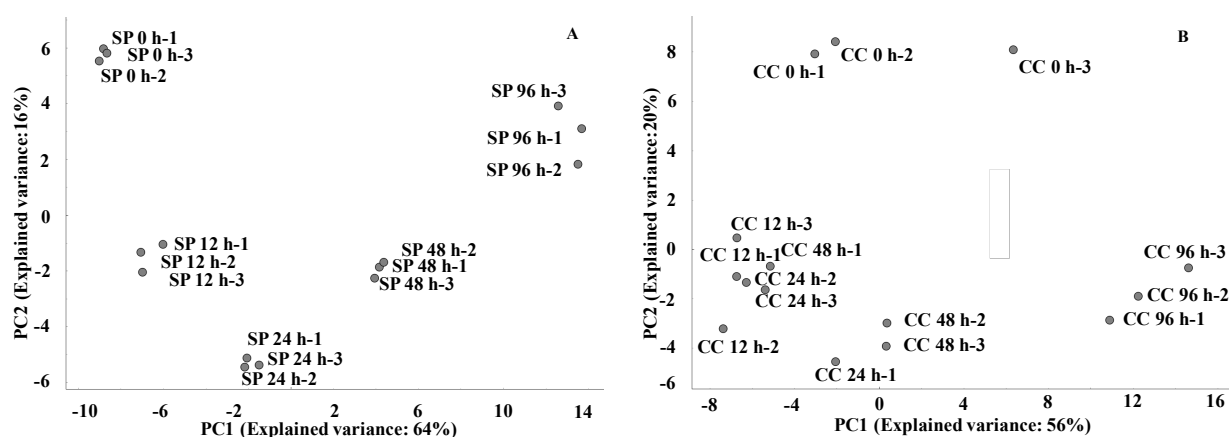


Figure 4. Principal component analysis of *Scenedesmus* sp. and *C. closterium* under nitrogen starvation. A: Samples from *Scenedesmus* sp.; B: Samples from *C. closterium*. Three biological replicates were performed at each time point.

The heat maps illustrated the alteration of the lipid and pigment molecules in the *C. closterium* (**Fig. 5A**) and the *Scenedesmus* sp. (**Fig. 5B**) during nitrogen starvation. All the molecules are listed in **Table S1** for *Scenedesmus* sp. and **S2** for *C. closterium* in the supplementary material. Moreover, the structures of most abundant molecules from different groups of glycerolipids in *Scenedesmus* sp. and *C. closterium* are shown in **Fig. 6A** and **6B** respectively. Sixty and seventy-two TAG molecules were identified in the *Scenedesmus* sp. and the *C. closterium* respectively and therefore, this study provided the most abundant TAG profiles in the two species of algae.

Generally, TAGs (>3 double-bond) were absent at 0 h and only present at 12 h of nitrogen starvation in the *Scenedesmus* sp.. Among the 60 TAGs in *Scenedesmus* sp., TAG 50:1(16:0/16:0/18:1), 52:1 (18:0/16:0/18:1), 50:2 (14:0/18:1/18:1), 52:2 (16:0/18:1/18:1), 50:3 (16:0/16:0/18:3), 52:3(16:0/18:1/18:2), 54:3 (18:0/18:0/18:3), 52:4 (18:1/16:0/18:3) and 52:4 (16:0/18:2/18:2) were the dominant TAG species at 96 h. The abundance of the major TAGs (≤ 3 double bonds), increased by 8 to 20-folds at 96 h when compared to their counterparts at 0 h, except for 52:1 (18:0/16:0/18:1) and 50:3 (16:0/16:0/18:3). 52:1 (18:0/16:0/18:1) increased by 3-folds at 96 h compared to 0 h, while no 50:3 (16:0/16:0/18:3) was synthesized at 0 h. 52:4 (18:1/16:0/18:3) and 52:4 (16:0/18:2/18:2) containing >3 double-bond increased by approximately 60-folds at 96 h, when compared to TAGs at 0 h. With respect to plastidial membrane lipids, a more complex pattern was adopted. MGDG 34:7 (16:4/18:3), as the most abundant MGDG, decreased significantly at 24 h under nitrogen starvation ($p < 0.05$). All DGDGs displayed the same tendency as the total DGDG amount, culminating at 48 h and decreasing at 96 h. A notable aspect is that the dominant DGDG, 34:3 (16:0/18:3), increased constantly during the whole process. PE 36:6 (C18:3/18:3), as the major PE at 0 h, decreased significantly at 12 h ($p < 0.05$). Likewise, most DGTS lipids with PUFA chains decremented dramatically at 12 h with an exception that the concentration of dominant DGTS 34:3 (16:0/18:3) increased significantly at 24 h ($p < 0.05$). The primary lyso-DGTS (18:3) fluctuated in a certain range during the whole process. DGTSs as a type of N-containing lipids tended to be involved in the first reaction to nitrogen starvation. DGTS 34:3 (16:0/18:3) and lyso-DGTS (18:3) might serve as the house-keeping lipids engaged in maintaining the whole integrity of the cell membrane.

Seventy-two TAG molecules in the *C. closterium* have been assigned at 96 h based on high-resolution and tandem MS data (**Fig. 5B**). Eight TAG molecules 46:1 (14:0/16:1/16:0), 48:1 (16:0/16:1/16:0&16:0/18:1/14:0), 52:1 (16:0/18:1/18:0&14:0/18:1/20:0), 48:2 (16:0/16:1/16:1&14:0/18:1/16:1), 50:2 (16:0/18:1/16:1&14:0/18:1/18:1), 52:5 (16:0/16:0/20:5), 52:5 (16:0/16:1/20:4) and 52:6 (16:0/16:1/20:5) were found to be the most predominant species in the *C. closterium*. The significant increase of the major TAGs only took place after 96 h nitrogen starvation. TAG 46:1 (14:0/16:1/16:0), 48:2 (16:0/16:1/16:1&14:0/18:1/16:1), 52:5 (16:0/16:0/20:5) and 52:6 (16:0/16:1/20:5) increased by 40-60% at 96 h. The most abundant MGDG molecule 36:8 (16:3/20:5) showed a significant decrease at 24 h ($p < 0.05$). The two

primary DGDG 36:7 (C16:2/C20:5) and 36:6 (C16:1/C20:5) decreased significantly at 96 h when compared to 0 h ($p < 0.05$). The SQDG 32:1 (16:0/16:1) increased within 24 h followed by a decrease at 96 h.

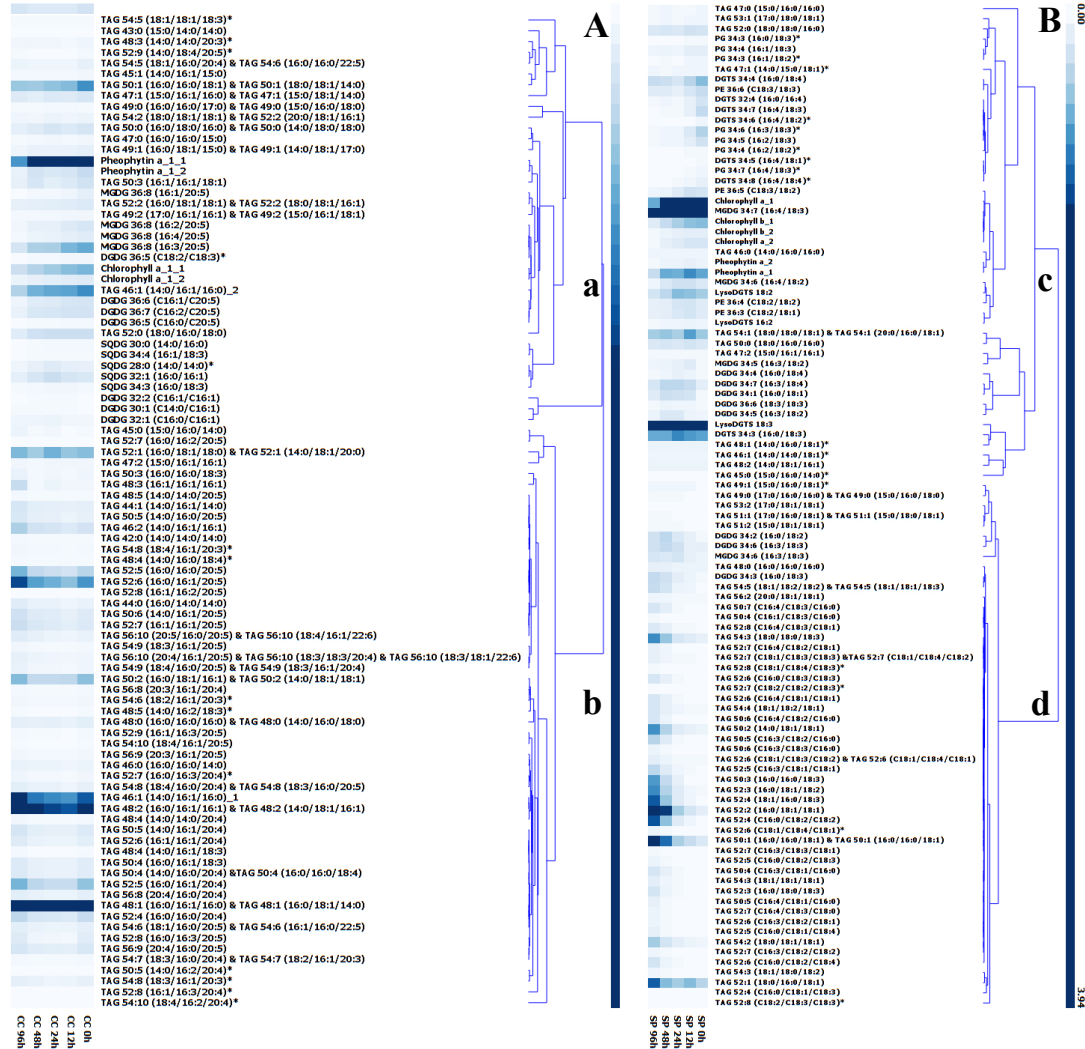


Figure 5. Heat map of glycerolipid and pigment molecules in *C. closterium* and *Scenedesmus* sp. under nitrogen starvation. A: glycerolipid and pigment molecules from *C. closterium*; B: glycerolipid and pigment molecules from *Scenedesmus* sp.. All the identified molecules were primarily clustered in 4 groups: molecules in group a and c displayed a decreasing trend during the time course; molecules in group b decreased at the beginning, then increased till 96 h; group d exhibited an increasing trend. *: compounds were tentatively identified due to the insufficient fragment information.

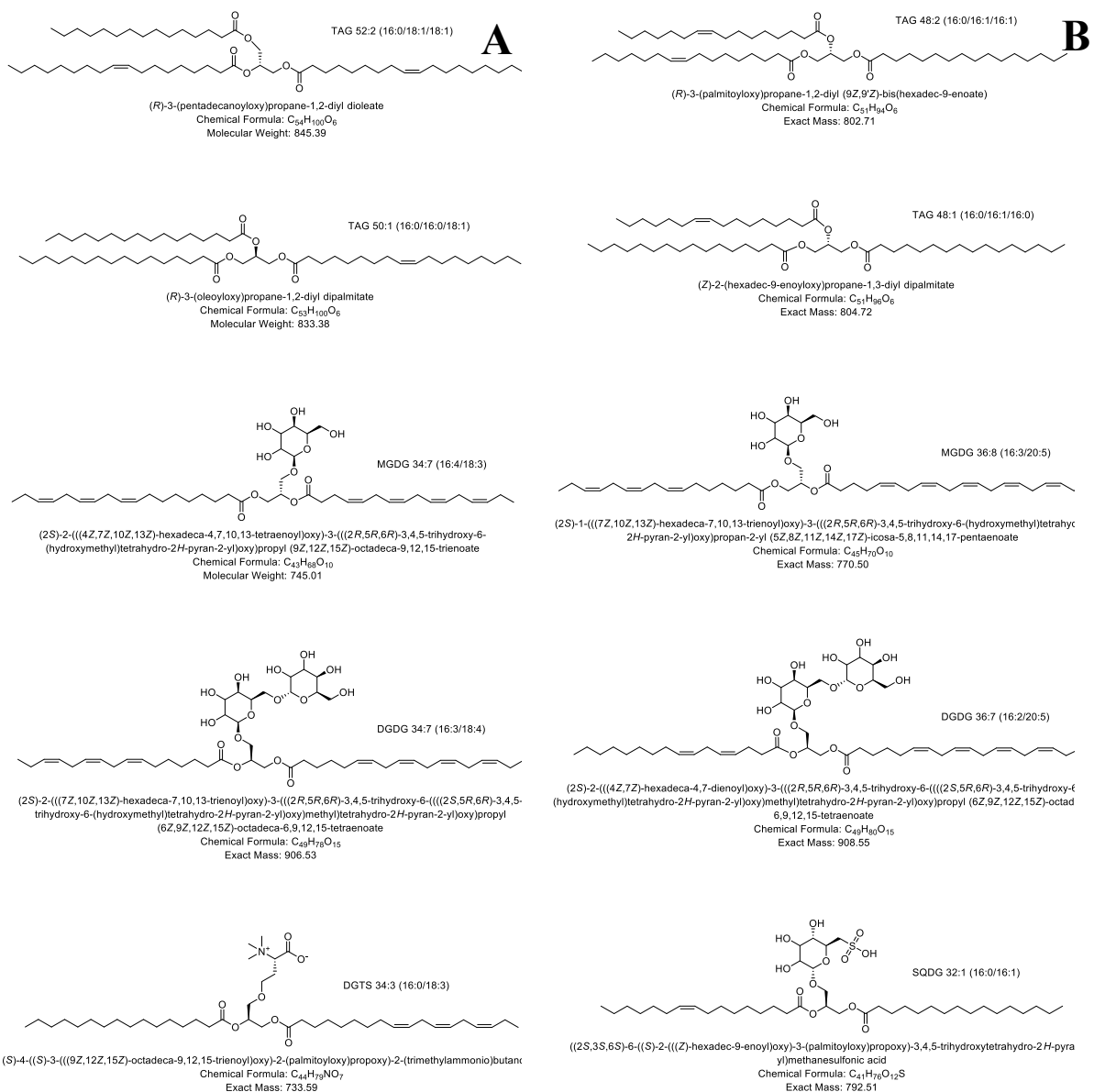


Figure 6. The structures of the representative molecules from different groups of glycerolipids. A: Molecules from *Scenedesmus* sp.; B: Molecules from *C. closterium*.

5.5 Discussion

5.5.1 Total lipid content and growth kinetics under nitrogen starvation

Despite the absence of nitrogen, both species continued growing, especially *C. closterium*, which doubled the cell concentration at 24 h. This might be explained by assuming that algae in nutrient-sufficient environment tend to assimilate more nutrients, including nitrogen, to form an internal reservoir in a vacuole which could support growth in a nitrogen-scarce or even nitrogen-free environment (Lavin and Lourenço, 2005). The existence of this internal reservoir was described in *Chlorella* sp. and *Nannochloropsis oculata* (Paes et al., 2016). The marine diatom *Fistulifera solaris* continued growing for 24 h in a nutrient free medium and then the growth was inhibited (Liang et al., 2015). It has been previously reported that *Scenedesmus obliquus* could accumulate as much as 20 % lipid in dry biomass after 5-day nitrogen starvation compared to 11 % in negative control, along with an increase of carbohydrate and decrease of protein content (Ho et al., 2012). These findings are in line with the lipid content of the *Scenedesmus* sp. after nitrogen starvation described in the current study. This could be interpreted by the fact that nitrogen is intimately connected to the carbon metabolism. The reduced availability of nitrogen led to the re-allocation of photosynthetic carbon flux into lipid synthesis (Alipanah et al., 2015). *P. tricornutum* produced significantly more lipid after 48 h cultivation in a nitrogen-free medium. However, the growth was suppressed when compared to the control after 48 h (Alipanah et al., 2015). These findings contrast with the lipid metabolism displayed by the *C. closterium* in the present study. The decrease of total lipid content in the *C. closterium* could possibly be explained by the rapid cellular reproduction within 12 h, which would require a significant amount of energy. Therefore, lipids, i.e., energy storage compounds, were consumed to provide energy due to the deficiency of photosynthetic ATP production.

5.5.2 Fatty acids profile under nitrogen starvation

Although *Scenedesmus* sp. and *C. closterium* were characterized by different fatty acids compositions, the concentrations of polyunsaturated fatty acids decreased in both species after 96 h of nitrogen starvation, but the saturated and monounsaturated fatty acids increased in response

to a nitrogen-free environment. Similar alterations of fatty acids happened in *Chlorella zofingiensis* under nitrogen starvation with an elevated saturated and monounsaturated fatty acids but a diminished polyunsaturated fatty acids ratio (Zhu et al., 2015). Likewise, the synthesis of saturated fatty acid of *P. tricornutum* increased in a nitrogen-depleted medium at 96 h compared to nitrogen-replete medium (Yodsuwan et al., 2017). Nevertheless, in another study, the levels of monounsaturated fatty acids (C14:1 and C16:1) decreased in the green algae *E. oleoabundans* under nitrogen deprived conditions (Matich et al., 2018). The decrease of polyunsaturated fatty could be considered as a consequence of the inhibition of the photosynthesis and degradation of the photosynthetic systems where PUFA are usually present. Since saturated/monounsaturated acyl chains are beneficial for biodiesel production and both the *Scenedesmus* sp. and the *C. closterium* feature high saturated/monounsaturated fatty acids contents, induced by nitrogen starvation, these two species appear to be suitable candidates for biodiesel production (Islam et al., 2013). The odd-numbered chain fatty acids were detected in both species, although in low concentration. Despite the fact that odd-numbered chain fatty acids (C15:0 and C17:0) have been identified in other studies (Branco-Vieira et al., 2017), the synthesis pathway remains unclear.

5.5.3 Relative quantitative analysis of glycerolipids and pigments

The reduction of photosynthetic pigments and the decrease of plastidial membrane lipids in nitrogen-free media indicated an inhibition of photosynthesis in the *Scenedesmus* sp. and the *C. closterium*. The decline in pigments was due to the degradation of the essential enzymes and structural proteins in the photosynthetic pathway; meanwhile, the N in pigments, as N-rich compounds, were presumably redirected to protein synthesis under nitrogen starvation (Levitan et al., 2015). Another previous study observed a shrunk volume of chloroplast and an increased volume of lipid droplets in the diatom *F. solaris* in a nutrient-starved environment (Liang et al., 2015).

In comparison to *Scenedesmus* sp., *C. closterium* adopted a different lipid mechanism triggered by nitrogen starvation. *C. closterium* in this study accumulated a high TAG content at 0 h, and as nitrogen starvation proceeded, TAG decreased to provide energy for the cell division. *Scenedesmus* sp. accumulated a very low amount of TAGs at 0 h, which then increased steadily.

TAGs only accounted for 1.8 % of the dry biomass of the *Scenedesmus* sp., in a nutrient-replete environment, which indicated most of the photosynthetically fixed carbon was partitioned into protein and carbohydrate to enhance biomass.

Plastidial membrane lipids were more abundant in *Scenedesmus* sp. than in *C. closterium*. As most of the MGDG, DGDG, and SQDG are mainly present in thylakoids membrane and have a substantial impact on the photosynthesis and growth, it can be proposed that photosynthetic apparatus in the *Scenedesmus* sp. is more developed in the *C. closterium* (Dormann et al., 1995). DGDG in *Scenedesmus* sp. increased within 48 h as a reaction of the compromised photosynthesis, but decreased during the whole process in *C. closterium*. The ratio of MGDG/DGDG in both species decreased significantly. Decreased MGDG, along with increased DGDG, was reported previously in *Arabidopsis* (Gaude et al., 2007) and *P. tricornutum* (Abida et al., 2015), yet both MGDG and DGDG decreased under nitrogen starvation in *Chlamydomonas reinhardtii* and *F. solaris* (Liang et al., 2015; Siaux et al., 2011). This could be explained that a bilayer-lipid (DGDG) has superiority over a non-bilayer-lipid (MGDG) in maintaining the integrity of thylakoids under nitrogen stress (Webb and Green, 1991). However, as the nitrogen starvation proceeded, the more photosynthetic machinery was degraded, and the DGDG started to decrease at 48 h of nitrogen starvation, which was reflected by the declining MGDG/DGDG ratio described in this study. Consequently, it can be hypothesized that the structure of the photosynthetic system in the *C. closterium* is more subjected to the nitrogen stress than in the *Scenedesmus* sp., due to the immediate reduction of DGDG.

5.5.4 Lipid and pigment molecules alteration

Results showed that the PUFA were mainly present in membrane lipids at 0 h in both species, while TAGs with PUFA acyl chain increased significantly at 96 h. Hence, we suggested that PUFA acyl chains were recycled by TAGs in both algae, which was observed in a previous study (Goncalves et al., 2016). Glycolipids, such as MGDG, DGDG, and SQDG, possess a variety of bioactive effects and high nutritional values due to the PUFA content, yet a lipidomic study of glycerol lipids has been only performed in a limited number of microalgae as reviewed by da Costa E. et al. (da Costa et al., 2016). Herein, we propose two new candidates to produce high-value

lipids for health by providing the annotation of glycolipid molecules in *Scenedesmus* sp. and *C. closterium*. Diacylglycerols, as precursors of TAG *de novo* synthesis, were synthesized by the acylation of the *sn*-2 position of lysophosphatidic acid catalyzed by lysophosphatidic acid acyltransferases (LPAAT) (Nobusawa et al., 2017). LPAAT in different organelles showed varied specificity. LPAAT in the chloroplast showed specific preference to C16 moiety substrate – which represents the “prokaryotic” pathway, while LPAAT in the endoplasmic reticulum preferred C18 – representing the “eukaryotic” pathway (Allen et al., 2014). As shown in **Table 1**, although TAGs were synthesized in both pathways, the ratio of TAGs from the two pathways differed during nitrogen starvation. Before the beginning of nitrogen starvation, TAGs were synthesized in both the “eukaryotic” and “prokaryotic” pathway in the *Scenedesmus* sp., but the decreased ratio of TAG with C16/C18 in the *sn*-2 position indicated that more TAGs were assembled in the endoplasmic reticulum than chloroplast during nitrogen starvation. In contrast, a majority of the TAGs in the *C. closterium* were synthesized by the “prokaryotic” pathway in the chloroplast at 0 h. During the nitrogen starvation, the ratio of TAG with C16/C18 in *sn*-2 position remained constant during the first 24 h. A significant increase of the ratio was observed at 48 h caused by an increase of TAGs synthesized by the “prokaryotic” pathway in the chloroplast. Compared to the rapid increase of TAGs in the *Scenedesmus* sp., the significant increase of TAGs only happened at 96 h in the *C. closterium*, revealing *Scenedesmus* sp., can switch to lipids production faster than *C. closterium*. The concentration of DGDG increased within 48 h in the *Scenedesmus* sp., while DGDG decreased at 24 h in the *C. closterium*. Interestingly, the concentration of DGDG 34:3 (16:0/18:3) increased at 96 h in *Scenedesmus* sp. indicating its essential function in photosystems of the *Scenedesmus* sp.. DGTS molecules in *Scenedesmus* sp. dropped immediately after nitrogen starvation as the first response of nitrogen starvation.

Table 1. The content of TAGs (% dry biomass) with C16 or C18 FA in the *sn*-2 position and ratio of TAG with C16 and C18 in the *sn*-2 position

Time (h)	<i>Scenedesmus</i> Sp.			<i>C. closterium</i>		
	% C16 <i>sn</i> -2	% C18 <i>sn</i> -2	Ratio of C16/C18 <i>sn</i> -2	% C16 <i>sn</i> -2	% C18 <i>sn</i> -2	Ratio of C16/C18 <i>sn</i> -2
0	0.75±0.06	0.99±0.15	0.76±0.1	11.89±0.1	1.75±0.06	6.79±0.16
12	1.08±0.16	1.46±0.15	0.74±0.04	8.66±0.63	1.28±0.08	6.77±0.21
24	1.19±0.06	1.88±0.17	0.64±0.04	9.25±0.20	1.42±0.04	6.53±0.21
48	2.00±0.11	4.11±0.18	0.49±0.01	10.22±0.10	1.01±0.05	10.09±0.57
96	3.49±0.17	7.53±0.23	0.46±0.01	14.84±1.36	1.41±0.04	10.53±1.17

If two or three molecules shared one mass/charge ratio, they were represented by the dominant one based on the fragment information in the calculation. Data were shown as mean±SD (n=3).

Our results suggest that *Scenedesmus* sp. and *C. closterium* adopted a different strategy to cope with nitrogen stress, specifically regarding TAG accumulation mechanisms. The TAGs content of the *C. closterium* decreased at 12 h, which might be induced by the rapid cell reproduction. The unique lipid metabolism that observed in the *C. closterium* is probably due to its benthic characteristics. Diatoms are more competitive in absorbing nutrients than other phytoplankton. Large diatoms, in particular, tend to have a relatively larger vacuole than in a small diatom where nitrogen could be stored (Litchman, 2007; Raven, 1987; Sicko-Goad et al., 1984). The growth of *Scenedesmus* sp. slowed down, but *C. closterium* duplicated rapidly during the first 48 h of nitrogen starvation. Furthermore, a decrease of cell size at 96 h compared to cells at was observed under a microscope (**Fig. S3**). Larger cells could be beneficial for ciliates defense, but they will have a lower area/volume, compared to smaller cells. A lower area/volume ration will not be harmful in a nutrient-rich environment, however, in a nutrient-limited environment, smaller cells are more favorable for nutrients uptake (Banse, 1976; Raven, 1998). Therefore, *C. closterium* improved the capability of nitrogen assimilation by reproducing smaller cells. Likewise, algae under nitrogen stress tended to strengthen the nitrogen assimilation apparatus as described in other studies, which supported this hypothesis (Levitan et al., 2015).

Apart from the knowledge we gained on lipid synthesis pathway, the shift from fast-growing to a lipid-producing mode which was observed in *Scenedesmus* sp. reflected its potential application in wastewater treatment in the next step. The synergy of wastewater treatment with algae cultivation was recognized as a sustainable and cost-efficient approach for biofuel production. In an ideal strategy, *Scenedesmus* sp. could be fed with the nutrients in the wastewater and at the same time fix carbon dioxide. The harvested biomass could be subject to nitrogen starvation before lipid extraction.

5.6 Conclusions

A detailed comparative lipidomic analysis of algae from different classes yielded information at the molecular level. Results revealed that the two algae species in our study (freshwater green alga and marine benthic diatom) exhibited different strategies of lipid metabolism in response to nitrogen starvation. Nitrogen starvation induced an increased level of saturated/monounsaturated fatty acids and decreased the production of polyunsaturated fatty acids, which is beneficial for biofuel production. TAG increased by more than 600 % and 20 % in the *Scenedesmus* sp. and *C. closterium* respectively after 96 h of nitrogen starvation. After nitrogen starvation, the TAGs of the *Scenedesmus* sp. and the *C. closterium* attributed 11 % and 17 % to the dry biomass, respectively. In comparison to the concomitant decrease of MGDG and DGDG in *C. closterium*, the increased DGDG in the *Scenedesmus* sp. indicated the important role in maintaining the integrity of photosystems in green algae. By providing the most abundant TAG profiles in the two species of oleaginous algae, more insights have been brought into the different metabolisms of lipid production. Under nitrogen stress, more TAGs were synthesized by the “eukaryotic pathway” than “prokaryotic pathway” in the *Scenedesmus* sp.. On the contrary, the increased TAGs were mainly synthesized by the “prokaryotic pathway” in the chloroplast of *C. closterium* reflecting the different strategies of *de novo* TAG biosynthesis in freshwater green algae and diatom.

Acknowledgement

We would like to thank Candice Thorstenson for the improvement of the language. The authors would also like to thank Dr. Jichang Han for the isolation the algae *Scenedesmus* sp. in a previous project funded by Phytolutions. This study was supported by OceanLab of Jacobs University and by the AnMBRA project. Song Wang was funded by China Scholarship Council.

Authors' contributions

Song Wang and Diana Sirbu designed the experiment, carried out the experiment, interpreted the data and drafted the manuscript. Laurenz Thomsen, Nikolai Kuhnert, Matthias S. Ullrich and Claudia Thomsen helped interpret data and gave critical comments on the manuscript.

5.7 Reference

- Abida, H., Dolch, L.J., Mei, C., Villanova, V., Conte, M., Block, M.A., Finazzi, G., Bastien, O., Tirichine, L., Bowler, C., Rebeille, F., Petroustos, D., Jouhet, J. and Marechal, E. (2015) Membrane glycerolipid remodeling triggered by nitrogen and phosphorus starvation in *Phaeodactylum tricornutum*. *Plant Physiology* **167**, 118-136.
- Adarme-Vega, T.C., Lim, D.K.Y., Timmins, M., Vernen, F., Li, Y. and Schenk, P.M. (2012) Microalgal biofactories: a promising approach towards sustainable omega-3 fatty acid production. *Microbial Cell Factories* **11**, 96.
- Alipanah, L., Rohloff, J., Winge, P., Bones, A.M. and Brembu, T. (2015) Whole-cell response to nitrogen deprivation in the diatom *Phaeodactylum tricornutum*. *Journal of Experimental Botany* **66**, 6281-6296.
- Allen, J.W., DiRusso, C.C. and Black, P.N. (2014) Triglyceride quantification by catalytic saturation and LC-MS/MS reveals an evolutionary divergence in regioisometry among green microalgae. *Algal Research* **5**, 23-31.
- Banse, K. (1976) Rates of growth, respiration and photosynthesis of unicellular algae as related to cell size-a review. *Journal of Phycology* **12**, 135-140.
- Becker, E.W. (2007) Micro-algae as a source of protein. *Biotechnology Advances* **25**, 207-210.
- Benavente-Valdes, J.R., Aguilar, C., Contreras-Esquivel, J.C., Mendez-Zavala, A. and Montanez, J. (2016) Strategies to enhance the production of photosynthetic pigments and lipids in chlorophyceae species. *Biotechnology reports (Amsterdam, Netherlands)* **10**, 117-125.
- Branco-Vieira, M., San Martin, S., Agurto, C., Santos, M., Freitas, M., Mata, T., Martins, A. and Caetano, N. (2017) Potential of *Phaeodactylum tricornutum* for Biodiesel Production under Natural Conditions in Chile. *Energies*. **11**, 54.
- Chew, K.W., Yap, J.Y., Show, P.L., Suan, N.H., Juan, J.C., Ling, T.C., Lee, D.J. and Chang, J.S. (2017) Microalgae biorefinery: High value products perspectives. *Bioresource Technology* **229**, 53-62.
- Christenson, L. and Sims, R. (2011) Production and harvesting of microalgae for wastewater treatment, biofuels, and bioproducts. *Biotechnology Advances* **29**, 686-702.
- Chu, W.L. (2017) Strategies to enhance production of microalgal biomass and lipids for biofuel feedstock. *Eur. J. Phycol.* **52**, 419-437.

- da Costa, E., Silva, J., Mendonca, S.H., Abreu, M.H. and Domingues, M.R. (2016) Lipidomic approaches towards deciphering glycolipids from microalgae as a reservoir of bioactive lipids. *Marine Drugs* **14**.
- Dormann, P., Hoffmann-Benning, S., Balbo, I. and Benning, C. (1995) Isolation and characterization of an *Arabidopsis* mutant deficient in the thylakoid lipid digalactosyl diacylglycerol. *Plant Cell* **7**, 1801-1810.
- Faried, M., Samer, M., Abdelsalam, E., Yousef, R.S., Attia, Y.A. and Ali, A.S. (2017) Biodiesel production from microalgae: Processes, technologies and recent advancements. *Renewable and Sustainable Energy Reviews* **79**, 893-913.
- Frada, M.J., Burrows, E.H., Wyman, K.D. and Falkowski, P.G. (2013) Quantum requirements for growth and fatty acid biosynthesis in the marine diatom *Phaeodactylum tricornutum* (Bacillariophyceae) in nitrogen replete and limited conditions. *Journal of Phycology* **49**, 381-388.
- Gaude, N., Bréhélin, C., Tischendorf, G., Kessler, F. and Dörmann, P. (2007) Nitrogen deficiency in *Arabidopsis* affects galactolipid composition and gene expression and results in accumulation of fatty acid phytyl esters. *Plant Journal* **49**, 729-739.
- Goncalves, E.C., Wilkie, A.C., Kirst, M. and Rathinasabapathi, B. (2016) Metabolic regulation of triacylglycerol accumulation in the green algae: identification of potential targets for engineering to improve oil yield. *Plant Biotechnology Journal* **14**, 1649-1660.
- Guillard, R.R.L. (1975) Culture of phytoplankton for feeding marine invertebrates. In: *Culture of Marine Invertebrates Animals* (Smith, W.L. and Chanley, M.H. eds), pp. 26-60. New York, USA: Plenum Press.
- Harwood, J.L. and Guschina, I.A. (2009) The versatility of algae and their lipid metabolism. *Biochimie*. **91**, 679-684.
- Ho, S.H., Chen, C.Y. and Chang, J.S. (2012) Effect of light intensity and nitrogen starvation on CO₂ fixation and lipid/carbohydrate production of an indigenous microalga *Scenedesmus obliquus* CNW-N. *Bioresource Technology* **113**, 244-252.
- Hu, Q., Sommerfeld, M., Jarvis, E., Ghirardi, M., Posewitz, M., Seibert, M. and Darzins, A. (2008) Microalgal triacylglycerols as feedstocks for biofuel production: perspectives and advances. *Plant Journal* **54**, 621-639.

- Islam, M.A., Magnusson, M., Brown, R.J., Ayoko, G.A., Nabi, M.N. and Heimann, K. (2013) Microalgal species selection for biodiesel production based on fuel properties derived from fatty acid profiles. *Energies* **6**, 5676-5702.
- Kumari, P., Kumar, M., Reddy, C.R.K. and Jha, B. (2013) 3 - Algal lipids, fatty acids and sterols. In: *Functional Ingredients from Algae for Foods and Nutraceuticals*, (Herminia Domínguez ed) pp. 87-134. Woodhead Publishing.
- Lavín, P.L. and Lourenço, S.O. (2005) An evaluation of the accumulation of intracellular inorganic nitrogen pools by marine microalgae in batch cultures. *Brazilian Journal of Oceanography* **53**, 55-68.
- Levitan, O., Dinamarca, J., Zelzion, E., Lun, D.S., Guerra, L.T., Kim, M.K., Kim, J., Van Mooy, B.A., Bhattacharya, D. and Falkowski, P.G. (2015) Remodeling of intermediate metabolism in the diatom *Phaeodactylum tricornutum* under nitrogen stress. *Proceedings of the National Academy of Sciences of the United States of America* **112**, 412-417.
- Li, J., Han, D., Wang, D., Ning, K., Jia, J., Wei, L., Jing, X., Huang, S., Chen, J., Li, Y., Hu, Q. and Xu, J. (2014) Choreography of transcriptomes and lipidomes of *Nannochloropsis* reveals the mechanisms of oil synthesis in microalgae. *Plant Cell* **26**, 1645-1665.
- Li, Y., Horsman, M., Wang, B., Wu, N. and Lan, C.Q. (2008) Effects of nitrogen sources on cell growth and lipid accumulation of green alga *Neochloris oleoabundans*. *Applied Microbiology and Biotechnology* **81**, 629-636.
- Liang, Y., Osada, K., Sunaga, Y., Yoshino, T., Bowler, C. and Tanaka, T. (2015) Dynamic oil body generation in the marine oleaginous diatom *Fistulifera solaris* in response to nutrient limitation as revealed by morphological and lipidomic analysis. *Algal Research* **12**, 359-367.
- Litchman, E. (2007) CHAPTER 16 - Resource Competition and the Ecological Success of Phytoplankton. In: *Evolution of Primary Producers in the Sea* (Falkowski, P.G. and Knoll, A.H. eds), pp. 351-375. Burlington: Academic Press.
- Makulla, A. (2000) Fatty acid composition of *Scenedesmus obliquus*- correlation to dilution rates. *Limnologica* **30**, 162-168.
- Matich, E.K., Ghafari, M., Camgoz, E., Caliskan, E., Pfeifer, B.A., Haznedaroglu, B.Z. and Atilla-Gokcumen, G.E. (2018) Time-series lipidomic analysis of the oleaginous green microalga species *Ettlia oleoabundans* under nutrient stress. *Biotechnology for Biofuels* **11**, 29.

- Miller, R., Wu, G., Deshpande, R.R., Vieler, A., Gartner, K., Li, X., Moellering, E.R., Zauner, S., Cornish, A.J., Liu, B., Bullard, B., Sears, B.B., Kuo, M.H., Hegg, E.L., Shachar-Hill, Y., Shiu, S.H. and Benning, C. (2010) Changes in transcript abundance in *Chlamydomonas reinhardtii* following nitrogen deprivation predict diversion of metabolism. *Plant Physiology* **154**, 1737-1752.
- Nobusawa, T., Hori, K., Mori, H., Kurokawa, K. and Ohta, H. (2017) Differently localized lysophosphatidic acid acyltransferases crucial for triacylglycerol biosynthesis in the oleaginous alga *Nannochloropsis*. *Plant Journal* **90**, 547-559.
- Paes, C.R.P.S., Faria, G.R., Tinoco, N.A.B., Castro, D.J.F.A., Barbarino, E. and Lourenco, S.O. (2016) Growth, nutrient uptake and chemical composition of *Chlorella sp.* and *Nannochloropsis oculata* under nitrogen starvation. *Latin American Journal of Aquatic Research* **44**, 275-292.
- Raven, J.A. (1987) The role of vacuoles. *New Phytologist* **106**, 357-422.
- Raven, J.A. (1998) The twelfth Tansley Lecture. Small is beautiful: the picophytoplankton. *Functional Ecology* **12**, 503-513.
- Rismani-Yazdi, H., Haznedaroglu, B.Z., Carol, H. and Jordan, P. (2012) Transcriptomic analysis of the oleaginous microalga *Neochloris oleoabundans* reveals metabolic insights into triacylglyceride accumulation. *Biotechnology for Biofuels* **5**, 74.
- Siaut, M., Cuiné, S., Cagnon, C., Fessler, B., Nguyen, M., Carrier, P., Beyly, A., Beisson, F., Triantaphylidès, C., Li-Beisson, Y. and Peltier, G. (2011) Oil accumulation in the model green alga *Chlamydomonas reinhardtii*: characterization, variability between common laboratory strains and relationship with starch reserves. *BMC Biotechnology* **11**, 7.
- Sicko-Goad, L.M., Schelske, C.L. and Stoermer, E.F. (1984) Estimation of intracellular carbon and silica content of diatoms from natural assemblages using morphometric techniques. *Limnology and Oceanography* **29**, 1170-1178.
- Sirbu, D., Corno, M., Ullrich, M.S. and Kuhnert, N. (2018) Characterization of triacylglycerols in unfermented cocoa beans by HPLC-ESI mass spectrometry. *Food Chemistry* **254**, 232-240.
- Solovchenko, A.E. (2012) Physiological role of neutral lipid accumulation in eukaryotic microalgae under stresses. *Russian Journal of Plant Physiology* **59**, 167-176.

- Wang, S., Verma, S.K., Hakeem Said, I., Thomsen, L., Ullrich, M.S. and Kuhnert, N. (2018) Changes in the fucoxanthin production and protein profiles in *Cylindrotheca closterium* in response to blue light-emitting diode light. *Microbial Cell Factories* **17**, 110.
- Wang, S., Zhang, L., Yang, G., Zhu, B. and Pan, K. (2015) Purification of a diatom and its identification to *Cylindrotheca closterium*. *Journal of Ocean University of China* **14**, 357-361.
- Webb, M.S. and Green, B.R. (1991) Biochemical and biophysical properties of thylakoid acyl lipids. *Biochimica et Biophysica Acta* **1060**, 133-158.
- Yaakob, Z., Ali, E., Zainal, A., Mohamad, M. and Takriff, M.S. (2014) An overview: biomolecules from microalgae for animal feed and aquaculture. *Journal of Biological Research-Thessaloniki* **21**, 6.
- Yang, D., Song, D., Kind, T., Ma, Y., Hoefkens, J. and Fiehn, O. (2015) Lipidomic analysis of *Chlamydomonas reinhardtii* under nitrogen and sulfur deprivation. *PLoS One* **10**, e0137948.
- Yodsuwan, N., Sawayama, S. and Sirisansaneeyakul, S. (2017) Effect of nitrogen concentration on growth, lipid production and fatty acid profiles of the marine diatom *Phaeodactylum tricoratum*. *Agriculture and Natural Resources* **51**, 190-197.
- Zhu, L.D., Li, Z.H. and Hiltunen, E. (2016) Strategies for lipid production improvement in microalgae as a biodiesel feedstock. *BioMed Research International*, 8792548.
- Zhu, S., Wang, Y., Shang, C., Wang, Z., Xu, J. and Yuan, Z. (2015) Characterization of lipid and fatty acids composition of *Chlorella zofingiensis* in response to nitrogen starvation. *Journal of Bioscience and Bioengineering* **120**, 205-209.

5.8 Supplementary material

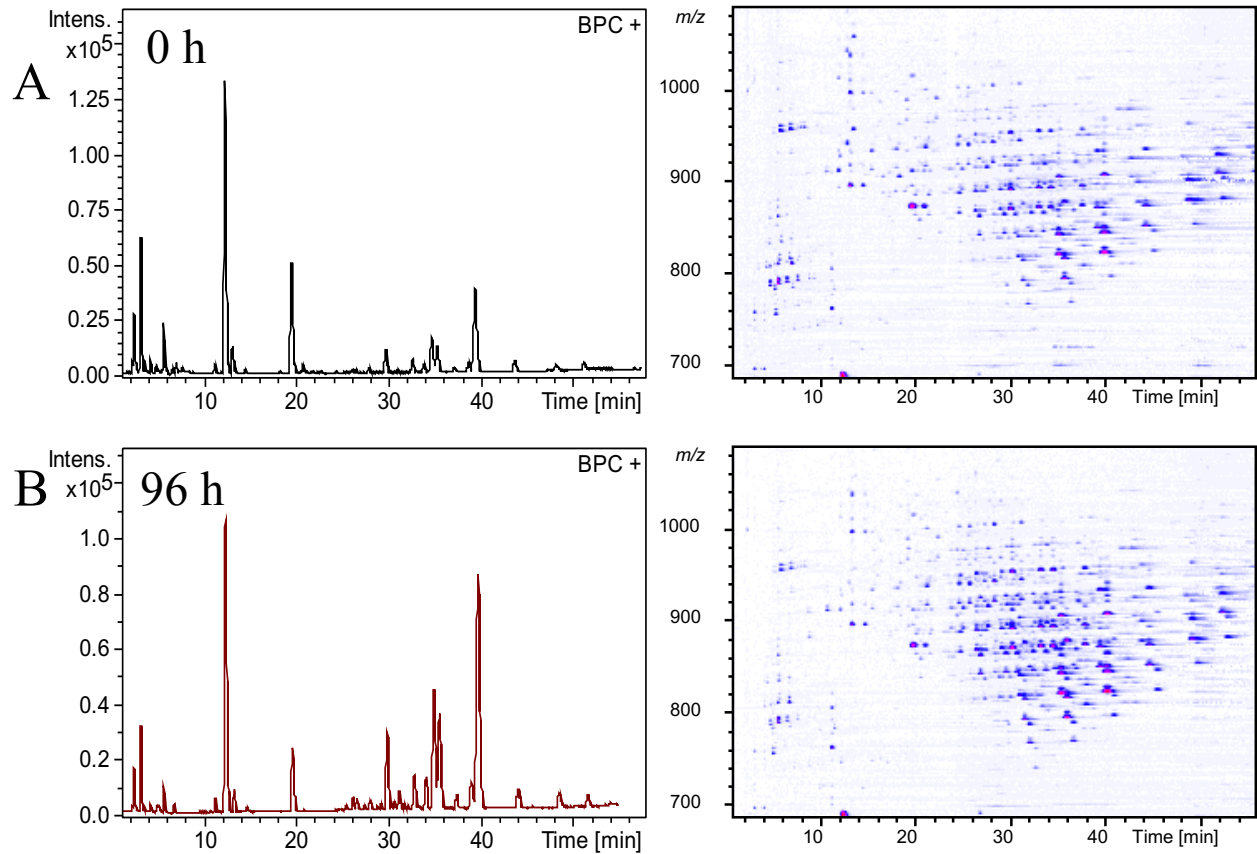


Figure S1: Representative chromatograms of A) lipid extract of *Cylindrotheca closterium* at 0 h (left panel) and its corresponding Two-dimensional (2D) map of reverse-phase high-resolution MS, and B) lipid extract of *Cylindrotheca closterium* at 96 h (left panel) and its corresponding Two-dimensional (2D) map of reverse-phase high-resolution MS.

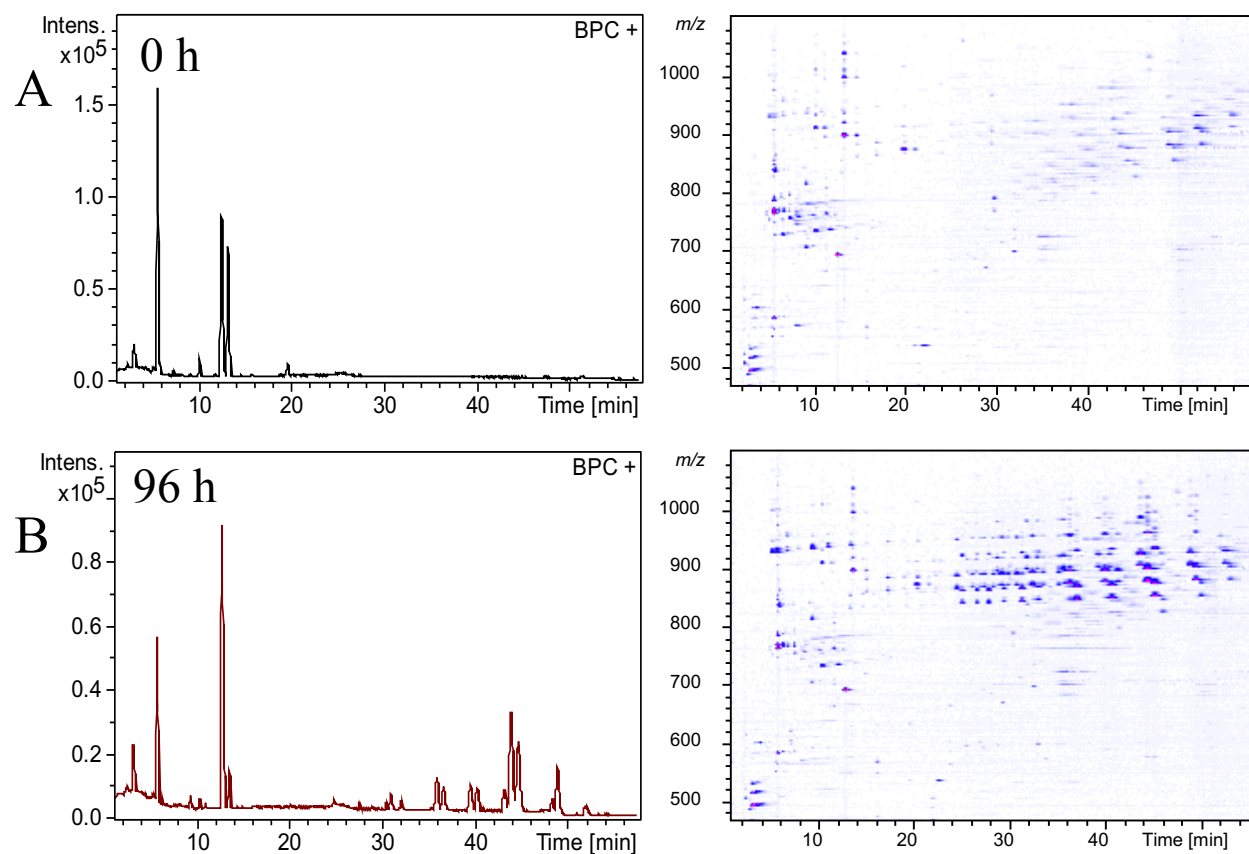


Figure S2: Representative chromatograms of a) lipid extract of *Scenedesmus* sp. at 0 h (left panel) and its corresponding Two-dimensional (2D) map of reverse-phase high-resolution MS, and b) lipid extract of *Scenedesmus* sp. at 96 h (left panel) and its corresponding Two-dimensional (2D) map of reverse-phase high-resolution MS.

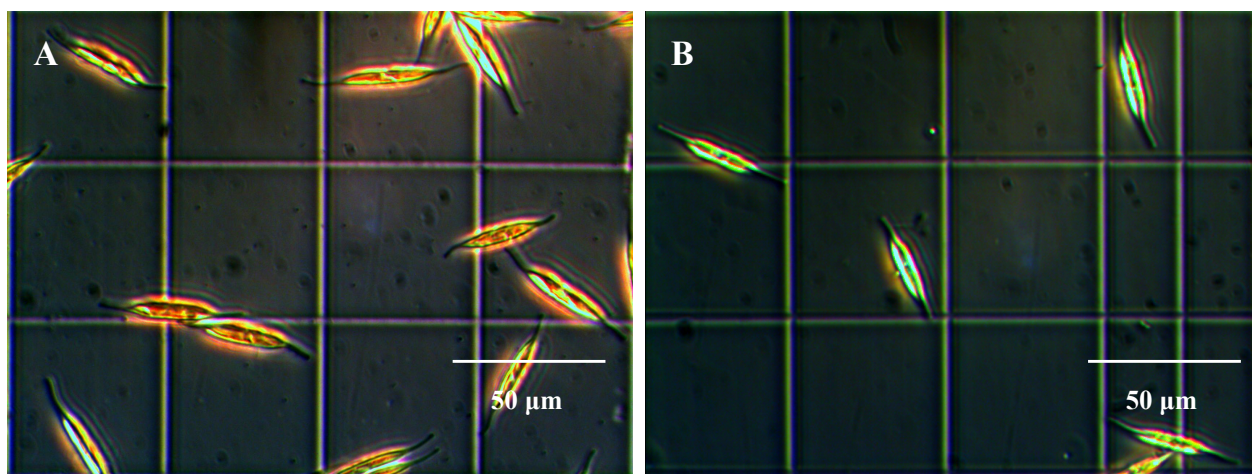


Figure S3. Microscopic observation of *C. closterium* cells before nitrogen starvation and after 96 h nitrogen starvation. A: Cells before nitrogen starvation; B: Cells after 96 h nitrogen starvation.

Table S1. Lipid molecular species in *Scenedesmus* sp. subdivided into homologous series

No.	Rt (min)	Molecular formulae	Theoretical	Experimental	Error [ppm]	Common Name
			mass [M+NH ₄] ⁺	mass [M+NH ₄] ⁺		
1	36.3	C ₄₇ H ₉₄ NO ₆	768.7076	768.7076	0.1	TAG 45:0 (15:0/16:0/14:0) *
2	40.6	C ₄₉ H ₉₈ NO ₆	796.7389	796.7372	2.1	TAG 46:0 (14:0/16:0/16:0)
3	42.6	C ₅₀ H ₁₀₀ NO ₆	810.7545	810.7522	2.9	TAG 47:0 (15:0/16:0/16:0)
4	45	C ₅₁ H ₁₀₂ NO ₆	824.7702	824.7691	1.3	TAG 48:0 (16:0/16:0/16:0)
5	47.2	C ₅₂ H ₁₀₄ NO ₆	838.7858	838.7856	0.3	TAG 49:0 (17:0/16:0/16:0) & TAG 49:0 (15:0/16:0/18:0)
6	49.1	C ₅₃ H ₁₀₆ NO ₆	852.8015	852.8024	1.1	TAG 50:0 (18:0/16:0/16:0)
7	52.4	C ₅₅ H ₁₁₀ NO ₆	880.8328	880.8344	1.9	TAG 52:0 (18:0/18:0/16:0)
8	36.2	C ₄₉ H ₉₆ NO ₆	794.7232	794.7215	2.1	TAG 46:1 (14:0/14:0/18:1) *
9	38.7	C ₄₁ H ₉₄ N ₉ O ₆	808.7322	808.7333	1.5	TAG 47:1 (14:0/15:0/18:1) *
10	40.4	C ₅₁ H ₁₀₀ NO ₆	822.7545	822.7523	2.7	TAG 48:1 (14:0/16:0/18:1) *
11	41.9	C ₅₂ H ₁₀₂ NO ₆	836.7602	836.7681	2.4	TAG 49:1 (15:0/16:0/18:1) *
12	44.1	C ₅₃ H ₁₀₄ NO ₆	850.7858	850.7858	0	TAG 50:1 (16:0/16:0/18:1) & TAG 50:1 (16:0/16:0/18:1) TAG 51:1 (17:0/16:0/18:1) & TAG 51:1 (15:0/18:0/18:1)
13	46.3	C ₅₄ H ₁₀₆ NO ₆	864.8015	864.7986	3.3	TAG 52:1 (18:0/16:0/18:1) TAG 53:1 (17:0/18:0/18:1)
14	48.6	C ₅₅ H ₁₀₈ NO ₆	878.8171	878.8178	0.7	TAG 54:1 (18:0/18:0/18:1) & TAG 54:1 (20:0/16:0/18:1)
15	50.1	C ₅₆ H ₁₁₀ NO ₆	892.8328	892.8320	0.9	TAG 47:2 (15:0/16:1/16:1)
16	51.7	C ₅₇ H ₁₁₂ NO ₆	906.8484	906.8487	0.3	TAG 48:2 (14:0/18:1/16:1) TAG 50:2 (14:0/18:1/18:1) TAG 51:2 (15:0/18:1/18:1) TAG 52:2 (16:0/18:1/18:1) TAG 53:2 (17:0/18:1/18:1) TAG 54:2 (18:0/18:1/18:1)
17	32.2	C ₄₉ H ₉₄ NO ₆	792.7076	792.7080	0.5	TAG 56:2 (20:0/18:1/18:1)
18	36.3	C ₅₁ H ₉₈ NO ₆	820.7389	820.7386	0.3	TAG 50:3 (16:0/16:0/18:3)
19	39.8	C ₅₃ H ₁₀₂ NO ₆	848.7702	848.7699	0.3	TAG 52:3 (16:0/18:1/18:2)
20	41.1	C ₅₄ H ₁₀₄ NO ₆	862.7858	862.7847	1.3	TAG 52:3 (16:0/18:0/18:3)
21	43.3	C ₅₅ H ₁₀₆ NO ₆	876.8015	876.8003	1.4	
22	45.5	C ₅₆ H ₁₀₈ NO ₆	890.8171	890.8163	0.9	
23	48	C ₅₇ H ₁₁₀ NO ₆	904.8328	904.8326	0.2	
24	51.3	C ₅₉ H ₁₁₄ NO ₆	932.8641	932.8646	0.6	
25	36.1	C ₅₃ H ₁₀₀ NO ₆	846.7545	846.7539	0.7	
26	39.1	C ₅₅ H ₁₀₄ NO ₆	874.7858	874.7848	1.2	
27	40.4	C ₅₅ H ₁₀₄ NO ₆	874.7858	874.7859	0.1	

Chapter 5

28	42.7	C ₅₇ H ₁₀₈ NO ₆	902.8171	902.8162	1	TAG 54:3 (18:1/18:1/18:1)
29	43.5	C ₅₇ H ₁₀₈ NO ₆	902.8171	902.8157	1.5	TAG 54:3 (18:1/18:0/18:2)
30	44.8	C ₅₇ H ₁₀₈ NO ₆	902.8171	902.8168	0.4	TAG 54:3 (18:0/18:0/18:3)
31	35.4	C ₅₅ H ₁₀₂ NO ₆	872.7702	872.7693	0.9	TAG 52:4 (18:1/16:1/18:2) *
32	38.3	C ₅₇ H ₁₀₆ NO ₆	900.8015	900.7992	2.5	TAG 54:4 (18:1/18:2/18:1)
33	34.8	C ₅₇ H ₁₀₄ NO ₆	898.7858	898.7840	2	TAG 54:5 (18:1/18:2/18:2) & TAG 54:5 (18:1/18:1/18:3)
34	24.4	C ₅₃ H ₉₂ NO ₆	838.6919	838.6909	1.3	TAG 50:7 (C16:4/C18:3/C16:0)
35	26	C ₅₃ H ₉₄ NO ₆	840.7076	840.7074	1.8	TAG 50:6 (C16:3/C18:3/C16:0)
36	27.2	C ₅₃ H ₉₄ NO ₆	840.7076	840.7073	0.3	TAG 50:6 (C16:4/C18:2/C16:0)
37	28.7	C ₅₃ H ₉₆ NO ₆	842.7232	842.7217	1.9	TAG 50:5 (C16:4/C18:1/C16:0)
38	30.5	C ₅₃ H ₉₆ NO ₆	842.7232	842.7223	1.1	TAG 50:5 (C16:3/C18:2/C16:0)
39	31.7	C ₅₃ H ₉₈ NO ₆	844.7389	844.7377	1.3	TAG 50:4 (C16:3/C18:1/C16:0)
40	32.2	C ₅₃ H ₉₈ NO ₆	844.7389	844.7389	0	TAG 50:4 (C16:1/C18:3/C16:0)
41	24	C ₅₅ H ₉₄ NO ₆	864.7076	864.7062	1.5	TAG 52:8 (C16:4/C18:3/C18:1)
42	25.6	C ₅₅ H ₉₆ NO ₆	866.7232	866.7239	0.8	TAG 52:7 (C16:3/C18:2/C18:2)
43	26.4	C ₅₅ H ₉₆ NO ₆	866.7232	866.7241	1	TAG 52:7 (C16:3/C18:3/C18:1)
44	26.7	C ₅₅ H ₉₆ NO ₆	866.7232	866.7217	1.8	TAG 52:7 (C16:4/C18:2/C18:1)
45	27.7	C ₅₅ H ₉₆ NO ₆	866.7232	866.7212	2.4	TAG 52:7 (C16:4/C18:3/C18:0)
46	28.2	C ₅₅ H ₉₈ NO ₆	868.7389	868.7379	1.1	TAG 52:6 (C16:3/C18:2/C18:1)
47	28.6	C ₅₅ H ₉₈ NO ₆	868.7389	868.7378	1.2	TAG 52:6 (C16:0/C18:3/C18:3)
48	29.1	C ₅₅ H ₉₈ NO ₆	868.7389	868.7374	1.7	TAG 52:6 (C16:0/C18:2/C18:4)
49	30.3	C ₅₅ H ₉₈ NO ₆	868.7389	868.7370	2.2	TAG 52:6 (C16:4/C18:1/C18:1)
50	31.6	C ₅₅ H ₁₀₀ NO ₆	870.7545	870.7522	2.7	TAG 52:5 (C16:0/C18:2/C18:3)
51	32.7	C ₅₅ H ₁₀₀ NO ₆	870.7545	870.7529	1.9	TAG 52:5 (C16:3/C18:1/C18:1)
52	34.5	C ₅₅ H ₁₀₀ NO ₆	870.7545	870.7531	1.6	TAG 52:5 (C16:0/C18:1/C18:4)
53	34.9	C ₅₅ H ₁₀₂ NO ₆	872.7702	872.7697	0.5	TAG 52:4 (C16:0/C18:2/C18:2)
54	36.2	C ₅₅ H ₁₀₂ NO ₆	872.7702	872.7702	0.1	TAG 52:4 (C16:0/C18:1/C18:3)
55	25	C ₅₇ H ₉₈ NO ₆	892.7379	892.7379	1.1	TAG 52:8 (C18:2/C18:3/C18:3) *
56	26	C ₅₇ H ₉₈ NO ₆	892.7379	892.7397	1	TAG 52:8 (C18:1/C18:4/C18:3) *
57	28.1	C ₅₇ H ₁₀₀ NO ₆	894.7545	894.7522	2.6	TAG 52:7 (C18:1/C18:3/C18:3)
58	29.7	C ₅₇ H ₁₀₀ NO ₆	894.7545	894.7553	0.9	TAG 52:7 (C18:2/C18:2/C18:3) *
59	31	C ₅₇ H ₁₀₂ NO ₆	896.7706	896.7712	1.1	TAG 52:6 (C18:1/C18:3/C18:2) & TAG 52:6 (C18:1/C18:4/C18:1)
60	32.1	C ₅₇ H ₁₀₂ NO ₆	896.7702	896.7711	1	TAG 52:6 (C18:1/C18:4/C18:1) *
61	5.1	C ₄₉ H ₈₂ NO ₁₅	924.5679	924.5683	0.4	DGDG 34:7 (16:3/18:4)
62	5.6	C ₄₉ H ₈₄ NO ₁₅	926.5835	926.5812	2.5	DGDG 34:6 (16:3/18:3)

Chapter 5

63	6.6	C ₄₉ H ₈₆ NO ₁₅	928.5992	928.5987	0.6	DGDG 34:5 (16:3/18:2)
64	6.6	C ₅₁ H ₈₈ NO ₁₅	954.6148	954.6162	1.4	DGDG 36:6 (18:3/18:3)
65	7.7	C ₄₉ H ₈₈ NO ₁₅	930.6148	930.6153	0.5	DGDG 34:4 (16:0/18:4)
66	9.2	C ₄₉ H ₉₀ NO ₁₅	932.6305	932.6307	0.3	DGDG 34:3 (16:0/18:3)
67	10.7	C ₄₉ H ₉₂ NO ₁₅	934.6461	934.6472	1.1	DGDG 34:2 (16:0/18:2)
68	13	C ₄₉ H ₉₄ NO ₁₅	936.6618	936.6610	0.8	DGDG 34:1 (16:0/18:1)
69	5.6	C ₄₃ H ₇₂ NO ₁₀	762.5151	762.5146	0.6	MGDG 34:7 (16:4/18:3)
70	6.1	C ₄₃ H ₇₄ NO ₁₀	764.5307	764.5312	0.7	MGDG 34:6 (16:3/18:3)
71	6.7	C ₄₃ H ₇₄ NO ₁₀	764.5307	764.5332	3.3	MGDG 34:6 (16:4/18:2)
72	7.3	C ₄₃ H ₇₆ NO ₁₀	766.5464	766.5448	2.1	MGDG 34:5 (16:3/18:2)
73	9.2	C ₄₂ H ₇₄ NO ₇	704.546	704.5440	2.7	DGTS 32:4 (16:0/16:4)
74	10.1	C ₄₄ H ₇₈ NO ₇	732.5773	732.5771	0.3	DGTS 34:4 (16:0/18:4)
75	11.8	C ₄₄ H ₈₀ NO ₇	734.5929	734.5905	3.3	DGTS 34:3 (16:0/18:3)
76	4.8	C ₄₄ H ₇₀ NO ₇	724.5147	724.5151	0.5	DGTS 34:8 (16:4/18:4) *
77	6.7	C ₄₄ H ₇₂ NO ₇	726.5303	726.5302	0.2	DGTS 34:7 (16:4/18:3)
78	7.3	C ₄₄ H ₇₄ NO ₇	728.546	728.5452	1.1	DGTS 34:6 (16:4/18:2) *
79	7.6	C ₄₄ H ₇₄ NO ₇	728.546	728.5471	1.6	DGTS 34:5 (16:4/18:1) *
80	6.5	C ₃₉ H ₇₉ NO ₁₀ P	752.5436	752.5460	3.2	PG 34:7 (16:4/18:3) *
81	7.5	C ₃₉ H ₈₁ NO ₁₀ P	754.5593	754.5610	2.2	PG 34:6 (16:3/18:3) *
82	8.4	C ₃₉ H ₈₃ NO ₁₀ P	756.5749	756.5750	0.1	PG 34:5 (16:2/18:3)
83	9.4	C ₃₉ H ₈₅ NO ₁₀ P	758.5911	758.5919	1.1	PG 34:4 (16:2/18:2) *
84	9.9	C ₃₉ H ₈₅ NO ₁₀ P	758.5911	758.5918	0.9	PG 34:4 (16:1/18:3)
85	11.4	C ₃₉ H ₈₇ NO ₁₀ P	760.6067	760.6055	1.6	PG 34:3 (16:1/18:2) *
86	12.2	C ₃₉ H ₈₇ NO ₁₀ P	760.6067	760.6050	2.2	PG 34:3 (16:0/18:3) *
87	9.9	C ₄₄ H ₇₇ NO ₈ P	778.5381	778.5377	0.5	PE 36:6 (C18:3/18:3)
88	11	C ₄₄ H ₇₉ NO ₈ P	780.5538	780.5534	0.5	PE 36:5 (C18:3/18:2)
89	12.4	C ₄₄ H ₈₁ NO ₈ P	782.5694	782.5682	1.5	PE 36:4 (C18:2/18:2)
90	14.6	C ₄₄ H ₈₃ NO ₈ P	784.5851	784.5860	1.2	PE 36:3 (C18:2/18:1)
91	3	C ₂₆ H ₄₄ NO ₆	466.3163	466.3154	1.9	LysoDGTS 16:2
92	3.3	C ₂₈ H ₄₈ NO ₆	494.3476	494.3466	2	LysoDGTS 18:2
93	3.7	C ₂₈ H ₅₀ NO ₆	496.3633	496.3627	1.1	LysoDGTS 18:3
94	10.3	C ₅₅ H ₇₁ MgN ₄ O ₆	907.5219	907.5231	1.4	Chlorophyll b_1
95	11.1	C ₅₅ H ₇₁ MgN ₄ O ₆	907.5219	907.5221	0.3	Chlorophyll b_2
96	13.4	C ₅₅ H ₇₃ MgN ₄ O ₅	893.5426	893.5425	0.1	Chlorophyll a_1
97	14.9	C ₅₅ H ₇₃ MgN ₄ O ₅	893.5426	893.5430	0.5	Chlorophyll a_2
98	19.7	C ₅₇ H ₇₅ MgN ₄ O ₂	871.5735	871.5718	2	Pheophytin a_1
99	20.9	C ₅₇ H ₇₅ MgN ₄ O ₂	871.5735	871.5719	1.8	Pheophytin a_2

*tentatively assigned

Table S2. Lipid molecular species in *C. closterium* subdivided into homologous series

No.	Rt (min)	Molecular formulae	Theoretical	Experimental	Error [ppm]	Common Name
			mass [M+NH ₄] ⁺	mass [M+NH ₄] ⁺		
1	32.5	C ₄₅ H ₉₀ NO ₆	740.6763	740.6752	1.4	TAG 42:0 (14:0/14:0/14:0)
2	34.3	C ₄₆ H ₉₂ NO ₆	754.6919	754.6904	2.1	TAG 43:0 (15:0/14:0/14:0)
3	36.3	C ₄₇ H ₉₄ NO ₆	768.7076	768.7054	2.9	TAG 44:0 (16:0/14:0/14:0)
4	38.3	C ₄₈ H ₉₆ NO ₆	782.7232	782.7256	3.1	TAG 45:0 (15:0/16:0/14:0)
5	40.5	C ₄₉ H ₉₈ NO ₆	796.7389	796.7402	1.7	TAG 46:0 (16:0/16:0/14:0)
6	42.6	C ₅₀ H ₁₀₀ NO ₆	810.7545	810.7544	0.2	TAG 47:0 (16:0/16:0/15:0)
7	45	C ₅₁ H ₁₀₂ NO ₆	824.7702	824.7709	0.9	TAG 48:0 (16:0/16:0/16:0) & TAG 48:0 (14:0/16:0/18:0)
8	47.3	C ₅₂ H ₁₀₄ NO ₆	838.7858	838.7822	4.4	TAG 49:0 (16:0/16:0/17:0) & TAG 49:0 (15:0/16:0/18:0)
9	49.2	C ₅₃ H ₁₀₆ NO ₆	852.8015	852.8029	1.7	TAG 50:0 (16:0/18:0/16:0) & TAG 50:0 (14:0/18:0/18:0)
10	52.3	C ₅₅ H ₁₁₀ NO ₆	880.8328	880.8310	2	TAG 52:0 (18:0/16:0/18:0)
11	31.8	C ₄₇ H ₉₂ NO ₆	766.6919	766.6920	0	TAG 44:1 (14:0/16:1/14:0)
12	33.6	C ₄₈ H ₉₄ NO ₆	780.7076	780.7099	3	TAG 45:1 (14:0/16:1/15:0)
13	35.6	C ₄₉ H ₉₆ NO ₆	794.7232	794.7217	1.9	TAG 46:1 (14:0/16:1/16:0)
14	37.5	C ₅₀ H ₉₈ NO ₆	808.7389	808.7383	0.7	TAG 47:1 (15:0/16:1/16:0) & TAG 47:1 (15:0/18:1/14:0)
15	39.8	C ₅₁ H ₁₀₀ NO ₆	822.7545	822.7555	1.2	TAG 48:1 (16:0/16:1/16:0) & TAG 48:1 (16:0/18:1/14:0)
16	41.8	C ₅₂ H ₁₀₂ NO ₆	836.7702	836.7692	1.2	TAG 49:1 (16:0/18:1/15:0) & TAG 49:1 (14:0/18:1/17:0)
17	44.1	C ₅₃ H ₁₀₄ NO ₆	850.7858	850.7873	1.7	TAG 50:1 (16:0/16:0/18:1) & TAG 50:1 (18:0/18:1/14:0)
18	48.6	C ₅₅ H ₁₀₈ NO ₆	878.8171	878.8192	2.4	TAG 52:1 (16:0/18:1/18:0) & TAG 52:1 (14:0/18:1/20:0)
19	51.6	C ₅₇ H ₁₁₂ NO ₆	906.8484	906.8484	0	TAG 46:1 (14:0/16:1/16:0)
20	31.3	C ₄₉ H ₉₄ NO ₆	792.7076	792.7068	1	TAG 46:2 (14:0/16:1/16:1)
21	33.1	C ₅₀ H ₉₆ NO ₆	806.7232	806.7213	2.4	TAG 47:2 (15:0/16:1/16:1)

Chapter 5

22	34.9	C ₅₁ H ₉₈ NO ₆	820.7389	820.7386	0.4	TAG 48:2 (16:0/16:1/16:1) &
						TAG 48:2 (14:0/18:1/16:1)
23	37	C ₅₂ H ₁₀₀ NO ₆	834.7545	834.7528	2.1	TAG 49:2 (17:0/16:1/16:1) &
						TAG 49:2 (15:0/16:1/18:1)
24	39.1	C ₅₃ H ₁₀₂ NO ₆	848.7702	848.7697	0.6	TAG 50:2 (16:0/18:1/16:1) &
						TAG 50:2 (14:0/18:1/18:1)
25	43.3	C ₅₅ H ₁₀₆ NO ₆	876.8015	876.8030	1.8	TAG 52:2 (16:0/18:1/18:1) &
						TAG 52:2 (18:0/18:1/16:1)
26	47.9	C ₅₇ H ₁₁₀ NO ₆	904.8328	904.8321	0.7	TAG 54:2 (18:0/18:1/18:1) &
						TAG 52:2 (20:0/18:1/16:1)
27	26	C ₅₁ H ₉₂ NO ₆	814.6919	814.6925	0.7	TAG 48:5 (14:0/16:2/18:3) *
28	27.1	C ₅₁ H ₉₂ NO ₆	814.6909	814.6909	1.2	TAG 48:5 (14:0/14:0/20:5)
29	28.7	C ₅₁ H ₉₄ NO ₆	816.7076	816.7073	0.4	TAG 48:4 (14:0/16:1/18:3)
30	29	C ₅₁ H ₉₄ NO ₆	816.7076	816.7071	0.5	TAG 48:4 (14:0/16:0/18:4) *
31	29.8	C ₅₁ H ₉₄ NO ₆	816.7076	816.7059	2	TAG 48:4 (14:0/14:0/20:4)
32	31.5	C ₅₁ H ₉₆ NO ₆	818.7232	818.7229	0.4	TAG 48:3 (16:1/16:1/16:1)
33	32.6	C ₅₁ H ₉₆ NO ₆	818.7232	818.7226	0.7	TAG 48:3 (14:0/14:0/20:3) *
34	25.6	C ₅₃ H ₉₄ NO ₆	840.7089	840.7079	1.2	TAG 50:5 (14:0/16:2/20:4) *
35	26.7	C ₅₃ H ₉₄ NO ₆	840.7089	840.7083	0.8	TAG 50:6 (14:0/16:1/20:5)
36	29.3	C ₅₃ H ₉₆ NO ₆	842.7232	842.7256	2.8	TAG 50:5 (14:0/16:1/20:4)
37	30.4	C ₅₃ H ₉₆ NO ₆	842.7320	842.7246	1.7	TAG 50:5 (14:0/16:0/20:5)
38	32.1	C ₅₃ H ₉₈ NO ₆	844.7389	844.7401	1.4	TAG 50:4 (16:0/16:1/18:3)
39	33.4	C ₅₃ H ₉₈ NO ₆	844.7389	844.7387	0.2	TAG 50:4 (14:0/16:0/20:4) &
						TAG 50:4 (16:0/16:0/18:4)
40	34.3	C ₅₃ H ₁₀₀ NO ₆	846.7545	846.7547	0.3	TAG 50:3 (16:1/16:1/18:1)
41	35.7	C ₅₃ H ₁₀₀ NO ₆	846.7545	846.7549	0.4	TAG 50:3 (16:0/16:0/18:3)
42	20.1	C ₅₅ H ₉₂ NO ₆	862.6919	862.6906	1.6	TAG 52:9 (16:1/16:3/20:5)
43	21.5	C ₅₅ H ₉₂ NO ₆	862.6919	862.6915	0.5	TAG 52:9 (14:0/18:4/20:5) *
44	22.9	C ₅₅ H ₉₄ NO ₆	864.7076	864.7065	1.3	TAG 52:8 (16:1/16:3/20:4) *
45	23.5	C ₅₅ H ₉₄ NO ₆	864.7076	864.7087	1.3	TAG 52:8 (16:1/16:2/20:5)
46	24.6	C ₅₅ H ₉₄ NO ₆	864.7076	864.7088	1.5	TAG 52:8 (16:0/16:3/20:5)
47	26.3	C ₅₅ H ₉₆ NO ₆	866.7232	866.7266	3.9	TAG 52:7 (16:1/16:1/20:5)
48	27	C ₅₅ H ₉₆ NO ₆	866.7232	866.7246	1.6	TAG 52:7 (16:0/16:2/20:5)
49	27.3	C ₅₅ H ₉₆ NO ₆	866.7232	866.7251	2.2	TAG 52:7 (16:0/16:3/20:4) *
50	28.8	C ₅₅ H ₉₈ NO ₆	868.7398	868.7394	0.6	TAG 52:6 (16:1/16:1/20:4)
51	29.9	C ₅₅ H ₉₈ NO ₆	868.7398	868.7412	2.7	TAG 52:6 (16:0/16:1/20:5)

Chapter 5

52	32.9	C ₅₅ H ₁₀₀ NO ₆	870.7545	870.7539	0.7	TAG 52:5 (16:0/16:1/20:4)
53	34.2	C ₅₅ H ₁₀₀ NO ₆	870.7545	870.7550	0.6	TAG 52:5 (16:0/16:0/20:5)
54	37.3	C ₅₅ H ₁₀₂ NO ₆	872.7702	872.7711	1.1	TAG 52:4 (16:0/16:0/20:4)
55	20.4	C ₅₇ H ₉₄ NO ₆	888.7089	888.7058	2	TAG 54:10 (18:4/16:1/20:5)
56	21.6	C ₅₇ H ₉₄ NO ₆	888.7089	888.7081	0.6	TAG 54:10 (18:4/16:2/20:4) *
57	23.6	C ₅₇ H ₉₆ NO ₆	890.7232	890.7240	0.9	TAG 54:9 (18:3/16:1/20:5)
58	24.9	C ₅₇ H ₉₆ NO ₆	890.7232	890.7234	0.2	TAG 54:9 (18:4/16:0/20:5) &
59	26.3	C ₅₇ H ₉₈ NO ₆	892.7389	892.7423	3.8	TAG 54:8 (18:4/16:1/20:3) *
60	27.4	C ₅₇ H ₉₈ NO ₆	892.7389	892.7392	0.3	TAG 54:8 (18:4/16:0/20:4) &
61	29.4	C ₅₇ H ₁₀₀ NO ₆	894.7545	894.7551	0.6	TAG 54:8 (18:3/16:1/20:3) *
62	30.6	C ₅₇ H ₁₀₀ NO ₆	894.7545	894.7555	1	TAG 54:7 (18:3/16:0/20:4) &
63	32.3	C ₅₇ H ₁₀₂ NO ₆	896.7702	896.7716	1.7	TAG 54:6 (18:2/16:1/20:3) *
64	33.4	C ₅₇ H ₁₀₂ NO ₆	896.7702	896.7734	3.6	TAG 54:6 (18:1/16:0/20:5) &
65	36.8	C ₅₇ H ₁₀₄ NO ₆	898.7858	898.7858	0	TAG 54:5 (18:1/16:0/20:4) &
66	38.3	C ₅₇ H ₁₀₄ NO ₆	898.7858	898.7800	1	TAG 54:5 (18:1/18:1/18:3) *
67	24.4	C ₅₉ H ₉₈ NO ₆	916.7389	916.7410	2.3	TAG 56:10 (20:4/16:1/20:5) & TAG 56:10 (18:3/18:3/20:4) & TAG 56:10 (18:3/18:1/22:6)
68	25.6	C ₅₉ H ₉₈ NO ₆	916.7389	916.7371	1.9	TAG 56:10 (20:5/16:0/20:5) & TAG 56:10 (18:4/16:1/22:6)
69	27.1	C ₅₉ H ₁₀₀ NO ₆	918.7545	918.7555	1.1	TAG 56:9 (20:3/16:1/20:5)
70	28.1	C ₅₉ H ₁₀₀ NO ₆	918.7545	918.7552	0.7	TAG 56:9 (20:4/16:0/20:5)
71	30	C ₅₉ H ₁₀₂ NO ₆	920.7702	920.7697	0.5	TAG 56:8 (20:3/16:1/20:4)
72	30.9	C ₅₉ H ₁₀₂ NO ₆	920.7702	920.7692	1.1	TAG 56:8 (20:4/16:0/20:4)
73	6	C ₅₁ H ₈₆ NO ₁₅	952.5992	952.5988	0.4	DGDG 36:7 (C16:2/C20:5)
74	7	C ₅₁ H ₈₈ NO ₁₅	954.6148	954.6124	2.6	DGDG 36:6 (C16:1/C20:5)
75	8.1	C ₅₁ H ₉₀ NO ₁₅	956.6305	956.6307	0.2	DGDG 36:5 (C16:0/C20:5)
76	10.7	C ₄₇ H ₉₀ NO ₁₅	908.6305	908.6314	1	DGDG 32:1 (C16:0/C16:1)
77	8.8	C ₄₇ H ₈₈ NO ₁₅	906.6148	906.6127	2.4	DGDG 32:2 (C16:1/C16:1)
78	8.9	C ₄₅ H ₈₆ NO ₁₅	880.5992	880.6004	1.4	DGDG 30:1 (C14:0/C16:1)
79	8.5	C ₅₁ H ₉₀ NO ₁₅	956.6305	956.6282	2.4	DGDG 36:5 (C18:2/C18:3) *
80	4.9	C ₄₅ H ₇₂ NO ₁₀	786.5151	786.5152	0.2	MGDG 36:8 (16:4/20:5)
81	5.7	C ₄₅ H ₇₄ NO ₁₀	788.5307	788.5302	0.7	MGDG 36:8 (16:3/20:5)
82	6.5	C ₄₅ H ₇₆ NO ₁₀	790.5456	790.5480	2.1	MGDG 36:8 (16:2/20:5)
83	7.7	C ₄₅ H ₇₈ NO ₁₀	792.5620	792.5612	1.1	MGDG 36:8 (16:1/20:5)
84	6.8	C ₄₁ H ₈₀ NO ₁₂ S	810.5396	810.5373	2.8	SQDG 32:1 (16:0/16:1)

Chapter 5

85	5.9	C ₄₃ H ₈₀ NO ₁₂ S	834.5396	834.5398	0.3	SQDG 34:3 (16:0/18:3)
86	5.2	C ₃₇ H ₇₄ NO ₁₂ S	756.4926	756.4903	3.1	SQDG 28:0 (14:0/14:0) *
87	6.9	C ₃₉ H ₇₈ NO ₁₂ S	784.5239	784.5257	2.3	SQDG 30:0 (14:0/16:0)
88	4.8	C ₄₃ H ₇₈ NO ₁₂ S	832.5239	832.5220	2.3	SQDG 34:4 (16:1/18:3)
89	13.4	C ₅₅ H ₇₃ MgN ₄ O ₅	893.5426	893.5408	2	Chlorophyll a_1
90	14.8	C ₅₅ H ₇₃ MgN ₄ O ₅	893.5426	893.5438	1.3	Chlorophyll a_1
91	19.7	C ₅₅ H ₇₅ N ₄ O ₅	871.5735	871.5724	0.9	Pheophytin a_1
92	21	C ₅₅ H ₇₅ N ₄ O ₅	871.5735	871.5710	2.6	Pheophytin a_1

*tentatively assigned

6. Conclusions and Prospective Researches

Humans are increasingly exposed to multi-resistant bacteria, which emphasizes the need for the discovery of alternative antibacterial substances. Metabolites synthesized by microalgae hold the promise as the feedstock for novel antibiotics with the progressing development in cultivation technology of microalgae. With the purification and identification methods developed in **Chapter 3**, the discovery of novel antibacterial substances can be conducted in microalgae from different classes with minor modifications. Additionally, *P. tricornutum* biomass could be tested as food supplements or feeds for animals as a substitution of antibiotics. In particular, *P. tricornutum*, due to its inhibitory effect against *Vibrio* species, could be of great interest in marine aquacultures, which are often contaminated by different *Vibrio* species.

The results on optimization of pigment synthesis in *C. closterium* in **Chapter 4** suggested that LED light illumination led to fucoxanthin yields comparable to those obtained with fluorescent light at the same photosynthetic active radiation and light regime. The use of blue LED light consumed considerably less energy as compared to fluorescent light illumination. Thus, our study proved that the application of LED light with a specific spectrum is a practical way to save energy in algal cultivation and allows indoor cultivation in “Algae Tower”. Nevertheless, the productivity of fucoxanthin decreased in our bag PBRs compared to bottle PBRs, which necessitated a modification of the LEDs configuration for current PBRs. For instance, a LED light with better penetration rate, novel materials for bag manufacturing, or the implementation of high-frequency pulsed LED might be suitable way on how to improve this situation. Due to the excellent property of rapid sedimentation, *C. closterium* could be easily harvested from our PBRs as a concentrated algal suspension before centrifugation. A significant amount of dewatering cost and energy could be saved in this stage. Consequently, implementing a low-cost and effective extraction and purification approach towards large-scale production would be developed in the next step. Furthermore, results of our study allowed the conclusion that fucoxanthin production was promoted by an increased photosynthetic efficiency. It is therefore tempting to speculate that future genetic engineering of the algae could help to upregulate the expression of key photosynthesis genes coded in the genome of the chloroplast. An increase in the bioavailability of CO₂ may also

favor the fucoxanthin synthesis by accelerating the turnover of photosynthesis. More transcriptomic and proteomic information is needed to elucidate the *de novo* biosynthesis pathway of fucoxanthin in diatom.

Two different mechanisms of lipid accumulation displayed by *Scenedesmus* sp. and *C. closterium*, under nitrogen starvation were unraveled by lipidomic analysis in **Chapter 5**. Neutral lipids in forms of triacylglycerols increased significantly in *Scenedesmus* sp. biomass after 96 h of nitrogen starvation. *Scenedesmus* sp. was initially isolated from a sewage plant in Germany exhibiting high resistance to adverse environmental conditions as well as a high growth rate at the same time. Therefore, it could serve as a valuable candidate to mitigate nutrients and harmful compounds from industrial wastewater. The biomass could subsequently be used for biofuels production after stress. In contrast, one had to harvest *C. closterium* at the late-exponential phase to get a lipid fraction rich in both fucoxanthin and the neutral lipid.

To summarize, the identified products, developed techniques, and determined culture conditions in this thesis intended to make progress towards an economically feasible large-scale production of algal biomass and high-value compounds. An ideal way of sustainable utilization of microalgal biomass is based on a bio-refinery concept (Chew et al., 2017). High-value compounds could be fractionated from total lipids after lipid extraction from algal biomass. Carbohydrates could be used as stock to produce bio-ethanol and bio-hydrogen by fermentation, while microalgal proteins have a broad prospect in animal feeds and food industry.

6.1 Reference

Chew, K.W., Yap, J.Y., Show, P.L., Suan, N.H., Juan, J.C., Ling, T.C., Lee, D.J. and Chang, J.S. (2017) Microalgae biorefinery: High value products perspectives. *Bioresource Technology* **229**, 53-62.